# The Application of Stem Cells from Human Exfoliated Deciduous Tooth in Translational Medicine : New Insights into Cryopreserved Tissue Bank and Stem Cell Therapy

馬, 蘭

https://doi.org/10.15017/1470545

出版情報：九州大学, 2014, 博士（歯学）, 課程博士
バージョン：

# トランスレーショナル医学における

# ヒト脱落乳歯幹細胞の応用

## –凍結組織バンクと幹細胞治療への新たな試み–

**2014**

馬　蘭

九州大学　歯学府歯学専攻

口腔保健推進学講座

小児口腔医学分野

指導教員
九州大学　大学院歯学研究院
口腔保健推進学講座　小児口腔医学分野
教授　野中　和明

研究指導者
九州大学　大学院歯学研究院
口腔常態制御学講座　分子口腔解剖学分野
講師　山座　孝義

# The Application of Stem Cells from Human Exfoliated Deciduous Tooth in Translational Medicine

## -New Insights into Cryopreserved Tissue Bank and Stem Cell Therapy-

**2014**


**Lan Ma**

Section of Pediatric Dentistry,

Division of Oral Health, Growth and Development,

Graduate School of Dental Science,

Kyushu University


**Supervisors**

**Prof. Kazuaki Nonaka, D.D.S., Ph.D.**
Section of Pediatric Dentistry,
Division of Oral Health, Growth and Development,
Faculty of Dental Science, Kyushu University

**Dr. Takayoshi Yamaza, D.D.S., Ph.D.**
Department of Molecular Cell Biology and Oral Anatomy,
Faculty of Dental Science, Kyushu University

## A part of the present thesis has been reported in the following paper.

1. **Ma L**, Makino Y, Yamaza H, Akiyama K, Hoshino Y, Song G, Kukita T, Nonaka K, Shi S, Yamaza T.

   Cryopreserved dental pulp tissues of exfoliated deciduous teeth is a feasible stem cell resource for regenerative medicine.

   PLoS One. 2012;7(12):e51777.

2. **Ma L**, Yamaza H, Hoshino Y, Aijima R, Kukita T, Song G, Zhao W, Nonaka K, Shi S, Yamaza T.

   SHED-based therapy ameliorates osteoporosis secondary in MRL/*lpr* mice through interleukin-17-impaired endogenous bone marrow mesenchymal stem cells

   Stem Cells. In submission

## A part of the present thesis has been reported in the following academic conferences.

1. **L. MA**, H. YAMAZA, Y. MAKINO, G. SONG, K. NONAKA, T. YAMAZA.

   Influence of Cryopreservation on the Properties of Stem Cells isolated from Cryopreserved Exfoliated Deciduous Teeth.

   International Symposium: Shaping the future of craniofacial sciences and therapeutics. Aug 2011. Beijing.

2. **Lan Ma**, Haruyoshi Yamaza, Yusuke Makino, So-ichiro Sonoda, Keitaro F. Masuda, Toshio Kukita, Kazuaki Nonaka, Takayoshi Yamaza.

   Isolation and characterization of mesenchymal stem cells isolated from cryopreserved exfoliated deciduous teeth.

   第 53 回歯科基礎医学会学術大会・総会　2011 年 9 月　岐阜

3. **Lan Ma**, Yusuke Makino, Haruyoshi Yamaza, Kentaro Akiyama, Guangtai Song, Toshio Kukita, Songtao Shi, Kazuaki Nonaka, Takayoshi Yamaza.

   Long Term Cryopreserved Dental Pulp Tissues of Exfoliated Deciduous Teeth is a Feasible Stem Cell Resource for Regenerative Medicine.

   Musculoskeletal Science: Bedside to Bench to Bedside in Gordon Research Conference. Aug 2012. Andover, NH, USA.

4. **Lan Ma**, Takayoshi Yamaza, Yusuke Makino, Haruyoshi Yamaza, Yoshihiro Hoshino, Keitaro F. Masuda, Toshio Kukita, Kazuaki Nonaka.

   Bone Regeneration using Stem Cells from Long-term Cryopreserved Dental Pulp Tissues of Exfoliated Deciduous Teeth.

   第 54 回歯科基礎医学会学術大会・総会、 2012 年 9 月 福島

5. **Lan Ma**, Yusuke Makino, Haruyoshi Yamaza, Kentaro Akiyama, Guangtai Song, Toshio Kukita, Songtao Shi, Kazuaki Nonaka, Takayoshi Yamaza.

   Long Term Cryopreserved Dental Pulp Tissues of Exfoliated Deciduous Teeth is a Feasible Stem Cell Resource for Regenerative Medicine.

   The 7th Kyudai international oral bioscience symposium. March 2013. Fukuoka.

6. **Lan Ma**, Haruyoshi Yamaza, Yoshihiro Hoshino, Toshio Kukita, Kazuaki Nonaka, Takayoshi Yamaza.

   Cryopreservation of Dental Pulp Tissues of Exfoliated Deciduous Teeth is a Suitable Stem Cell Bank for Regenerative Medicine

   The 24th fukuoka international symposium on pediatric/maternal-child health research. Aug 2013. Fukuoka.

# TABLE OF CONTENTS

## LIST OF TABLES

## LIST OF FIGURES

## LIST OF ABBREVIATIONS

AA: ascorbic acid

Ab: antibody

AGG: aggrecan

ALB: albumin

ALP: alkaline phosphatase

alphaMEM: alpha Modification of Eagle's Medium

ANA: anti-nuclear antibody

APC: allophycocyanin

B: bone

bFGF: basic fibroblast growth factor

BMCs: bone marrow nucleated cells

BMC-hBMMSC: bone marrow cells isolated from hBMMSC-transplanted MRL/lpr mice

BMC-MRL/lpr: bone marrow cells isolated from non-transplanted MRL/lpr mice

BMC-SHED: bone marrow cells isolated from SHED-transplanted MRL/lpr mice

BMC-WT: bone marrow cells isolated from wild-type mice

BMD: bone mineral density

BrdU: bromodeoxyuridine

BV: blood vessel

BV/TV: bone volume/trabecular volume

C3: complementary 3

Calvarial-WT: calvarial cells isolated form wild-type mice

CathK: cathepsin K

CFSE: carboxyfluorescein diacetate succinimidyl ester

CFU-F: colony-forming unit fibroblasts

CM: conditioned medium

CM-hBMMSC: conditional medium from BMC-hBMMSC cultures

CM-MRL/lpr: conditional medium from BMC-MRL/lpr cultures

CM-SHED: conditional medium from BMC-SHED cultures

ColX: type X collagen

CT: connective tissue

Ctr: calcitonin receptor

CTX: C-terminal telopeptides of type I collagen

D: dentin

DAPI: 4', 6-diamidino-2-phenylindole

DMSO: dimethyl sulfoxide

DP: dental pulp

DPSCs: dental pulp stem cells

dsDNA: double strand DNA

DSPP: dentin sialophosphoprotein

EGM-2: endothelial cell growth media kit

EGF: epidermal growth factor

EDTA: ethylenediaminetetraacetic acid

ELISA: enzyme linked immunosorbent assay

ES: embryonic stem cells

FBS: fetal bovine serum

FDA: U.S. Food and Drug Administration

FITC: fluorescein isothiocyanate

GAPDH: glyceraldehyde 3-phosphate dehydrogenase

GVHD: graft-versus-host-disease

HA/TCP: hydroxyapatite tricalcium phosphate

hBMMSCs: human bone marrow MSCs

hBMMSC-T: hBMMSC- transplanted MRL/*lpr* mice

hCD146: human CD146

H&E: hematoxylin and eosin

HEK: HEK293 cells

H.I. HEK: heat inactivated HEK,

H.I. SHED-Cryo: heat inactivated SHED-Cryo

H.I. SHED-Fresh: heat inactivated SHED-Fresh

hMt: human specific mitochondria

HSC: hematopoietic stem cell

IFNg: interferon gamma

IgG: Immunoglobulin G

IgG1: Immunoglobulin G1

IgG2a: Immunoglobulin G2a

IgG2b: Immunoglobulin G2b

IgM: Immunoglobulin M

IL-6: interleukin 6

IL-17: interleukin 17

iPS: induced pluripotent stem cells

ITS: insulin-transferring-selene mixture

LN: lymph nodes

LNGFR: low affinity nerve growth factor

LPL: lipoprotein lipase

*lpr*: MRL/lpr mice

M-CSF: macrophage colony stimulating factor

mCD146: mouse CD146

microCT: micro-computed tomography

MNCs: multinucleated cells

MRL/*lpr* : non-transplanted MRL/*lpr* mice

MSCs: mesenchymal stem cells

MSC-hBMMSC: BMMSCs isolated from hBMMSC-transplanted MRL/*lpr* mice

MSC-MRL/*lpr*: BMMSCs isolated from non-transplanted MRL/*lpr* mice

MSC-SHED: BMMSCs isolated SHED-transplanted MRL/*lpr* mice

MSC-WT: BMMSCs isolated from wild-type mice

MW: molecular weight markers

Nfatc1: nuclear factor of activated T-cells, cytoplasmic 1

NIH: National Institutes of Health

ns: no significance

OCN: osteocalcin

OCT4: octamer 4

P3: Passaged 3

PAS: Periodic acid-Schiff staining

PBMNCs: human peripheral blood mononuclear cells

PBS: phosphate buffered saline

PCR: polymerase chain reaction

PD: population doubling

PDL: periodontal ligament

PerCP: peridinin-chlorophyll-protein complex

PFA: paraformaldehyde

PGE2: prostaglandin $E_2$

Pi: inorganic phosphate

PPARg2: peroxisome proliferator activated receptor-gamma2

RB: regenerated bone

RBM: regenerated bone marrow

R-PE: R-phycoerythrin

RT-PCR: reverse transcription polymerase chain reaction

RUNX2: runt-related gene 2

SCAP: stem cells from apical papilla

SD: standard deviation

SHED: human exfoliated deciduous teeth

SHED-Cryo: SHED from the cryopreserved deciduous dental pulp tissues

SHED-Fresh: SHED from fresh deciduous dental pulp tissues

SHED-T: SHED-transplanted MRL/lpr mice

SLE: systemic lupus erythematosus

SQ: starting quantity

sRANKL: soluble receptor activator for nuclear factor κB ligand

SSEA-4: stage-specific embryonic antigen-4

Tb.N: trabecular number

Tb.Sp: trabecular separation

Tb.Spac: trabecular space

Tb.Th: trabecular thickness

TC: gomori trichrome staining

TGFbeta1: transforming growth factor beta1

Th17: helper T cells

TRAP: tartrate-resistant acid phosphate

TRAP+ MNCs: TRAP-positive multinucleated cells

UCMSCs: umbilical cord-derived MSCs

VD3:1a, 25-$(OH)_2$ vitamin $D_3$

# ABSTRACT

Human exfoliated deciduous teeth have been considered to be a promising source for translational medicine because they contain unique postnatal stem cells from human exfoliated deciduous teeth (SHED), capable of multipotency and immunomodulatory function. However many considerations including preservation technique of deciduous teeth should be covered before clinical application. In the part I of this study, cryopreserved dental pulp tissues of human exfoliated deciduous teeth was evaluated to be a retrievable and practical source for cell-based therapy. SHED isolated from the cryopreserved tissues for over 2 years (SHED-Cryo) owned stem cell properties including clonogenicity, self-renew, stem cell marker expression, multipotency, *in vivo* tissue regenerative capacity and *in vitro* immunomodulatory. Next, SHED-Cryo were transplanted into systemic lupus erythematosus (SLE) model MRL/*lpr* mice and bone defect model mice, and improved SLE-like disorders (short lifespan, elevated autoantibody levels, nephritis-like renal dysfunction, increased IL-17-secreting helper T cells, and secondary osteoporosis) and critical calvarial bone-defects

The aim of the part II was focused on the therapeutic mechanism of SHED transplantation to osteoporotic disorders secondary in SLE. Secondary osteoporosis in SLE leads the patients to lose their quality of life by fragility fractures. Current study showed that systemic transplanted SHED could ameliorate bone loss in SLE model MRL/*lpr* mice. However, the therapeutic mechanism to the bone regeneration has not been fully understood. Systemically transplanted SHED as well as human bone marrow mesenchymal stem cells (hBMMSCs) recovered the reduction of bone density and structures in MRL/*lpr* mice with enhanced osteoblastogenesis and suppressed osteoclastogenesis. More importantly, we found that the negative bone metabolic turnover

in the secondary osteoporosis is mediated by impaired recipient BMMSCs, which may act as an endogenous source for osteoporosis in SLE. To overcome the bone dysfunction, MSC transplantation re-established functionally impaired recipient BMMSCs of MRL/*lpr* mice through the suppression of IL-17 in the recipient bone marrow, regulating positive bone metabolism via osteoblasts and osteoclasts.

Taken together, the cryopreservation technique of dental pulp tissues of deciduous teeth provides a suitable and desirable approach for translational medicine. Furthermore, IL-17 and endogenous BMMSCs might be a therapeutic target of SHED-based therapy to SLE and osteoporosis secondary. These findings present a new insight into cryopreserved tissue banking and stem cell therapy, indicating the great potential of SHED in translational medicine.

# PART I

# Cryopreserved Dental Pulp Tissues of Exfoliated Deciduous Teeth are a Feasible Stem Cell Resource for Regenerative Medicine

## 1.1 INTRODUCTION

Mesenchymal stem cells (MSCs) have been isolated from a variety of fetal and adult tissues and considered as an ideal candidate source for cell-based therapy due to their unique properties such as multipotency and immunomodulatory functions [1]. Many researchers have investigated to apply MSCs as progenitors of osteoblasts for bone tissue engineering. Clinical evidences also support the efficacy of MSC-based skeletal tissue regeneration [2, 3]. On the other hand, MSCs exert striking regulatory effects on immune cells such as T- and B-lymphocytes, dendritic cells, and natural killer cells [4, 5]. This immunological traits of MSCs lead to take clinical advantages to immune diseases such as acute graft-versus-host-disease (GVHD) [4, 6], hematopoietic stem cell (HSC) engraftment [7, 8] and SLE [9].

Recent discovery has evaluated that fresh dental pulp tissues of human exfoliated deciduous teeth preserve MSC population, termed SHED [10]. SHED display typical stem cell properties including clonogenicity, cell proliferation and multipotency to differentiate into odontoblast/osteoblast-, adipocyte-, and neural cell-like cells [10]. SHED also express a unique *in vivo* tissue regeneration capability of forming dentin/pulp and bone/bone marrow structures when subcutaneously transplanted into immunocompromised mice [10]. SHED implantation govern bone repair in critical-sized bone defects in mouse calvarias [11] and swine mandible [12]. Moreover, systemic SHED-transplantation exhibited effective improvement on SLE-like disorders including hyper-autoantibody levels, renal dysfunction and hyperactivity of IL-17-producing helper T (Th17) cells, in MRL/*lpr* mice [13]. Therefore SHED are considered to be a feasible and promising cell source for cell-based tissue engineering and immune therapy in regenerative medicine.

Exfoliated deciduous teeth possess advantages of minimal invasiveness and easily accessible tissue source in comparison with other human tissues such as bone marrow and adipose tissue [10]. However, the effective preservation of deciduous teeth has remained a primary concern for clinical applications of SHED. In addition, SHED isolation is impractical immediately after the exfoliation of deciduous teeth because the opportunity of the exfoliation is unpredictable. Recently, cryopreservation of human cells and tissues is amenable to be a reliable and feasible approach for stem cell storage [14]. Herein, we cryopreserved dental pulp tissues of exfoliated deciduous teeth for over 2 years and investigated the effects of the long term cryopreservation on the recovering of SHED properties including *in vitro* and *in vivo* biological and immunological properties. Furthermore, we assessed the therapeutic efficacy of the recovered SHED from the cryopreserved deciduous dental pulp tissues on immune modulation and bone regeneration in SLE model-MRL/*lpr* and bone defect model-immunocompromised mice.

## 1.2 MATERIALS AND METHODS

### *1.2.1 Ethics statement*

Procedures using human samples (exfoliated deciduous teeth and peripheral blood) were conducted in accordance with the Declaration of Helsinki and approved by the Kyushu University Institutional Review Board for Human Genome/Gene Research (Protocol Number: 393-01). We obtained written informed consent from all the children's parents on the behalf of the children participants involved in this study. All animal experiments were approved by the Institutional Animal Care and Use Committee of Kyushu University (Protocol Number: A21-044-1) and conformed to all the guidelines outlined in the Guide for the Care and Use of Laboratory Animals by the National Institutes of Health (NIH).

### *1.2.2 Human subjects*

Human exfoliated deciduous teeth were collected as discarded biological/clinical samples from children (5-7-year-old) at Department of Pediatrics of Kyushu University Hospital. Human peripheral blood mononuclear cells (PBMNCs) were collected from healthy volunteers (28-34 year-old).

### *1.2.3 Cryopreservation of deciduous dental pulp tissues of exfoliated deciduous teeth and isolation and culture of SHED*

A protocol for the cryopreservation of dental pulp tissues of exfoliated deciduous teeth was summarized in **Figure 1**. Dental pulp tissues were separated from exfoliated deciduous teeth. Half of the samples were mixed with a cryopreserved medium at 4$^{o}$C and kept overnight at -80$^{o}$C. The cryopreserved medium consisted of 10% dimethyl sulfoxide (DMSO) (Sigma, St Louis, MO) and 90% fetal bovine serum (FBS) (Equitech-Bio,

Kerrville, TX). They were transferred into liquid nitrogen and stored for over 2 years (25-30 months). The other half of fresh deciduous dental pulp tissues were treated to isolate SHED (SHED-Fresh). SHED-Cryo, as well as SHED-Fresh, were isolated by an adherent colony-forming unit fibroblasts (CFU-F) method [10, 13, 15]. The cryopreserved tissues were quickly thawed at 37$^{o}$C. Both cryopreserved and fresh dental pulp tissues were digested with 0.3% collagenase type I (Worthington Biochemicals, Lakewood, NJ) and 0.4% dispase II (Sanko Junyaku, Tokyo, Japan) in phosphate buffered saline (PBS, pH 7.4) for 60 min at 37$^{o}$C. Single-cell suspensions were obtained through a 70-μm-cell strainer (BD Bioscience, San Jones, CA). The cells (1x10$^{6}$) were seeded on T-75 flasks, washed with PBS after 3 hours and cultured at 37$^{o}$C in 5% $CO_2$ with a growth medium containing 15% FBS (Equitech-Bio), 100 μM L-ascorbic acid 2-phosphate (WAKO Pure Chemical, Osaka, Japan), 2 mM L-glutamine (Nacalai Tesque, Kyoto, Japan) and 100 U/ml penicillin and 100 μg/ml streptomycin (Nacalai Tesque) in alpha Modification of Eagle's Medium (alphaMEM) (Invitrogen, Carlsbad, CA) and subsequently cultured for 14-16 days until obtaining adherent colonies. The adherent colonies-forming cells were recognized as SHED as described before [10, 13]. The colonies-forming cells were passed and sub-cultured in the growth medium. The medium was changed twice a week.

### *1.2.4 Antibodies*

Antibodies used in this study are summarized in the **Table 1**.

**Table 1. List of antibodies in Part I**

| Names of antibodies | Types of antibodies | Names of Suppliers |
|---|---|---|
| anti-CD3 antibody | purified | eBioscience (San Diego, CA) |
| anti-CD4 antibody | R-PE-conjugated | eBioscience (San Diego, CA) |
| anti-CD8a antibody | FITC-conjugated | eBioscience (San Diego, CA) |
| anti-CD14 antibody | R-PE -conjugated | eBioscience (San Diego, CA) |
| anti-CD28 antibody | purified | eBioscience (San Diego, CA) |
| anti-CD31 antibody | purified | eBioscience (San Diego, CA) |
| anti-CD34 antibody | R-PE-conjugated | eBioscience (San Diego, CA) |
| anti-CD45 antibody | R-PE-conjugated | eBioscience (San Diego, CA) |
| anti-CD73 antibody | R-PE-conjugated | eBioscience (San Diego, CA) |
| anti-CD105 antibody | R-PE-conjugated | eBioscience (San Diego, CA) |
| anti-CD146 antibody | R-PE-conjugated | eBioscience (San Diego, CA) |
| anti-interferon γ antibody | APC-conjugated | eBioscience (San Diego, CA) |
| anti-interleukin 17A antibody | R-PE-conjugated | eBioscience (San Diego, CA) |
| anti-human mitochondria | purified | Millipore (Billerica, MA) |
| anti-neurofilament M antibody | purified | Sigma (St Louis, MO) |
| anti-STRO-1 antibody | purified | abcam (Cambridge, MA) |
| anti-tubulin βIII antibody | purified | Sigma (St Louis, MO) |

APC: allophycocyanin
FITC: fluorescein isothiocyanate
PerCP: Peridinin-chlorophyll-protein complex
R-PE: R-phycoerythrin

### *1.2.5 Mice*

C57BL/6J and Balb/cA-nu/nu mice (female, 6 week-old) were purchased from CLEA Japan. (Tokyo, Japan). C57BL/6J MRL/*lpr* mice (female, 6 week-old) were from Japan SLC. (Shizuoka, Japan). They were housed in temperature- and light-controlled environmental conditions with a 12-hour light and dark cycle, and permitted ad *libitum* consumption of water and standard pellet chow.

### *1.2.6 Histology of cryopreserved dental pulp tissues of exfoliated deciduous teeth*

Cryopreserved deciduous pulp tissues were fixed with 4% paraformaldehyde (PFA) in PBS and immersed in O.C.T. compound (Sakura Finetek Japan, Tokyo, Japan). The frozen specimens were cut into 6-μm thick sections. Some sections were stained with hematoxylin and eosin (H&E). The others were immunostained with anti-STRO-1 and anti-human CD146 antibodies by using SuperPicture kit (Invitrogen). Subclass-matched antibodies were used for negative controls for immunohistochemistry. The sections were observed under a microscope BIORVO BZ-9000 (Keyence Japan, Osaka, Japan).

### *1.2.7 CFU-F assay*

Cells ($10x10^3$) isolated from frozen/fresh deciduous dental pulp tissues were seeded on 100-mm culture dishes and cultured in the growth medium for 16 days. The flasks were treated with 4% PFA and 0.1% toluidine blue in PBS for 18 hours. Colonies containing >50 cells were recognized as single colony clusters under a microscope as described previously [10, 13]. The numbers of the colonies were counted.

### *1.2.8 Population doubling assay*

Cells were seeded on T-75 culture flasks (BD Bioscience). When the cells reached at sub-confluent condition, the cells were passed. These steps were repeated until the cells lost dividing capability. The population doubling score was calculated at every passage according to the equation: $\log_2$ (number of final harvested cells/number of initial seeded cells) and the total scores were determined by adding up each population doubling score in each sample as described in previous reports [10, 13].

### *1.2.9 Bromodeoxyuridine (BrdU) incorporation assay*

Passaged 3 (P3) SHED were seeded at $1x10^3$ per well on 35-mm dishes and cultured in the growth medium for 2 days. BrdU reagent (Invitrogen) was added at 1:100 in the medium and subsequently cultured additionally for 24 hours. The cells were fixed in 70% ethanol for 15 min, treated with the BrdU staining kit (Invitrogen) and lightly stained with hematoxylin according to the company's instruction. Seven images were randomly selected to calculate BrdU-positive nuclei number in each sample. Cell proliferation capacity was shown as a percentage of BrdU-positive nuclei over total nucleated cells [13].

### *1.2.10 Telomerase activity assay*

Telomerase activity was measured by a telomere repeat amplification protocol assay using the quantitative telomerase detection kit (Allied Biotech, Inc., Ijamsville, MD) applied with real-time PCR as referred to our previous reports [13, 19]. As positive control, HEK293T cells were used. Some extracts from each cell were heated at 85$^{o}$C for 10 min and used as negative control samples. The average starting quantity (SQ) of fluorescence units was used to compare the telomerase activity among the samples.

### *1.2.11 Flow cytometric analysis for SHED*

P3 SHED were cultured at 50-60% confluent condition. Cells ($100x10^3$/100 ml) were stained with primary specific antibodies. Subclass-matched antibodies were used as controls. Flow cytometry was analyzed on FACSCalibur flow cytometer (BD Bioscience) [13]. The number (percentage) of positive cells was determined using CellQuest software (BD Bioscience) by comparison with the corresponding control cells stained with

corresponding subclass-matched antibody in which a false-positive rate of less than 1% was accepted.

### *1.2.12 Immunofluorescence for cultured cells*

The cells were fixed with 4% PFA in PBS, and blocked with PBS containing 10% normal serum matched to secondary antibodies. The samples were incubated with the specific antibodies to cell surface markers or subclass-matched antibodies overnight at 4$^{o}$C and treated with CF 633-conjugated-secondary antibodies (Biotium, Hayward, CA). Finally, they were stained with 4', 6-diamidino-2-phenylindole (DAPI) (Dojindo, Kumamoto, Japan) and observed under BIORVO microscope (BZ-9000, Keyence Japan). Numbers of cells positive to the specific antibodies and nuclei stained with DAPI were counted and shown as a percentage of positive cells over total nucleated cells.

### *1.2.13 Semi-quantitative RT-PCR*

Total RNA was isolated from the cultures using TRIzol (Invitrogen) and digested with DNase I. The cDNA was synthesized from 100 ng of total RNA using Revatra Ace (TOYOBO, Osaka, Japan). The specific primer pairs are listed in **Table 2**. PCR was performed using gene specific primers and RT-PCR Quick Taq HS DyeMix (TOYOBO) at 94°C for 2 min for one cycle and then react for 40 cycles with denature at 94°C for 45 sec, annealing at 56°C for 45 sec, extension at 72°C for 60 sec as one cycles, with a final 10-min extension at 72°C. After amplification, 5 ml of each amplified PCR product was analyzed by 2 % agarose gel electrophoresis, and visualized by ethidium bromide staining. The intensity of bands was measured by using Image-J soft ware and normalized to an internal control gene, *glyceraldehyde 3-phosphate dehydrogenase (GAPDH)*.

### *1.2.14 In vitro multipotent assay*

***In vitro* dentinogenic/osteogenic induction assay**: SHED (P3, $5x10^3$) were grown on 60-mm dishes in the growth medium until confluent condition and induced with an dentinogenic/osteogenic medium supplemented with 1.8 mM potassium dihydrogen phosphate (Sigma, St. Louis, MO) and 10 nM dexamethasone (Sigma) in the growth medium. The dentinogenic/osteogenic medium were changed twice a week. One week after the induction, dentinogenic/osteogenic markers were analyzed by semi-quantitative reverse transcription polymerase chain reaction (RT-PCR) and alkaline phosphatase (ALP) activity test [13]. For mineralized nodule assay, the cultures were stained with 1% Alizarin Red-S (Sigma) at 4 weeks post induction. The Alizarin red-positive area was analyzed using NIH image software Image-J and shown as a percentage of Alizarin red-positive area over total area [13].

***In vitro* chondrogenic induction assay:** SHED (P3, $2x10^6$) were aggregated in a 15 mL tube and cultured with Dulbecco's modified Eagle's medium (Invitrogen) supplemented with 15% FBS (Equitech-Bio), 2 mM L-glutamine (Nacalai Tesque), 100 μM L-ascorbate-2-phosphate (Wako Pure Chemicals), 2 mM sodium pyruvate (Nacalai Tesque), 1% insulin-transferring-selene mixture (ITS) (BD Biosciences), 100 nM dexamethasone (Sigma), 10 ng/ml transforming growth factor beta1 (TGFbeta1) (PeproTech, Rocky Hill, NJ) and 100 U/ml penicillin and 100 μg/ml streptomycin (Nacalai Tesque). The chondrogenic medium was changed twice a week. After 3-week induction, chondrocyte-specific genes were analyzed by semi-quantitative RT-PCR.

***In vitro* adipogenic induction assay**: Cultured SHED (P3, $5x10^3$/dish) were cultured until the confluent condition and induced in an adipogenic medium with the growth medium plus 500 μM isobutyl-methylxanthine (Sigma), 60 μM indomethacin (Sigma), 0.5 μM hydrocortisone (Sigma) and 10 μM insulin (Sigma). After 6-week induction,

**Table 2. List of primer pairs for RT-PCR in Part I**

*albumin* (GenBank accession no. NM_000477.5)
sense: 5'-ATGGATGATTTCGCAGCTTT-3' (1787-1806)
antisense: 5'- TGGCTTTACACCAACGAAAA-3' (2005-1986)

*aggrecan(AGG)* (NM_013227)
sense: 5'-GCAGAGACGCATCTAGAAATTG-3' (7062-7083)
antisense: 5'-GGTAATTGCAGGGAACATCATT-3' (7656-7677)

*alkaline phosphatase* (*ALP*) (X14390)
sense: 5’-ACGTGGCTAAGAATGTCATC-3’ (nucleotide 322-341)
antisense: 5’-CTGGTAGGCGATGTCCTTA-3’ (nucleotide 779-797)

*collagen, type X* (*ColX*) (NM_000493)
sense: 5'-CACCAGGCATTCCAGGATTCC-3' (1463-1483)
antisense: 5'-AGGTTTGTTGGTCTGATAGCTC-3'(2265-2286)

*dentin sialophosphoprotein* (*DSPP*) (NM_014208)
sense: 5′-GGCAGTGACTCAAAAGGAGC-3′ (1630-1649)
antisense: 5′-TGCTGTCACTGTCACTGCTG-3′ (1815-1834)

*GAPDH* (M33197)
sense: 5′-AGCCGCATCTTCTTTTGCGTC-3′ (12-32)
antisense: 5′-TCATATTTGGCAGGTTTTTCT-3′ (807-827)

*lipoprotein lipase* (*LPL*) (X14390)
sense: 5′-ATGGAGAGCAAAGCCCTGCTC-3′ (118-138)
antisense: 5′-GTTAGGTCCAGCTGGATCGAG-3′ (661-681)

*low-affinity neural growth factor* (*LNGFR*) (NM_002507)
sense: 5’-CACCTCCAGAACAAGACCTC-3’ (775-794)
antisense: 5’-GAGCCGTTGAGAAGCTTCTC-3’ (1167-1186)

*NANOG* (NM_024865)
sense: 5’-TCCTCCATGGATCTGCTTATTCA-3’ (382-404)
antisense: 5’-CAGGTCTTCACCTGTTTGTAGCTGAG-3’ (616-641)

*NESTIN* (NM_006617)
sense: 5’-CAGCGTTGGAACAGAGGTTGG-3’ (852-872)
antisense: 5’-TGGCACAGGTGTCTCAAGGGTAG-3’ (1218-1240)

*NOTCH1* (NM_017617)
sense: 5’-CACCCAGAACTGCGTGCA-3’ (3840-3857)
antisense: 5’-GGCAGTCAAAGCCGTCGA-3’ (4547-4564)

*octamer4 (OCT4)* (NM_203289)
sense: 5’-GACAGGGGGAGGGGAGGAGCTAGG-3’ (1495-1518)
antisense: 5’-CTTCCCTCCAACCAGTTGCCCCAAAC-3’ (1613-1638)

←**Table 2. List of primer pairs for RT-PCR in Part I**

*osteocalcin* (*OCN*) (X53698)
sense: 5′-CATGAGAGCCCTCACA-3′ (18-33)
antisense: 5′-AGAGCGACACCCTAGAC-3′ (316-332)

*peroxisome proliferator activated receptor-γ2* (*PPARg2*) (AB451337)
sense: 5′-CTCCTATTGACCCAGAAAGC-3′ (23-42)
antisense: 5′-GTAGAGCTGAGTCTTCTCAG-3′ (350-369)

*runt-related gene 2 (RUNX2)* (L40992)
sense: 5′-CAGTTCCCAAGCATTTCATCC-3 (880–900)
antisense: 5′-TCAATATGGTCGCCAAACAG-3′ (1304–1323)

*SOX9* (NM_000346)
sense: 5'-GAACGCACATCAAGACGGAG-3' (1553-1572)
antisense: 5'-TCTCGTTGATTTCGCTGCTC-3' (2164-2183).

cultures were stained with 0.3% Oil red O (Sigma) to detect lipid droplets. The samples stained with Oil red O were treated with isopropanol and the absorbance of the extracts were measured at 520 nm. Adipocyte-specific genes were also analyzed by semi-quantitative RT-PCR.

***In vitro*** **endothelial cell induction assay:** P3 SHED ($5x10^3$ cells) were seeded on fibronectin-coated 35-mm dishes (BD Biosciences) and cultured by using a commercial available endothelial cell growth media kit, EGM-2, (Lonza, Basel, Switzerland) according to the manufacture's instruction for 7 days. The endothelial growth medium was changed every 2 days. The cultures were fixed. Endothelial cell differentiation was determined by immunofluorescence with anti-CD31 and CD34 antibodies.

***In vitro*** **neuronal cell induction assay**: P3 SHED ($5x10^3$ cells/well) were plated in laminin-coated 35-mm dishes (BD Biosciences) and cultured in a neurogenic medium containing supplemented with 1xN2 supplement (Invitrogen), 10 ng/ml basic fibroblast growth factor (bFGF) (PeproTech), 10 ng/ml epidermal growth factor (EGF) (PeproTech), 100 U/ml penicillin and 100 μg/ml streptomycin in Neurobasal A (Invitrogen) for 21 days

according to the recent study [10]. The medium was changed with 50% of fresh medium twice a week. Neural cell differentiation was determined by immunofluorescence with anti-*glial fibrillary acidic protein*, anti-neural filament M, and anti-bIII tubulin antibodies.

***In vitro* hepatic induction assay**: P3 SHED (P3, $5x10^3$) were seeded on fibronectin-coated 35-mm dishes (BD Biosciences) and cultured with Iscove's modified Dulbecco's medium (Invitrogen) supplemented with 10 nM dexamethasone (Sigma), 1% ITS (BD Biosciences), 20 ng/ml EGF (PeproTech), 10 ng/ml bFGF (PeproTech), 20 ng/ml hepatocyte growth factor (PeproTech) and 20 ng/ml oncostain M (PeproTech) for 4 weeks. Hepatocyte-specific gene albumin was assayed by semi-quantitative RT-PCR.

### *1.2.15 In vivo tissue regeneration assay*

Xenogenic transplantation was performed as previously [13, 16]. Cultured SHED (P3) in the growth medium ($4x10^6$) were mixed with a carrier, hydroxyapatite tricalcium phosphate (HA/TCP) (40 mg, Zimmer Inc., Warsaw, IN). The mixtures were subcutaneously transplanted into the dorsal surface of 8-10-week-old Balb/c *nude*/*nude*. The implants were harvested eight weeks after the surgery, fixed with 4% PFA and decalcified with 10% EDTA. Frozen sections were cut and used for H&E staining or immunofluorescence.

### *1.2.16 In vivo self-renewal assay*

In vivo self-renewal assay with a sequential transplantation was referred to a recent study [17]. SHED (P3) ($4x10^6$) were implanted with HA/TCP carrier (40 mg) (Zimmer) into primary Balb/c *nu*/*nu* mice. Eight weeks after the transplantation, the primary implants were harvested and treated with 0.4% dispase II (Sanko Junyaku) for 60 min at $37^oC$ to obtain single cells from the implants. The cells were stained with R-PE-conjugated anti-

human CD146 and magnetic-beads-conjugated anti-R-PE antibodies (Miltenyi Biotec, Bergisch Gladbach, Germany) and sorted magnetically to obtain human CD146-positive cells. The purity was confirmed by flow cytometry with anti-human CD146 or anti-mouse CD146 antibody. The sorted cells were seeded at low density and cultured to obtain attached CFU-F. Expanded CFU-F-forming cells (P1) ($4x10^6$) were subcutaneously transplanted with HA/TCP carriers (40 mg) (Zimmer) into secondary immunocompromised mice for 8 weeks. Secondary implants were assayed by H&E staining and immunofluorescence.

### *1.2.17 Histological analysis of implant tissues.*

Implant tissue samples were fixed with 4% PFA in PBS overnight and decalcified with 5% EDTA solution (pH 7.4). Frozen sections were cut and treated with H&E staining and immunofluorescence with anti-human mitochondria, anti-STRO-1 or anti-human CD146 antibody. To measure newly-formed area of mineralized tissue, seven fields were randomly selected, and newly-formed area within each field was calculated by NIH image-J soft ware, and shown as a percentage over total tissue area as described before [13, 16].

### *1.2.18 Single colonies-derived cell assay*

As referred to a previous study [18], cells isolated from cryopreserved deciduous dental pulp tissues were seeded at 1, 2 or 4 cells per well on 24-well multiplates with the growth medium. The wells containing more than two attached cells were excluded from further analysis. The single cell-attached wells were cultured for 14-16 days and obtained CFU-F-forming cells. The single colony-forming cells were used for population doubling, BrdU incorporation and dentinogenic/osteogenic analyses.

### *1.2.19 Induction assay of Th17 cells*

Induction of Th17 cells was performed as previously [13]. Human $CD4^+CD25^-$ T cells were magnetically sorted from human PBMNCs using $CD4^+CD25^+$ regulatory T cell isolation kit (Miltenyi Biotec). They ($1x10^6$/well) were activated by plate-bounded anti-CD3 (5 μg/ml) and soluble anti-CD28 (1 μg/ml) antibodies for 3 days and loaded on SHED ($20x10^3$/well) with recombinant human TGFbeta1 (2 μg/ml, PeproTech) and interleukin 6 (IL-6) (50 mg/ml, PeproTech) for 3.5 days. T cells were stained with anti-PerCP-conjugated CD4 and FITC-conjugated anti-CD8a antibodies, treated with R-PE-conjugated anti-IL-17 and APC-conjugated anti-interferon gamma (IFNg) antibodies using Foxp3 staining buffer kit (eBioscience, San Diego, CA) and analyzed on FACSCalibur (BD Biosciences). IL-17 levels in the culture supernatants were analyzed by enzyme linked immunosorbent assay (ELISA) with a commercial available kit (R&D Systems) according to the manufacture's instruction.

### *1.2.20 Systemic transplantation of SHED into MRL/lpr mice*

The protocol for systemic transplantation of SHED into MRL/*lpr* mice was referred to our previous reports [9, 13]. Briefly, SHED ($0.1x\ 10^6$/10g body weight) or PBS were systemically infused into MRL/*lpr* mice via the tail vein at the age of 16 weeks old. Their survival was inspected daily until died. Peripheral blood, urine, kidney, axial lymph nodes and long bones were collected from MRL/*lpr* mice at the age of 20 weeks old according to our previous studies [9, 13].

### *1.2.21 Assay for autoantibodies, immunoglobulins, biomarkers and cytokines in peripheral blood serum, urine and tissue samples*

Biological factors in mouse biological samples were measured by ELISA with commercial available kits (anti-double strand DNA [dsDNA] IgG and IgM, anti-nuclear antibody [ANA], albumin and complementary 3: alpha diagnostic [San Antonio, TX]; IL-17 and nuclear factor κB ligand [sRANKL] [R&D Systems]; C-terminal telopeptides of type I collagen [CTX]: Nordic Bioscience [Herlev, Denmark]] according to the manufactures' instructions. Creatinine (R&D Systems) and urine protein (Bio Rad, Hercules, CA) were also assayed by colorimetry according to the manufactures' instructions.

### *1.2.22 Flow cytometric analysis for mouse peripheral blood Th17*

To measure Th17 cells, mouse PBMNCs were incubated with PerCP-conjugated anti-CD4, FITC-conjugated anti-CD8a, followed by the treatment with R-PE-conjugated anti-IL-17 and APC-conjugated anti-IFNg antibodies using a Foxp3 staining buffer kit (eBioscience). The stained cells were analyzed on FACSCalibur (BD Bioscience).

### *1.2.23 Histopathological analysis of mouse Kidney*

Kidney samples were fixed with 4% PFA in PBS overnight. After washed with PBS, some samples were processed for paraffin embedding and cut into 6-mm thick paraffin sections. The others were cut into 8-mm thick cryosections. The paraffin sections were treated with H&E, Gomori trichrome or Periodic Acid Schiff (PAS) staining. The cryosections were stained with anti-mouse complementary 3 antibody and treated with CF 633-conjugated-secondary antibodies (Biotium). Finally, they were stained with DAPI (Dojindo) and observed under BIORVO microscope (BZ-9000, Keyence Japan).

### *1.2.24 In vivo tracing assay of SHED*

To trace the trafficking of SHED transfused in MRL/*lpr* mice, carboxyfluorescein diacetate succinimidyl ester (CFSE) labeling was applied. Single suspended SHED population ($10x10^6$/ml) was incubated with CFSE solution (Invitrogen) for 10 min at 37°C. The labeled cells ($1x10^6$) were intravenously injected into the tail vein of MRL/*lpr* mice. Lymph nodes, kidneys and femurs of the mice were harvested either 24 h or 1 week after the infusion. The tissue samples were fixed with 4% PFA in PBS overnight. Only bone samples were treated with 10% EDTA. All of the samples were cut into 6-mm frozen sections, stained with DAPI (Dojindo) and observed under a microscope.

### *1.2.25 Bone phenotype analysis*

The femoral bone samples were fixed with 4% PFA in PBS overnight and analyzed by micro-computed tomography (microCT) with Skyscan 1076 scanner (Skyscan, Kontich, Belgium). Bone mineral density (BMD) and bone structural parameters including bone volume/trabecular volume (BV/TV), trabecular thickness (Tb.Th), trabecular number (Tb.N), trabecular separation (Tb.Sp) and trabecular space (Tb.Spac) were calculated using CT Analyzer software (Skyscan) according to the manufacture's instruction. After microCT analysis, the bone samples were decalcified with 10% EDTA and cut into 6-mm paraffin sections. The paraffin sections were treated with H&E staining. Some sections were stained with a tartrate-resistant acid phosphate (TRAP) staining solution containing 0.01% naphthol AS-MX phosphate (Sigma), 50 mM tartrate (Sigma), 0.06% fast red violet LB salt (Sigma) in 0.1 M acetate buffer (pH 5.0) for 10 min or staining. TRAP-positive cells were counted and quantified as previously [19].

### *1.2.26 In vitro osteoclastic and osteogenic assays*

Bone marrow were flashed out from bone cavity of femurs and tibias with heat-inactivated 3% FBS (Equitech-Bio) in PBS. For osteoclastic assay, the bone marrow nucleated cells (BMCs) were seeded at $1x10^6$ per well on the 24-well culture plates with 10 ng/ml macrophage colony stimulating factor (M-CSF) (R&D Systems) and 25 ng/ml sRANKL (PeproTech) in alphaMEM for 5-6 days. The medium was changed on Day 3. The cultures were treated with TRAP staining [19] and the TRAP-positive cells with muitinuclear (n>3) were counted [19]. The BMCs ($1x10^6$) were also seeded on 35-mm culture dishes and cultured in an osteogenic medium containing 10% FBS (Equitech-Bio), 2 mM L-glutamine (Nacalai Tesque), 100 mM L-ascorbic acid 2-phosphate (WAKO pure chemicals), 2 mM beta-glycerophosphate (Sigma), 10 nM dexamethasone (Sigma), 100 U/ml penicillin and 100 μg/ml streptomycin (Nacalai Tesque) in alphaMEM [20]. Four weeks after the induction, the osteogenic cultures were stained with 1% Alizarin Red (Sigma) and mineralized area was quantified.

### *1.2.27 Bone regeneration in calvarial bone defects*

The bone defect models in calvarial bone were generated on immunocompromised mice as described before [11]. Briefly, P3 SHED ($4x10^6$) were mixed with HA/TCP carriers (40 mg) (Zimmer). Calvarial bones, especially parietal bones, were removed to make a critical defect area. The mixtures of SHED and HA/TCP were placed on the defect area and the calvarial skins were sutured. Twelve weeks after the implantation, the calvariae were fixed with 4% PFA in PBS overnight and imaged by Skyscan 1076 scanner (Skyscan). Then, the samples were decalcified with 10% EDTA and cut into 6-μm thick paraffin sections. The sections were treated with H&E staining and TRAP staining. Some of sections were used for immunofluorescence with anti-human CD146 antibody.

### *1.2.28 Statistical analysis*

Student's *t*-test was used to analyze significance between 2 groups. A *P* value of less than 0.05 was considered as a significant difference.

## 1.3 RESULTS

### 1.3.1 SHED-Cryo possess MSC properties.

SHED have been elucidated to possess MSC characteristics including clonogenicity, self renew, multipotency, *in vivo* regeneration and *in vitro* immunomodulatory functions [10, 13]. Here, we demonstrated the effects of cryopreservation of deciduous pulp tissues on these SHED properties. Dental pulp tissues were removed from exfoliated deciduous teeth and frozen in the freezing medium (10% DMSO and 90% FBS) at -80$^{o}$C overnight followed by the preservation in a liquid nitrogen-filled tank for over 2 years (**Figure 1**). The remaining tooth bodies were returned to the donor children. The long-term cryopreserved tissues were quickly thawed at 37$^{o}$C before used (**Figure 1**). Histological analysis confirmed that the cryopreserved tissues showed dense connective tissues containing blood vessels and nerve fibers (**Figure 2A**), but not odontoblastic cells. The odontoblast layer may be lost because of mechanical damage or freezing fracture of the pulp samples. Early MSC markers STRO-1 and CD146-positive cells were detected at the perivascular area (**Figure 2B**) as dental pulp stem cells (DPSCs) were localized around the blood vessels in adult dental pulp tissues [21]. These data suggested a possibility that the cryopreserved deciduous pulp tissues retained MSCs.

Next, we isolated MSCs from the cryopreserved dental pulp tissues of exfoliated deciduous teeth, SHED-Cryo, by CFU-F approach (**Figure 1**), which is a classical and standard method [15]. When seeded at low density, single cells were adhered to the plastic culture dishes and then divided to generate cell clusters (**Figure 2C**). The clonogenic cell clusters exhibited different size and varied density (**Figure 2D**). The colony forming efficiency of SHED-Cryo showed similar to that of SHED-Fresh (**Figure 2E**). BrdU incorporation assay demonstrated that the proliferation capacity of SHED-Cryo maintained at a high level (**Figure 2F**) similar to that of SHED-Fresh (**Figure 2G**).

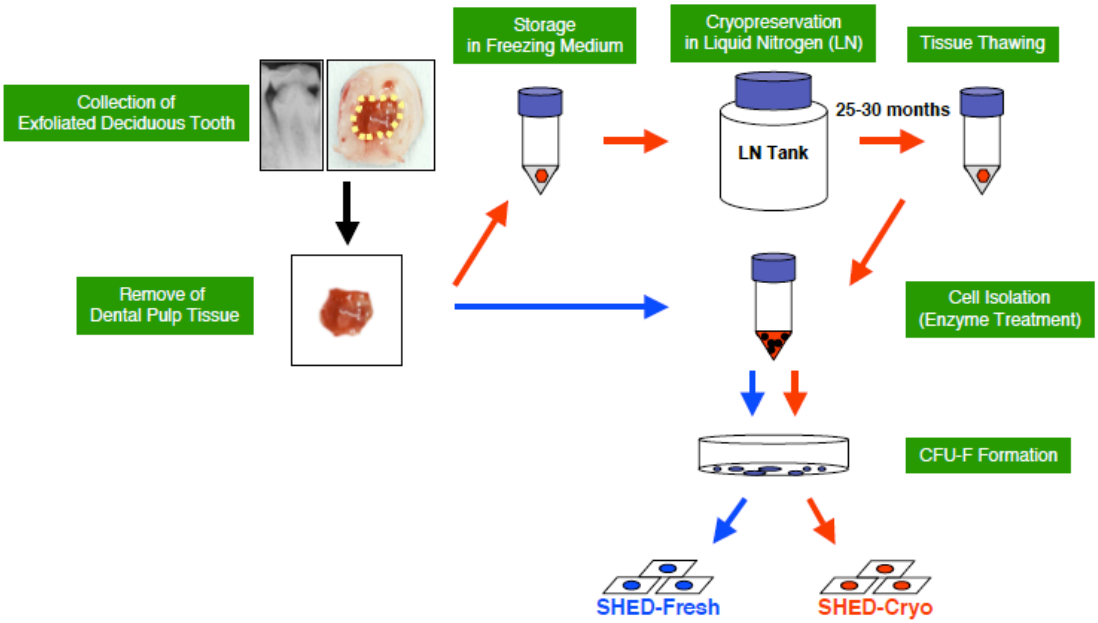


**Figure 1. A scheme of the cryopreservation and isolation of MSCs from dental pulp tissues of exfoliated deciduous teeth.** Deciduous dental pulp tissues in the remnant crown (yellow-dot circled region) were removed *en bloc* mechanically, stored in a freezing medium and preserved in a liquid nitrogen tank over 2 years. The frozen tissues were thawed at 37°C and treated with an enzyme solution. SHED-Cryo, as well as SHED-Fresh, were obtained by CFU-F method.

(Ma et al. PLoS One, 2012)

Flow cytometric analysis verified that SHED-Cryo were positive to STRO-1, CD146, CD73 and CD105 but negative to hematopoietic cell markers CD34, CD45 and CD14 (**Figure 2H**). SHED-Cryo were also positive to CD90 (over 95%) and the positive level in SHED-Cryo was similar to that in SHED-Fresh (data not shown). SHED-Cryo shared the immunophenotype with SHED-Fresh (**Figure 2I**). RT-PCR demonstrated that SHED-Cryo expressed genes for embryonic stem cells, *NANOG* and *OCT4*, and for neural crest cells, *NOTCH1*, *NESTIN* and *LNGFR* (**Figure 2J**), as seen in SHED-Fresh (**Figure 2K**). Expression of a neural crest cell marker, Nestin, was also detected in SHED-Cryo by flow cytometry (**Figure 2L**) and the expression in SHED-Cryo showed a similar level to that in SHED-Fresh (data not shown). Recent studies [22, 23] demonstrated the effect of cryopreservation on the expression of NANOG, OCT4 and Nestin in deciduous teeth stem

cells and may support, at least in partially, present cryopreserved effect of deciduous dental pulp tissues on SHED properties. Taken together, these data suggested that SHED-Cryo retained primitive MSC properties likely to SHED-Fresh.

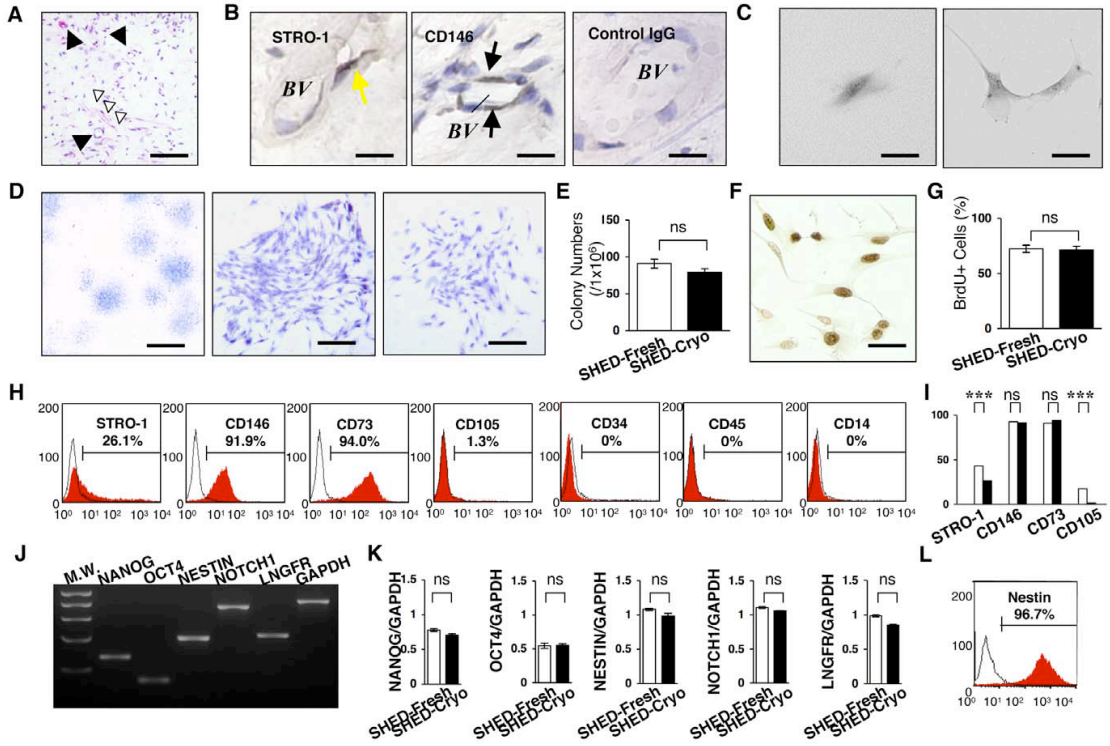


**Figure 2. Clonogenicity, cell proliferation capacity and stem cell marker expression of SHED-Cryo.** (**A**) Histology of cryopreserved dental pulp tissue of exfoliated deciduous teeth. Black arrowheads: blood vessel, white arrowheads: nerve fibers. H&E staining. (**B**) Localization of MSC markers in the cryopreserved deciduous pulp tissues. Yellow arrows: STRO-1-positive cells, black arrows: CD146-positive cells. *BV*: blood vessel, Control: subclass-matched antibody staining. (**C-E**) CFU-F assay. Formation of a clonogenic cell cluster from a single attached cell (**C**). Images of attached colonies of SHED-Cryo. Toluidine blue staining (**D**). Comparison of CFU-F number (**E**). (**F, G**) Cell proliferation assay. Immunostaining of BrdU-positive nuclei. (**F**). Comparison of cell proliferation (**G**). (**H, I**) Flow cytometry of MSC markers in SHED-Cryo. Representative histograms (**H**). Comparison of STRO-1, CD146, CD73 and CD105. Black columns: SHED-Cryo, white columns: SHED-Fresh (**I**). (**J, K**) Gene expression of embryonic stem and neural crest cell markers. MW: molecular weight markers (**J**). Comparative analysis of *NANOG*, *OCT4, NESTIN, NOTCH1* and *LNGFR* (**K**). (**L**) Flow cytometry of Nestin in SHED-Cryo. **A, B:** n=3. **C-L:** n=5 for all group. **A-E:** Bar= 30 µm (**A**), 5 µm (**B, C**, **F**), 1 mm (**D**, left) 25 mm (**D**, middle and right). **G, I, K:** ***$P$<0.005. ns: no significance. The graph bars represent mean±SD.

(Ma et al. PLoS One, 2012)

### 1.3.2 SHED-Cryo shows multipotency.

Four weeks after dentinogenic/osteogenic induction, SHED-Cryo were capable of forming Alizarin Red-positive nodules (**Figure 3A**). SHED-Cryo showed a high ALP activity (**Figure 3B**) and expressed odontoblast/osteoblast-specific genes *RUNX*2*, ALP*, *OCN*, and *DSPP* (**Figure 3C**) after the 1-week induction. SHED-Cryo expressed chondrocyte-specific genes for *SOX9*, *AGG* and *ColX* 3 weeks after chondrogenic culture (**Figure 3D**). SHED-Cryo expressed adipocyte-like phenotypes including accumulation of Oil red-O-positive droplets (**Figure 3E**) and expression of adipocyte-specific genes *LPL* and *PPARg2* (**Figure 3F**) 6 weeks after adipogenic induction. SHED-Cryo expressed albumin gene, one of hepatocyte-specific genes, 4 weeks after hepatogenic induction (**Figure 3G**). Immunofluorescence revealed that SHED-Cryo expressed endothelial cell markers CD31 and CD34 1 week after endothelial cell-induction (**Figure 3H**) and neural cell markers neurofilament M and tubulin bIII 3 weeks after neural cell-induction (**Figure 3I**). SHED-Cryo also exhibited similar capabilities of differentiating into odontoblasts/osteoblasts, adipocytes, chondrocytes, hepatocytes, endothelial cells and neural cells to SHED-Fresh (**Figure 3**). These data indicated that SHED-Cryo maintained multipotency as MSCs.

### 1.3.3 SHED-Cryo showed *in vivo* mineralized tissue regeneration.

Eight weeks after subcutaneous transplantation of SHED-Cryo with HA/TCP carriers into immunocompromised mice (**Figure 4**), dentin/pulp-like complex and bone/bone marrow-like structures were formed around the surface of HA/TCP by histological analysis (**Figure 5A**).

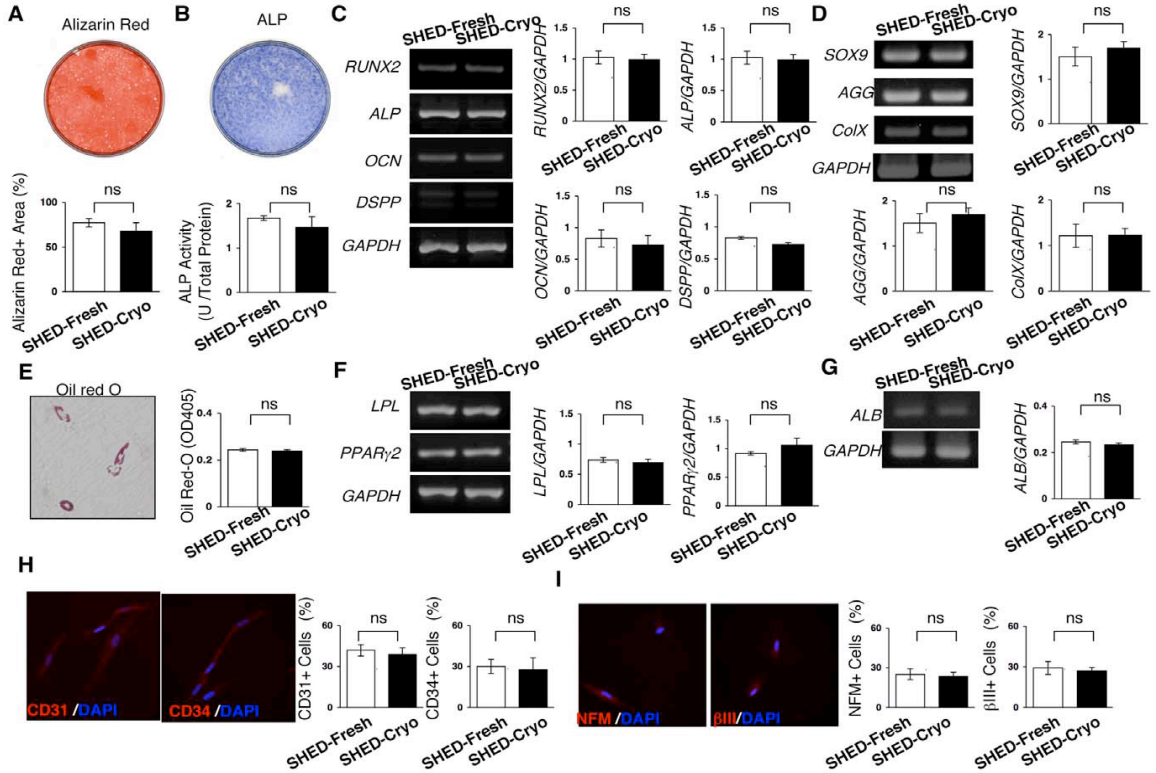


**Figure 3. Multipotency of SHED-Cryo.** (**A-C**) Dentinogenic/osteogenic differentiation capacity. Images of Alizarin Red staining (**A**) and ALP activity (**B**) of SHED-Cryo. Comparison of Alizarin Red-positive (Alizarin Red+) area (**A**), ALP activity (**B**) and odontoblast/osteoblast-specific genes, *RUNX, ALP, OCN, and DSPP* (**C**). (**D**) Chondrogenic differentiation capacity. Comparison of chondrocyte-specific genes, *SOX9*, *AGG* and *ColX*. (**E, F**) Adipogenic differentiation assay. Representative image of Oil Red-O staining and comparison of Oil Red-O accumulation (**E**). Comparison of adipocyte-specific genes *LPL* and *PPARgamma2* (**F**). (**G**) Hepatogenic differentiation capacity. Comparison of hepatocyte-specific gene *albumin (ALB)*. (**H**) Endothelial cell differentiation assay. Comparison of endothelial cell marker expression. (**H**) Neural cell differentiation assay. Comparison of neural cell markers. **A-I:** n=5 for all group. ns: no significance. The graph bars represent mean±SD.

(Ma et al. PLoS One, 2012)

Immunofluorescence showed that human mitochondria-positive cells were arranged on mineralized matrix (**Figure 5C**). Human specific STRO-1 and CD146 antibodies-positive cells were also detectable on the regenerated mineralized matrix (**Figure 5D**). On the other hand, control transplant-tissues that implanted only HA/TCP without SHED-Cryo did not express any mineralized tissue and human specific antibody-positive cells (**Figure 6**). Therefore these results suggested that SHED-Cryo were responsible cells for

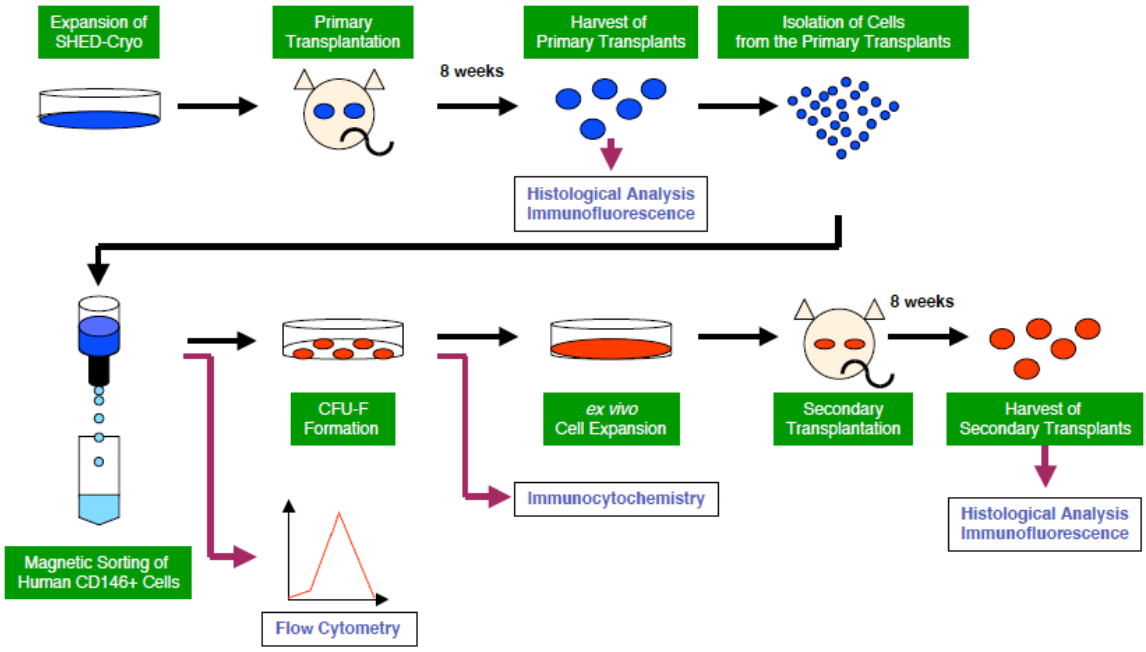


**Figure 4. A scheme of *in vivo* tissue regeneration and self-renewal assays of SHED-Cryo.** SHED-Cryo were subcutaneously transplanted with HA/TCP carrier into immunocompromised mice. Eight weeks after the implantation, the primary transplants were harvested. Some transplants were used for histological and immunofluorescent analyses. Cells were isolated from the other primary transplants and stained with human-specific CD146 antibody. Human CD146-positive cells were magnetically sorted. The purity of the cells was confirmed by flow cytometry as described in Materials and Methods. The CD146-positive cells were seeded at low density to obtain CFU-F-forming cells. The colony-forming cells were expanded and transplanted secondarily into immunocompromised mice. The secondary transplants were harvested 8 weeks after the implantation and analyzed morphologically.

(Ma et al. PLoS One, 2012)

mineralized tissue formation in the implant tissues. SHED-Cryo formed similar amount of the regenerated mineralized tissues when compared to SHED-Fresh (**Figure 5B**). These data indicated that SHED-Cryo retained a unique *in vivo* regenerative capacity likely to SHED-Fresh. Although the origin of bone marrow cells are host cells in bone marrow MSC-implants [24, 25], the origin of cells in bone marrow and dental pulp in SHED-implants have not been elucidated. Furthermore study will be needed to clarify the origin of the dental pulp cells and bone marrow cells in the SHED-implants in future.

### 1.3.4 SHED-Cryo retain self-renewal capability.

To evaluate self-renewal capability of SHED-Cryo, sequential transplantation, which is one of traditional and gold standard methods to identify the self-renewal capability of stem cells [17], was performed (**Figure 4**). CD146 is considered to be a critical cell surface marker for human MSCs [18]. Cell population was isolated from the primary implants and stained with human CD146 antibody. Human CD146 antibody-positive cells were purified by a magnet sorting system. Flow cytometric analysis confirmed that the sorted cells were positive to human CD146 (>95%) but negative to mouse CD146 (0%) (**Figure 5E**), evaluating the high purity of the sorting cells as human stem cells. When the sorted cells were seeded at low density, they were capable of forming CFU-Fs that exhibited positive to human CD146 by immunostaining (**Figure 5F**), indicating that the CD146-positive human cells maintained as intact MSCs in the transplant tissues after the long-term implantation. When the colony-forming cells were secondarily transplanted into immunocompromised mice for 8 weeks, the secondary implants contained similar dentin/pulp complex-like structures (**Figure 5G**) to the mineralized structural complexes in the primary transplants. Cells positive to anti-human CD146 or anti-human specific mitochondria antibodies were localized on the mineralized matrix (**Figure 5H**). Population doubling and telomerase activity are associated with self-renewal potential of stem cells [26]. Population doubling assay indicated a prolonged and time-limited cell proliferation in SHED-Cryo (**Figure 5I**). Telomerase activity test revealed the lower activity in SHED-Cryo (**Figure 5J**). Collectively, these results verified that SHED-Cryo represented a self-renewal capacity.

### 1.3.5 SHED-Cryo are heterogeneous population.

To identify the heterogeneity of SHED-Cryo, total 17 clonogenic single-colonies were acquired from a cryopreserved dental pulp tissue of exfoliated deciduous tooth. Each single-colony-derived SHED-Cryo showed various population-doubling score, diverse cell proliferation capacity and varied Alizarin red-positive area (**Figure 5K**). These findings indicated that SHED-Cryo displayed heterogeneous as seen in SHED-Fresh [10].

### 1.3.6 Immunomodulatory properties of SHED-Cryo *in vitro*.

To explore whether SHED-Cryo display immunomodulatory capacity to Th17 cells as seen in SHED-Fresh (**Figure 5L**) [13], SHED-Cryo were co-cultured with anti-CD3 and anti-CD28 antibodies-activated human $CD4^{+}CD25^{-}$ T cells under the stimulation with IL-6 and TGFb1. SHED-Cryo were able to inhibit both the differentiation of $CD4^{+}IL17^{+}IFNg^{-}$ Th17 cells and the secretion of IL-17 (**Figure 5L**), suggesting that SHED-Cryo maintained *in vitro* inhibitory effect on Th17 cells.

### 1.3.7 SHED-Cryo transplantation prolongs the life span and improves autoimmune disorder and renal dysfunction in MRL/*lpr* mice.

SLE-like autoimmune disorders appear around age 7-8 weeks in MRL/*lpr* mice and levels of Peripheral levels of autoimmune antibodies increase extremely from about 12 weeks of age in MRL/*lpr* mice. To evaluate the therapeutic potency of SHED-Cryo in severed SLE condition as seen in previous studies [13], SHED-Cryo were intravenously transfused to human SLE model MRL/*lpr* mice at the age of 16 weeks old (**Figure 7**). Kaplan-Meyer curve demonstrated that systemic SHED-Cryo-transplantation significantly prolonged the lifespan of MRL/*lpr* mice (**Figure 8A**). Mantel-Haenszel test evaluated that the median survival time was 155.0, 219.0 and 212.5 days in control, SHED-Fresh

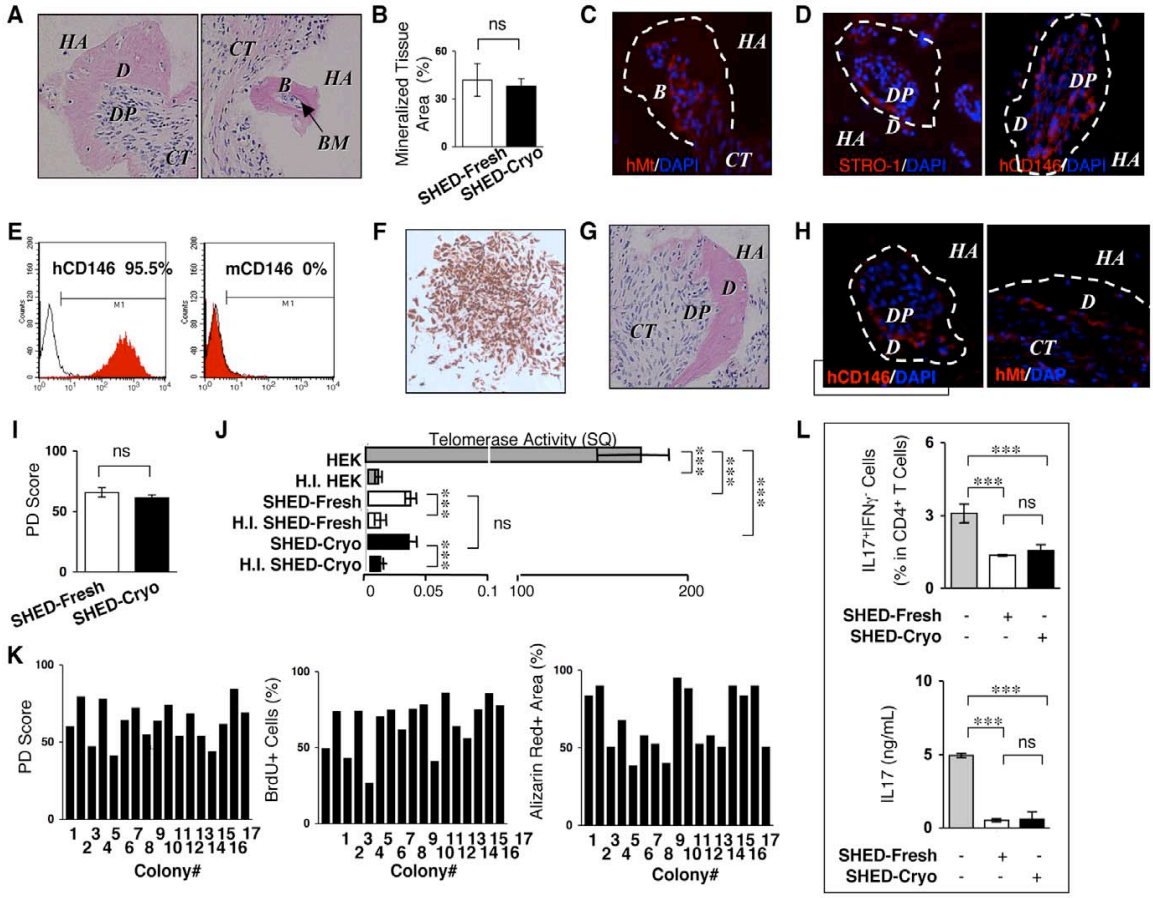


**Figure 5. Tissue regeneration capability, self-renewal potency, heterogeneity and *in vitro* immunomodulatory functions of SHED-Cryo.** (**A-D**) Images of primary transplant tissues of SHED-Cryo. H&E staining (HE) (**A**). Comparison of newly formed-mineralized tissue (**B**). Immunofluorescence with anti-human specific mitochondria (hMt) (**C**) and anti-STRO-1/human CD146 (hCD146) (**D**) antibodies. (**E, F**) Purity of hCD146 antibody-sorted cells from primary transplants. Flow cytometry with hCD146 and mouse CD146 (mCD146). (**E**). Immunocytochemistry with hCD146 antibody of sorted cell-derived CFU-F (**F**). (**G, H**) *in vivo* self-renewal assay. Images of secondary transplant tissues. H&E staining (**G**). Immunofluorescence with anti-hCD146/anti-Mt antibodies. (**H**). (**I**) Comparison of PD scores. (**J**) Comparison of telomerase activity. (**K**) Single-colony-derived cell assay with 17 single cell colonies from a cryopreserved deciduous pulp tissues. (**L**) *In vitro* direct immunosuppressive effects of SHED-Cryo on human Th17 cells. **A-J, L**: n=5 for all group. **A, C**, **D, F, H**: *B*: bone, *BM*: bone marrow, *CT*: connective tissue, *D*: dentin, *DP*: dental pulp, *HA*: HA/TCP, **I**: HEK: HEK293 cells, H.I. HEK: heat inactivated HEK, H.I. SHED-Cryo: heat inactivated SHED-Cryo, H.I. SHED-Fresh: heat inactivated SHED-Fresh. **C**, **D, H**: Dot lined areas: mineralized tissue. Nuclei are counterstained with DAPI. **B, H, I, L:** ***$P$<0.005, ns: no significance. The graph bars represent mean±SD.

(Ma et al. PLoS One, 2012)

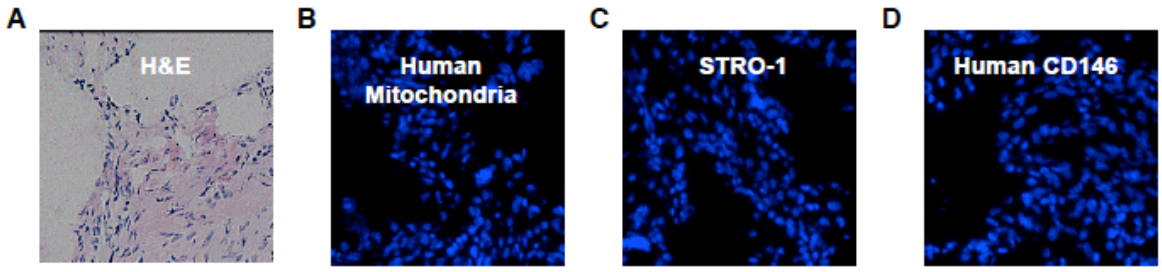


**Figure 6. Images of primary transplant tissues with HA/TCP alone. (A)** H&E staining (HE). **(B-D)** Immunofluorescence with anti-human specific mitochondria (hMt) **(B)**, anti-STRO-1 **(C)** and hCD146 **(D)** antibodies.
(Ma et al. PLoS One, 2012)

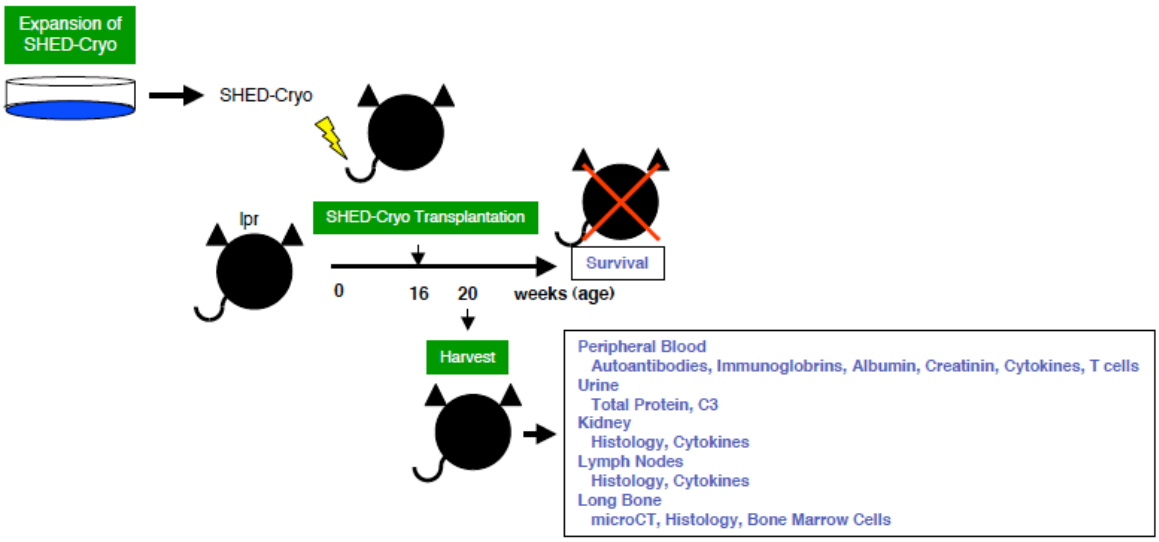


**Figure 7. A scheme of the transplantation of SHED-Cryo into MRL/*lpr* mice (*lpr*).** SHED-Cryo were infused into MRL/*lpr* mice via the tail vein at the age of 16 weeks. The mice were maintained until died for the survival assay. At 20-week-old, some mice were harvested and biological samples were collected to assess the therapeutic efficacy.
(Ma et al. PLoS One, 2012)

transplanted and SHED-Cryo-transplanted MRL/*lpr* mice, respectively. Elevated serum autoantibodies including ANA and anti-dsDNA IgG and IgM antibodies, which are critical clinical markers in human SLE therapy, were markedly decreased in SHED-Cryo transplanted MRL/*lpr* mice **(Figure 8B)**. Increased peripheral immunoglobulins including IgG1, IgG2a, IgG2b and IgM were also significantly reduced in SHED-Cryo-transplanted

mice (**Figure 9**). Histopathological analysis demonstrated that SHED-Cryo-transplantation prevented renal nephritis associated with hypercellularity, mesangial matrix hyperplasia and basal membrane disorder in MRL/*lpr* mice (**Figure 8C**). Immunofluorescence showed that complementary 3-deposition in glomeruli of the kidney in MRL/*lpr* mice was disappeared after SHED-Cryo-transplantation (**Figure 8C**). SHED-Cryo-transplantation elevated serum albumin level and reduced urine protein (**Figure 8D**), meanwhile, decreased serum creatinine in MRL/*lpr* mice (**Figure 8D**). SHED-Cryo-transplantation displayed similar therapeutic effects on the lifespan, autoantibody levels and renal function in MRL/*lpr* mice with SHED-Fresh-transplantation (**Figures 8 and 9**). These findings provided that SHED-Cryo retained therapeutic efficacy on MRL/*lpr* mice.

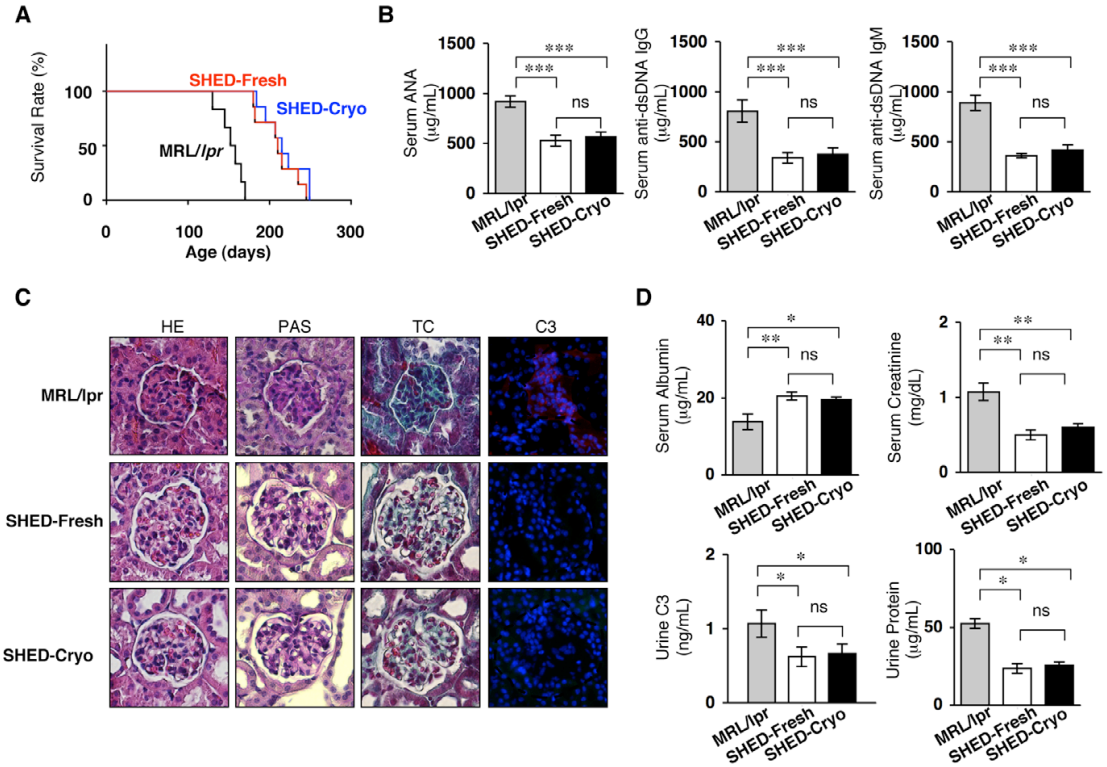


**Figure 8**. **Systemic SHED-Cryo-transplantation improves lifespan and SLE-like disorders in MRL/*lpr* mice.** (**A**) Kaplan-Meier survival curve of MRL/*lpr* mice. (**B**) ELISA of serum autoantibodies, ANA and anti-dsDNA IgG and IgM antibodies. (**C**) Histopathology of kidneys. *G* and dot-circled area: glomerular. HE: H&E staining, TC: Gomori trichrome staining, PAS: Periodic acid-Schiff staining, C3: Immunofluorescence of C3. DAPI staining. (**D**) Levels of serum albumin and creatinine and urine protein and C3. **A-D**: MRL/*lpr*: control group, SHED-Cryo: SHED-Cryo-transplant group, SHED-Fresh: SHED-Fresh-transplant group. **A**: n=7, **B-D**: n=5 for all group. **B, D**: **P*<0.05, ***P*<0.01, ****P*<0.005, ns: no significance. The graph bars represent mean±SD.

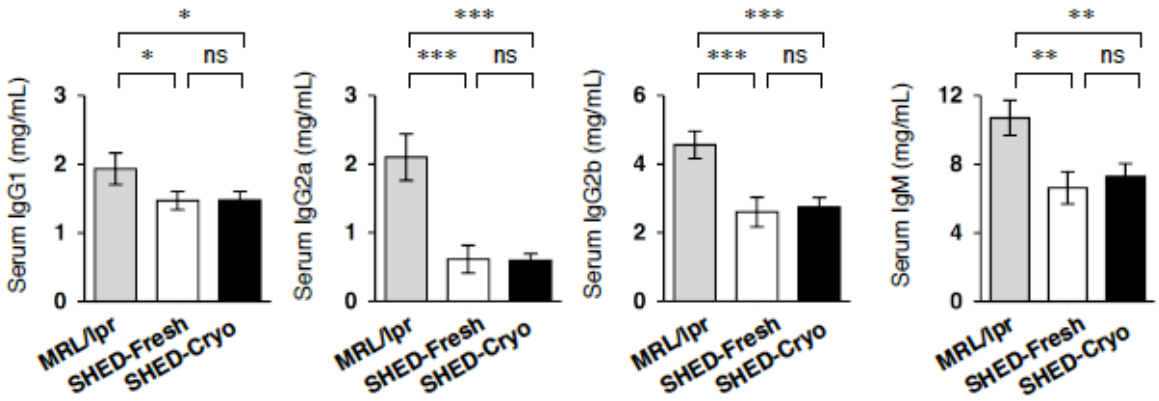


**Figure 9. Systemic SHED-Cryo-transplantation improves levels of serum immunoglobulins in MRL/*lpr* mice.** n=5 for all group. **P*<0.05, ***P*<0.01, ****P*<0.005, ns: no significance. The graph bars represent mean±SD. MRL/lpr: non-transplanted group, SHED-Fresh: SHED-Fresh-infused group, SHED-Cryo: SHED-Cryo-infused group.
(Figure 8-9: Ma et al. PLoS One, 2012)

### 1.3.8 Transplantation of SHED-Cryo suppresses peripheral Th17 cells in MRL/*lpr* mice.

Th17 cell regulation is a critical therapeutic strategy for SLE treatment [27]. The present study showed that the levels of peripheral Th17 cells and IL-17 were remarkably reduced in SHED-Cryo-received MRL/*lpr* mice at the age of 20 weeks old (**Figures 10A-10C**). This Th17-cell suppressive effect was similar to the effect of SHED-Fresh-transplantation on MRL/*lpr* mice (**Figures 10B and 10C**) [13], suggesting that SHED-Cryo maintained *in vivo* immunomodulatory functions.

### 1.3.9 Systemically infused SHED-Cryo home to lymph node and kidney in MRL/*lpr* mice and regulate the local immune microenvironment.

To assess the homing ability of SHED-Cryo into sites of tissue injury, CFSE-labeled SHED-Cryo were intravenously injected into MRL/*lpr* mice at the age of 16 weeks old. The high frequency of CFSE-positive SHED-Cryo was observed in the lymph nodes and kidneys, particularly in the glomeruli, on one day after the transplantation (**Figures 10D**

**and 11**). The frequency of CFSE-positive SHED-Cryo decreased gradually in both tissues from the 2nd day to 7th day after the transplantation (**Figures 10D and 11**). The localization of SHED-Cryo were similar to that of SHED-Fresh (**Figures 10D and 11**). The levels of inflammatory cytokines IL-17 and IL-6 in the lymph nodes and kidneys were significantly reduced in SHED-Cryo-transfused MRL/*lpr* mice, as well as SHED-Fresh-transfused mice, when compared to control MRL/*lpr* mice **(Figure 10E)**. Taken together, these *in vivo* studies suggested that SHED-Cryo were capable of homing to lesional sites and might improve the pathological environments of damaged tissues.

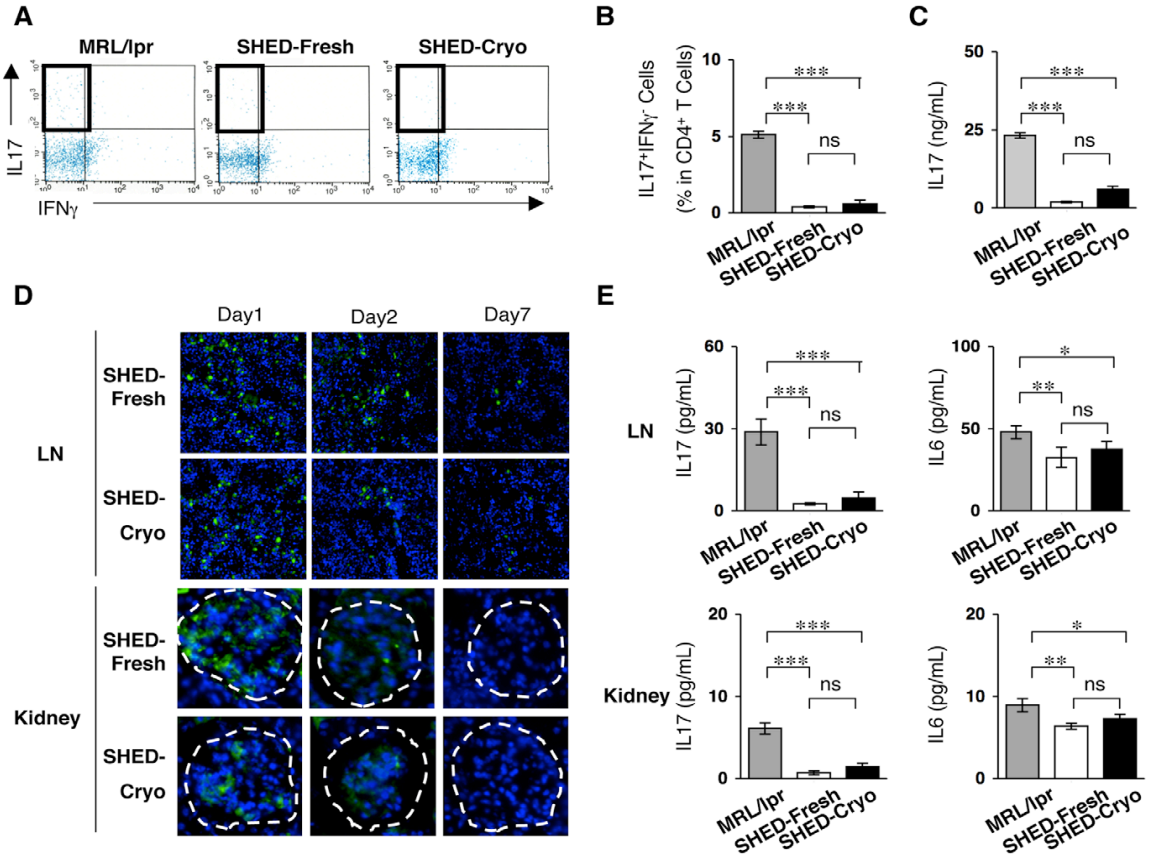


**Figure 10. SHED transplantation suppresses circulating and local levels of Th17 cells in MRL/*lpr* mice.** (**A, B**) Flow cytometry of peripheral $CD4^{+}IL17^{+}IFNg^{-}$ Th17 cells. (**C**) Serum levels of IL-17. (**D**) Homing of systemically infused CFSE-labeled SHED-Cryo and SHED-Fresh to lymph node (LN) and kidney of MRL/*lpr* Mice after 1- (Day 1), 2- (Day 2) or 7- (Day 7) day transplantation. Dot-circled area: glomerular. (**E**) ELISA of IL-17 an IL-6 levels in lymph node and kidney. **A**-**E**: n=5 for all group. MRL/*lpr*: control group, SHED-Cryo: SHED-Cryo-transplant group, SHED-Fresh: SHED-Fresh-transplant group. **B, C, E**: **P*<0.05, ***P*<0.01, ****P*<0.005, ns: no significance. The graph bars represent mean±SD.

(Ma et al. PLoS One, 2012)

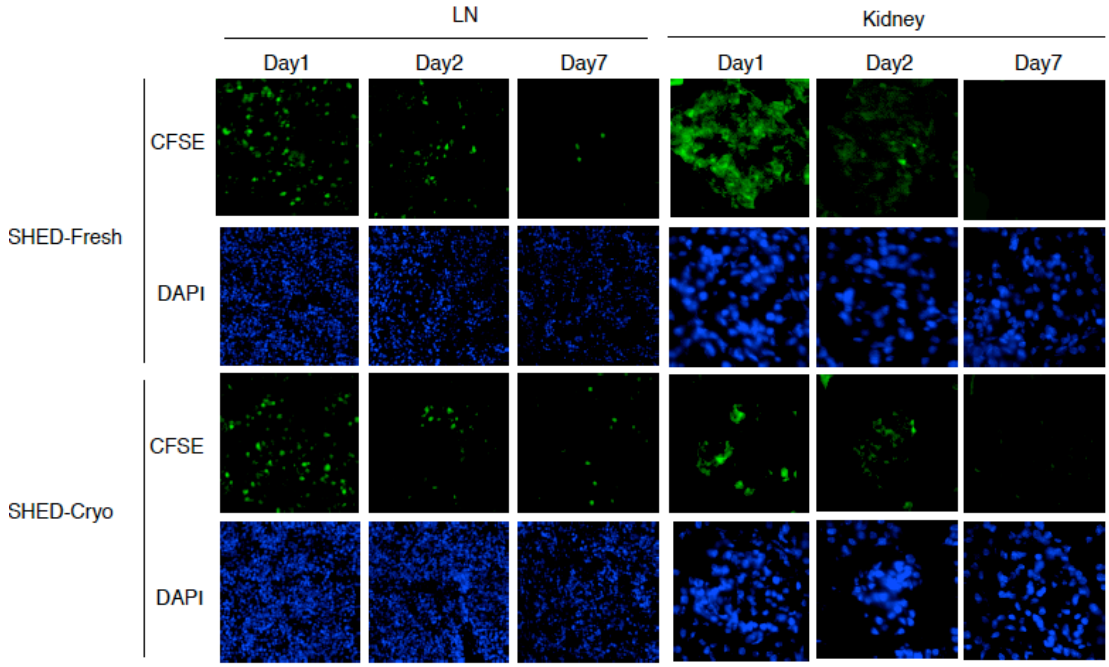


**Figure 11. Homing of systemically infused SHED-Cryo to lymph node and kidney of MRL/*lpr* Mice.** Images of CFSE-labeled SHED-Cryo and SHED-Fresh in lymph nodes (LN) and kidneys of MRL/*lpr* mice 1 (Day 1) or 7 (Day 7) days after the transplantation. SHED-Fresh: SHED-Fresh-infused group, SHED-Cryo: SHED-Cryo-infused group.
(Ma et al. PLoS One, 2012)

### 1.3.10 Systemic SHED-Cryo-transplantation improves osteoporotic skeletal disorder in MRL/*lpr* mice.

The homing ability of SHED-Cryo into bone sites were analyzed 1 day after the infusion into MRL/*lpr* mice at the age of 16 weeks old. The CFSE-positive SHED-Cryo was sparsely observed in the bone marrow space of MRL/*lpr* mice (**Figure 12**). The frequency of CFSE-positive SHED-Cryo was similar to that of SHED-Fresh (**Figure 12**). MRL/*lpr* mice expressed a remarkable osteoporotic bone-loss in their long bones (**Figures 13A-13D**). Systemic SHED-Cryo-transplantation was capable of increasing BMD and recovering trabecular bone structure in the long bones of MRL/*lpr* mice (**Figures 13A and 13B**). TRAP-positive cells were significantly reduced in the long bones of SHED-Cryo-infused group compared to the non-infused control group (**Figure**

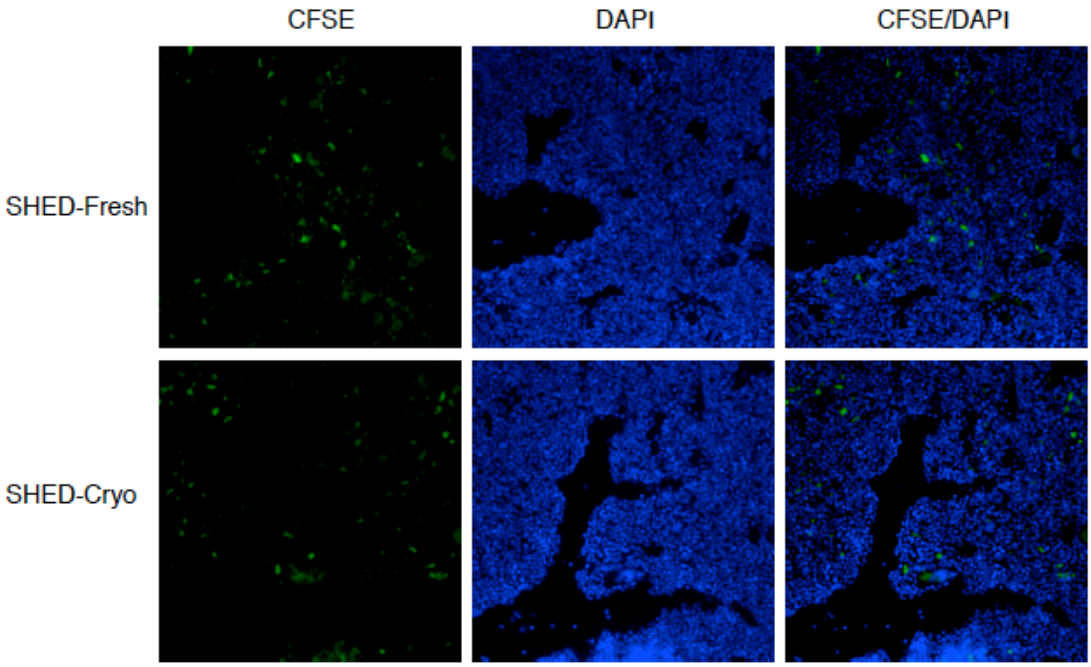


**Figure 12. Homing of systemically infused SHED-Cryo to bone of MRL/*lpr* Mice.** Images of CFSE-labeled cells in bone of MRL/*lpr* mice 1 (Day 1) or 7 (Day 7) days after the transplantation. SHED-Fresh: SHED-Fresh-infused group, SHED-Cryo: SHED-Cryo-infused group.

(Ma et al. PLoS One, 2012)

**13E**). SHED-Cryo-transplantation markedly reduced serum levels of sRANKL and CTX in MRL/*lpr* mice (**Figure 13F**). Flow cytometry revealed that $CD4^{+}IL\text{-}17^{+}IFNg^{-}$ Th17 cells were significantly reduced in bone marrow cells of SHED-Cryo- and SHED-Fresh-transplanted MRL/*lpr* mice compared to the control MRL/*lpr* mice (**data not shown**), suggesting that immunomodulatory functions of SHED-Cryo and SHED-Fresh may contribute to reduce the bone reduction in MRL/*lpr* mice. To examine *ex vivo* osteoclastogenesis and osteogenesis, BMCs were isolated from control, SHED-Fresh-transplanted and SHED-Cryo-transplanted MRL/*lpr* mice, termed control-, SHED-Fresh- and SHED-Cryo-BMCs, respectively. When BMCs were induced with M-CSF and sRANKL, the number of TRAP-positive multinucleated cells was significantly reduced in SHED-Cryo-BMCs than in control-BMCs (**Figure 13G**). Osteogenic analysis showed that Alizarin Red-positive area was shared larger in SHED-Cryo-BMCs than control-

BMCs (**Figure 13H**). SHED-Cryo-transplanted MRL/*lpr* mice expressed similar bone regenerative effects to SHED-Fresh-transplanted MRL/*lpr* mice (**Figure 13**). These data indicated that SHED-Cryo-transplantation improved osteoporotic disorder in MRL/*lpr* mice. Furthermore studies will be needed to evaluate the therapeutic mechanism of SHED to osteoporotic disorder in immune diseases likely SLE.

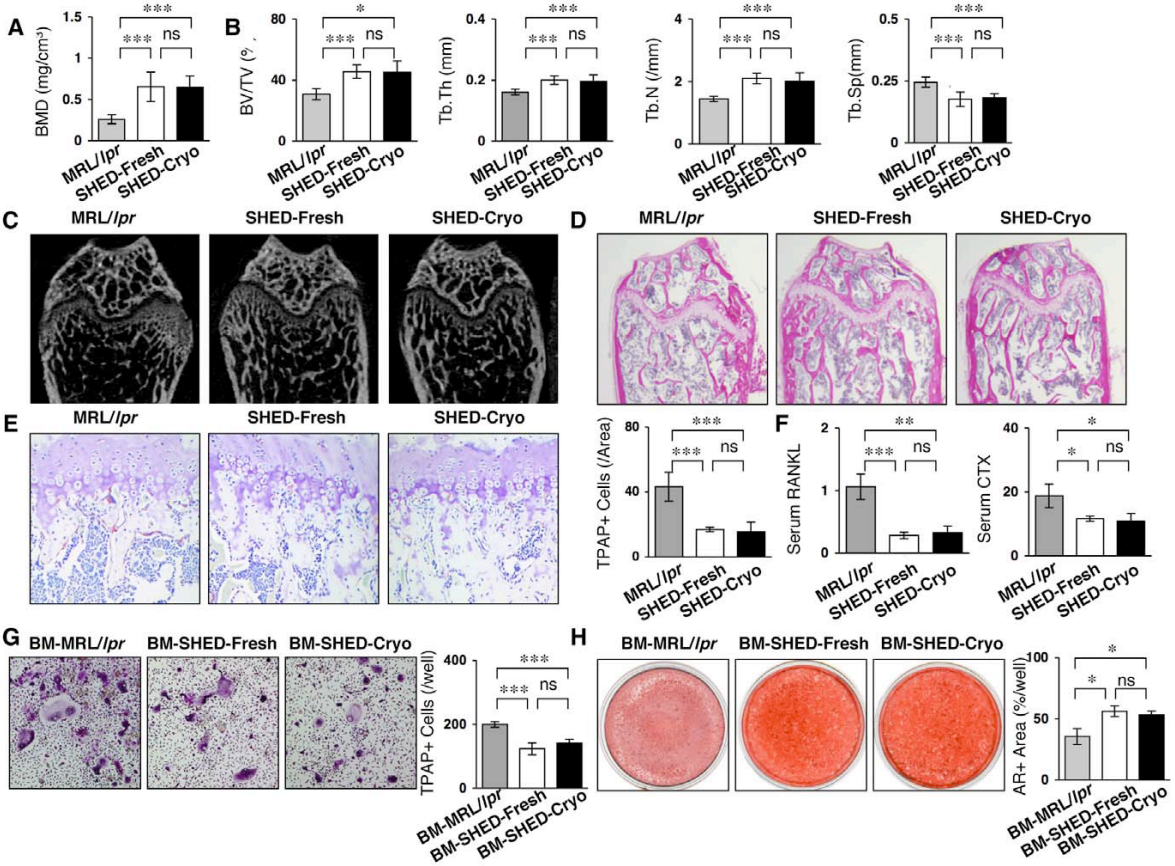


**Figure 13. SHED-Cryo transplantation ameliorates osteoporotic bone disorder in MRL/*lpr* mice. (A, B)** MicroCT analysis of tibiae. BMD (**A**). Trabecular parameters, BV/TV, Tb.Th, and Tb.N along with increased Tb.Sp (**B**). (**C, D**) MicroCT (**C**) and histological (**D**) images of trabecular bone structures of tibiae. H&E staining (**D**). (**E**, **F**) *In vivo* osteoclast activity. TRAP staining (**E**). ELISA of serum sRANKL and CTX (**F**). (**G**) *Ex vivo* sRANKL-induced osteoclastogenesis. TRAP+ cells: TRAP-positive osteoclast-like cells. (**H**) *Ex vivo* osteogenic capacity. Alizarin red-positive (AR+) area after four-week induction. **A-H:** n=5 for all groups. **A-F:** MRL/*lpr*: control group, SHED-Cryo: SHED-Cryo-transplant group, SHED-Fresh: SHED-Fresh-transplant group, **G, H:** BM-MRL/*lpr*: control MRL/*lpr* mice-derived bone marrow cells, BM-SHED-Cryo: SHED-Cryo-transplanted mice-derived bone marrow cells, BM-SHED-Fresh: SHED-Fresh-transplanted mice-derived bone marrow cells. **A, B, E, F:** **P*<0.05, ****P*<0.005 (vs. MRL/*lpr*). **G, H:** **P*<0.05, ***P*<0.01, ****P*<0.005 (vs. BM-MRL/*lpr*), ns: no significance. **A, B, E-H:** The graph bars represent mean±SD.

(Ma et al. PLoS One, 2012)

### 1.3.11 SHED-Cryo-implantation repairs the calvarial bone defects in immunocompromised mice.

From the present *in vivo* tissue regeneration capability of SHED-Cryo, we hypothesized that SHED-Cryo could regenerate bone tissues in bone defects, as seen in SHED-Fresh (**Figures 15A-15C**) [11]. We generated critical calvarial bone defects on immunocompromised mice and implanted SHED-Cryo with HA/TCP carrier onto the defect area (**Figure 14**).

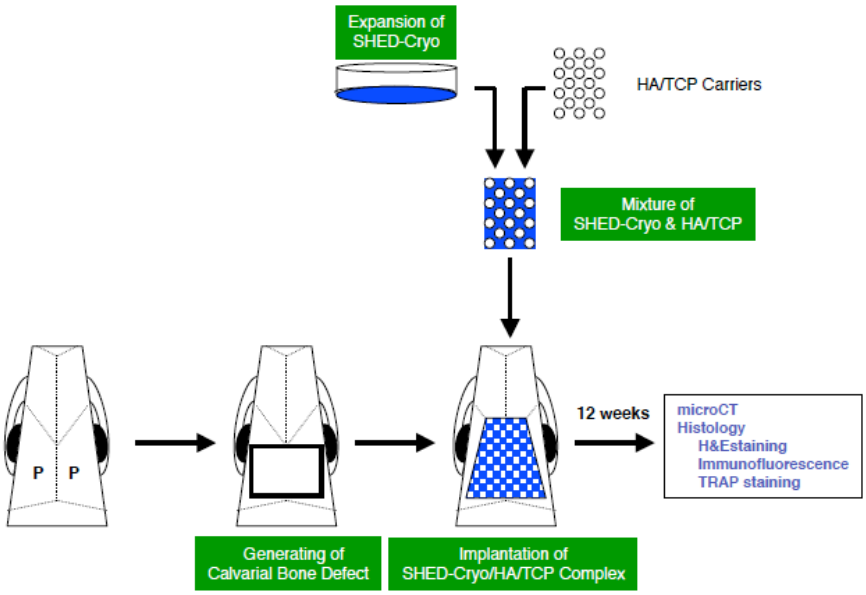


**Figure 14. A scheme of the transplantation of SHED-Cryo into calvarial bone defect of immunocompromised mice.** SHED-Cryo were expanded and mixed with HA/TCP carriers. Calvarial bones, especially parietal bone area (P), were removed to generate a bone defect on immunocompromised mice. SHED & HA/TCP mixtures were implanted to cover over the defect area. Twelve weeks after the implantation, the samples were harvested and analyzed by microCT and histology.
(Ma et al. PLoS One, 2012)

SHED-Cryo-implantation was able to regenerate the calvarial defects with a large amount of bone-like structures and bone-marrow-like components compared to implantation with only HA-TCP (**Figures 15A-15C**). The amount of regenerated bone and bone marrow at SHED-Cryo-implanted sites was similar to that at SHED-Fresh implanted sites (**Figures 15A-15C**). Immunofluorescence with anti-human CD146

antibody revealed that SHED-Cryo were responsible cells for bone regeneration in SHED-Cryo- and SHED-Fresh-implanted group, but not in HA/TCP-implanted group (**Figure 15B**). These findings suggested that SHED-Cryo and SHED-Fresh could be differentiated into bone-forming cells to contribute to repair the bone defect. A large number of TRAP-positive osteoclast-like cells were found in the regenerated bone tissues in SHED-Cryo-transplanted sites, as well as in that of SHED-Fresh-transplanted sites, but less in HA/TCP-transplanted sites (**Figure 15D**), suggesting that the regenerated bone tissues might indicate a physiological bone-remodeling ability by osteoclasts and osteoblasts. These data implied that SHED-Cryo were a useful cell source for tissue engineered bone regeneration. Implanted MSCs are impaired by host lymphocytes through secreting the pro-inflammatory cytokines IFNg and TNFalpha to suppress MSC-mediated bone regeneration [28]. On the other hand, deciduous teeth stem cells are capable of regenerating bone tissues in the calvarial defects of non-immunosuppressed rats [29]. Furthermore study will be necessary to clarify the kinetics of SHED under immunocompetent conditions for future clinical tissue engineering.

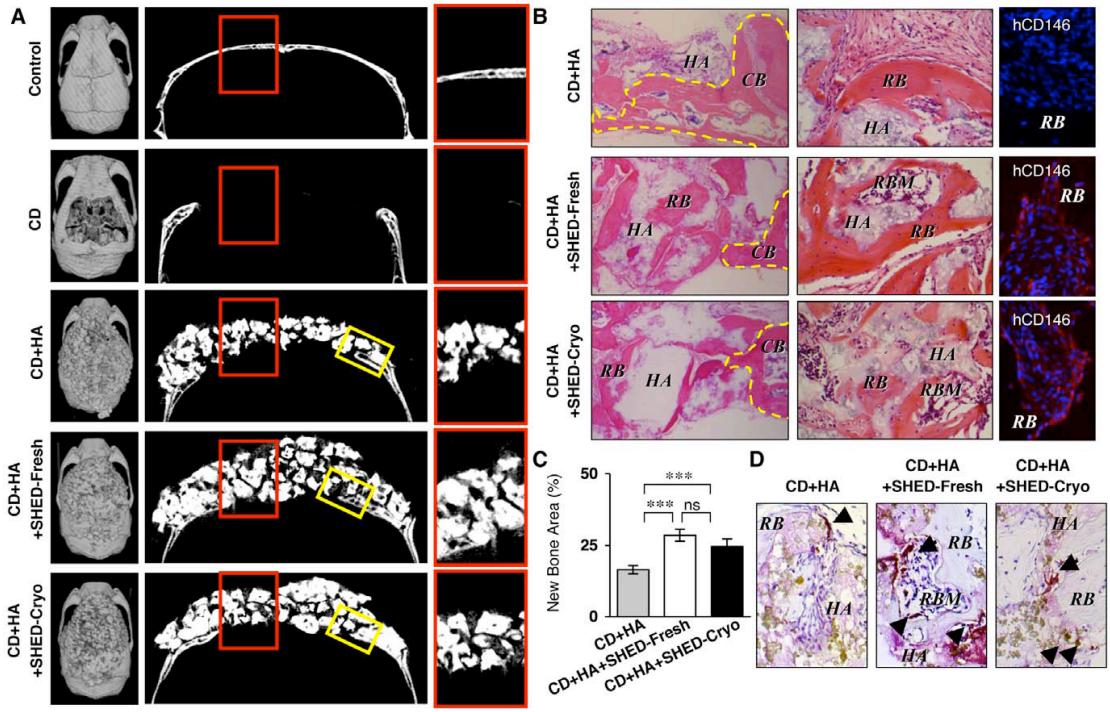


**Figure 15. SHED-Cryo are capable of repairing critical calvarial bone defects in immunocompromised mice.** (**A**) MicroCT images of mouse calvariae. Left panels: cranial images, middle panels: sagittal images, right panels: images of red-bowed area in riddle panels. (**B**) Histology of bone regeneration in mouse calvariae. Left panels: edge parts of the defect area (yellow-boxed area in Figure 7A). H&E staining; middle panels: middle parts of the defect area (red red-bowed area in Figure 7A). H&E staining; right panels: immunofluorescence with anti-human CD146 antibody (hCD146). DAPI staining. CB, yellow dot-circled area: calvarial bone, HA: HA/TCP, RB: regenerated bone, RBM: regenerated bone marrow. (**C**) Regenerated bone area in the defect area. (**D**) Distribution of osteoclasts. Arrowheads: TRAP-positive cells. TRAP staining. **A-D:** n=5 for all groups. Control: control (non-defect) group, CD: calvarial defect group, CD+HA: HA/TCP-implanted group, CD+HA+SHED-Fresh: SHED-Fresh-implanted group, CD+HA+SHED-Cryo: SHED-Cryo-implanted group. **C:** ***$P$<0.005, ns: no significance. The graph bars represent mean±SD.

(Ma et al. PLoS One, 2012)

## 1.4 DISCUSSION

Since SHED has been identified in dental pulp of deciduous tooth and characterized as MSCs [10], deciduous dental pulp tissues have been considered a promising stem cell source. SHED or deciduous teeth stem cells express multipotency into several lineage cells including of dentin/bone-forming cells [10, 30], endothelial cells [30], neural cells [10, 31] and myocytes [22] *in vitro* and *in vivo*. SHED or deciduous teeth stem cells were also applied for tissue-engineering in large animal models including bone defects, muscular dystrophy and dentin defects [12, 32-33], as well as small animal models including bone defect and spinal cord injury [11, 29, 34]. Recent study demonstrates *in vitro* immunomodulatory functions of SHED and evaluates the immune therapeutic efficacy on SLE-like model mice [13]. Herein, we demonstrated the feasibility of cryopreserved dental pulp tissue of human deciduous teeth in SHED-based bone tissue engineering and immune therapy. Our results indicate that long-term cryopreservation of human dental pulp tissues of deciduous teeth provides a great potential in future translational researches and clinical applications.

Postnatal stem cells have offered great promise to care diverse diseases. Besides HSCs have acquired outstanding and extensive success in a variety of human diseases such as leukemia, aplastic anemia and autoimmune diseases over half century [35, 36]. To date, MSCs also admit to regenerative medicine for GVHD [6], skeletal reconstruction [2, 3] and SLE [9]. Several challenges have remained to concern quality and safety in respective processes of MSC transplantation such as the cell processing and preserving *ex vivo*. Traditional bone marrow MSCs significantly reduced their frequency and multipotency donor-age-dependently [37-40]. Aspiration of bone marrow accompanies sever invasion to the donors possibly [41]. These significant disadvantages promote to seek alternative resources with accessible and least invasive approaches, and novel MSC

populations have been identified from various sources such as adipose tissue, cord blood and dental pulp [42-44]. While the isolation process of MSCs is intricate, clinically applicable processing for storing and banking of the resources can offer great advantages for MSC-based therapy as well as the reduction of the number of staffing required for cell processing. Cryopreservation of stem cells has provided several utilities such as long-term storage, adjusting a therapeutic cell dose, reducing contamination for safety and quality in the clinical applications [33, 45]. This approach has been used widely and successfully in bone marrow transplantation [46] and HSC transplantation [47]. Therefore, cryopreserved store and banking of MSC resources would be a variable, indispensable and practical approach for stem cell-based therapy.

SHED have been considered to be a primary promising source for regenerative medicine [10]. Exfoliated deciduous teeth represent the most easily, least invasively accessible and feasible resource because of their natural fate (exfoliation) and clinical abolition. SHED offered profound therapeutic efficacy to skeletal defects [11, 12] and autoimmune disease [13]. On the other hand, several tasks have remained to be solved in SHED processing and banking. It is generally hard to expect a chance of the exfoliating of deciduous teeth and to maintain the tissue activity of the interests for a while after the harvesting. In addition, isolation process of SHED accompanies with several complicated, arduous and time-consuming steps and attentive operations. Recent discoveries about functional MSCs recovered from cryopreserved intact dental pulp and periodontal ligament (PDL) tissues of adult human third molars suggest that the least minimal processing may be adequate for the banking of samples [48, 49]. Recovered MSCs after the cryopreservation can still maintain the immunomodulatory capacity *in vitro* [50, 51]. Deciduous teeth stem cells is known to maintain the stem cell property and multipotency after the long-term cryopreservation [22, 23]. In the present study, we firstly demonstrate

that stem cells are capable of recovering from human dental pulp tissues of exfoliated deciduous teeth after long-term (over 2 years) cryopreservation. The recovered SHED retained superior MSC properties such as self-renew, multipotency, *in vivo* dentin/bone-regeneration and *in vitro* immunomodulatory function. In addition, transplantation of SHED-Cryo showed critical therapeutic efficiency on both immune and skeletal disorders in MRL/*lpr* mice and bone defects in the calvariae of immunocompromised mice. Taken together, these data suggest that long-term cryopreservation of dental pulp tissues of deciduous teeth is an innocuous and designable approach for clinical banking of stem cells and gives great advantages in immune therapy and bone tissue engineering of regenerative medicine. Furthermore, the present pulp tissue banking system could allow children and their parents to return the “baby teeth” bodies as the most precious souvenirs to the children's growing.

Current studies indicate that the biological recovery of the PDL stem cells and adult DPSCs are inferior to the freshly isolated stem cells after the cryopreservation of PDL tissues [49] and adult teeth [48]. Whereas, cryopreserved stem cells from apical papilla (SCAP) show a similar biological and immunomodulatory functions to freshly isolated SCAP [50]. Apical papillae have a responsibility to form and extend tooth roots at the developing stage [52, 53], indicating that apical papillae are an active tissue biologically. Cryopreserved deciduous teeth stem cells can also maintain the stem cell property and multipotency [22, 23]. The present study demonstrated that cryopreservation of deciduous dental pulp did not affect the biological and immunological properties of SHED. Moreover, SHED show higher cell proliferation capability than adult DPSCs [10], suggesting that deciduous pulp tissues maintain greater biological activity than adult dental pulp tissues. The discrepancy of the functionally recovery efficiency among deciduous dental pulps, adult PDLs and adult dental pulps after the cryopreservation

might depend on the age and/or potential activity of donor samples, supporting the feasibility of the cryopreservation of deciduous dental pulp tissues.

In conclusion, present cryopreservation of dental pulp tissues of human exfoliated deciduous teeth does not affect on the biological, immunological and therapeutic functions of SHED. Therefore, cryopreserved approach of deciduous dental pulp tissues not only serve as a most clinically desirable banking approach, but also provide sufficient number of SHED for critical therapeutic benefits to stem cell-based immune therapy and tissue engineering in regenerative medicine.

# PART II

# SHED-based Therapy Ameliorates Osteoporosis Secondary in MRL/*lpr* Mice through Interleukin-17-impaired Endogenous Bone Marrow Mesenchymal Stem Cells

## 2.1 INTRODUCTION

Osteoporosis is the most common bone disease and defined as a reduction of bone strength [54]. The bone loss is not only primary related with age or postmenopausal, but also secondary affected by the underlying risk factors such as deficiencies, diseases or drugs [55]. SLE is a refractory and chronic multiorgan-autoimmune disease. As recent medical advancements have successfully elongated the lifespan of patients with SLE, many clinical researchers put more attention to the organ damages associated with the systemic chronic inflammation and/or the long-term medications for the quality of life [56]. Osteoporosis secondary frequently occurs in SLE patients and cause fragility fracture to scare their life [57]. Unfortunately, the safety and efficient treatments for SLE-associated osteoporosis have not been developed.

MSCs are typical adult stem cells with capabilities of self-renew and multipotency [58]. Recent studies have been elucidated that MSCs express immunomodulatory effects on immune cells [59,60], and MSC-based cell therapy has been greatly focused on the treatment of various immune diseases such as acute GVHD [6] and inflammatory bowel disease [61]. Previous allogeneic transplantation of hBMMSCs and human umbilical cord-derived MSCs (UCMSCs) governs a successful therapeutic efficacy on refractory SLE patients [9,62-63]. SHED, as we discussed in Part I, is a promising stem cell choice for clinical treatment. However, it has been unclear whether SHED-transplantation gives a treatment efficacy to the skeletal disorders in SLE patients.

MRL/*lpr* mice are well known to express human SLE-like disorders including short lifespan, abundant autoantibodies, glomerulonephritis and breakdown of self-tolerance [64]. MRL/*lpr* mice also exhibit severe trabecular bone reduction associated with excessive osteoclastic bone resorption and limited osteoblastic bone formation [9]. Currently, systemic transplantation of human MSCs including BMMSCs, UCMSCs,

SHED, and human supernumerary tooth-derived stem cells improve the primary autoimmune disorders such as elevated autoimmune antibodies, renal dysfunction and abnormal immunity in MRL/*lpr* mice [13,65-68]. In addition, the SHED-transplantation showed similar therapeutic recovery to the bone loss in MRL/*lpr* mice with hBMMSC-transplantation [13,67], indicating that this xenogenic transplant system of SHED into MRL/*lpr* mice might be a potential therapeutic approach for SLE patients who suffer from secondary osteoporosis. Unfortunately little has been understood about the SHED-mediated therapeutic mechanism to the skeletal disorder in MRL/*lpr* mice.

Osteoporosis is led by the disruption of the balance between the formation and resorption of bone associated with abnormal development of osteoclasts and osteoblasts. Increasing evidences have shown that BMMSCs from both SLE patients and SLE model MRL/*lpr* mice exhibited the reduced bone-forming capacity in vitro and in vivo [9,69]. Therefore osteogenic deficiency of endogenous BMMSCs might explain the origin of osteoporosis in SLE, speculating impaired BMMSCs might be a therapeutic target to the osteoporosis. However, little is known how endogenous BMMSCs are damaged functionally and how MSC-transplantation restores the reduced bone formation via endogenous BMMSCs in the bone marrow under SLE condition. Herein, we used MRL/*lpr* mice to examine the therapeutic efficacy and mechanism of systemically transplanted SHED, as well as transplanted hBMMSCs, on the secondary osteoporotic disorders in SLE. Moreover, we especially focused on the pathological and clinical responsibilities of endogenous BMMSCs for dysregulating bone metabolism through osteoblasts and osteoclasts in the inflammatory bone disorder in SLE.

## 2.2 MATERIALS AND METHODS

### 2.2.1 *Human subjects*

Human exfoliated deciduous teeth were obtained as clinically discarded biological samples from five patients (5-7-year-old) at Department of Pediatric Dentistry of Kyushu University Hospital under the approval by the Kyushu University Institutional Review Board for Human Genome/Gene Research (Protocol Number: 393-01). We obtained written informed consent from all the children's parents on the behalf of the children participants. Human bone marrow cells were purchased from AllCells (Barkley, CA).

### 2.2.2 *Mice*

C57BL/6J-*lpr/lpr* mice (female, 8 week-old) and pregnant and young-adult C57BL/6J mice (female, 8 week-old) were purchased from Japan SLC. (Shizuoka, Japan) and CLEA Japan (Tokyo, Japan), respectively. All animal experiments were approved by the Institutional Animal Care and Use Committee of Kyushu University (Protocol Number: A21-044-1).

### 2.2.3 *Human MSCs isolation and culture*

Human MSCs were isolated based on adherent CFU-F method [15]. Bone marrow cells (AllCells) were seeded at $10x10^6$/flask on T-75 culture flasks as previously [25]. According to previous reports [13], dental pulp tissues of human exfoliated deciduous teeth were minced and digested with 0.3% collagenase type I (Worthington Biochemicals, Lakewood, NJ) and 0.4% dispase II (Sanko Junyaku, Tokyo, Japan) for 60 min at $37^oC$. Single cell suspensions were obtained by passing through a 70-μm cell strainer (BD Bioscience, San Jones, CA) and seeded at $1x10^6$/flask on T-75 culture flasks. After 3 hours, non-adherent cells were removed by washing with PBS. Adherent cells were

cultured at 37$^{o}$C in 5% $CO_2$. The growth medium contained 15% FBS (Equitech-Bio, Kerrville, TX), 100 mM L-ascorbic acid 2-phosphate (Wako, Osaka, Japan), 2 mM L-glutamine (Nacalai, Kyoto, Japan), 100 U/ml penicillin and 100 mg/ml streptomycin (Nacalai) in alphaMEM (Invitrogen, Carlsbad, CA). After 14-16 days, adherent colonies-forming cells are passed and sub-cultured. The growth medium was changed twice a week.

To determine the isolated cells as MSCs, the cultured P3 cells ($100x10^3$/100 ml) were stained with specific antibodies to stem cell markers (each 1 mg/ml) (eBioscience, San Diego, CA), and the positive cell number was analyzed on FACSVerse flow cytometer (BD Biosciences). The numbers were determined by comparison with the corresponding control cells stained with corresponding subclass-matched antibody in which a false-positive rate of less than 1% was accepted. Each isolated cells were positive to CD73, CD90, CD105 and CD146 and negative to CD11b, CD14, CD35 and CD45 (data not shown). Furthermore, each P3 cells were cultured under osteogenic, chondrogenic and adipogenic conditions [67, 68], and expressed capacities of differentiating into osteoblasts (odontoblasts in case of SHED), chondrocytes and adipocytes (data not shown). These findings proved our isolated cells as MSCs based on the standard MSC criteria [70].

### 2.2.4 *Systemic MSC transplantation into MRL/lpr mice*

Cultured human MSCs (P3) of hBMMSCs and SHED were removed and washed with PBS 3 times. The donor cells ($0.1x\ 10^6$/10g body weight) were intravenously infused into MRL/*lpr* mice via the right cervical vein at ages of 16 weeks according to previous method [13]. The mice were harvested at the age of 20 weeks. Age-matched MRL/*lpr* mice receiving PBS were used as controls.

### 2.2.5 *ELISA of biological (blood serum, bone marrow) and culture (culture supernatant) samples*

CTX, IL-17 and sRANKL in the samples were measured by using ELISA kits (IL-17, sRANKL: R&D Systems, Minneapolis, MN; CTX, Nordic Bioscience Diagnostics A/S, Herlev, Denmark).

### 2.2.6 *Micro-computed tomographic bone analysis*

Femoral bones of mice were analyzed by microCT with Skyscan 1076 microCT system (Skyscan, Kontich, Belgium) [19]. Density values were calibrated using hydroxyl apatite phantoms (BMD values of 0.25 and 0.75 g/cm$^3$, Skyscan). BMD and bone structural indices (BV/TV, Tb.Th, Tb.N, Tb.Sp, and Tb.Spac) were calculated.

### 2.2.7 *Histological bone analysis*

Tibiae were fixed with 4 % PFA in PBS and decalcified with 10 % EDTA. Paraffin sections were cut into 6 mm-thick sections, and stained with H&E or TRAP staining [25]. Numbers of osteoblasts per bone surface were counted on five representative images [24]. TRAP-positive cell-number per total bone area in the bone metaphysis was analyzed on five representative images by NIH Image-J. For immunofluorescence, frozen sections were cut into 6-mm-thick sections. The cryosections were treated with non-immune IgG and reacted with anti-mouse IL-17 antibody (Santa Cruz, Santa Cruz, CA) or the subclass-matched antibody. The sections were stained with CF 633-conjugated-secondary antibody (Biotium, Hayward, CA) and DAPI (Dojindo).

### 2.2.8 *In vivo tracing of human MSCs*

MSCs ($10x10^6$) were incubated with 10 mM CFSE (Invitrogen) in PBS for 10 min at 37°C. The CFSE-labeled MSCs ($1x10^6$ per mouse) were intravenously infused into MRL/*lpr* mice at the age of 16 week old. One or seven days after the infusion, long bones were fixed with 4% PFA in PBS and decalcified with 10% EDTA. The frozen sections were cut and stained with DAPI (Dojindo, Kumamoto, Japan).

### 2.2.9 *Assay for Th17 cells in mouse bone marrow*

Mouse BMCs from mouse long bones (femurs and tibias) were treated with 0.82% $NH_4Cl$ in PBS for 15 min at room temperature. BMCs ($0.1x10^6$ per 100 ml) were incubated with PerCP-conjugated anti-CD4 antibody (1 mg) (eBioscience) and treated with R-PE-conjugated anti-IL-17 (eBioscience) and APC-conjugated IFNg (eBioscience) antibodies (each 1 mg). As controls, the isotype-matched antibodies were used. The number of $CD4^+IL\text{-}17^+IFNg^-$ Th17 cells (per $10x10^3$) was measured on FACSVerse (BD Biosciences).

### 2.2.10 *Culture and Stimulation of mouse BMCs*

BMCs were cultured in Dulbecco's Modified Eagle's Medium (DMEM, Nacalai) supplemented with 10% FBS (Equitech-Bio), 50 μM 2-mercaptoethanol (Invitrogen), 10 mM HEPES (Nacalai), 1 mM sodium pyruvate (Nacalai), 1% non-essential amino acid (Nacalai), 2 mM L-glutamine (Nacalai), 100 U/ml penicillin and 100 mg/ml streptomycin (Nacalai) with plate-bound anti-CD3 (eBioscience) (1 mg/ml) and soluble anti-CD28 (eBioscience) (1 mg/ml) antibodies on 24-well multiplates. The conditioned medium (CM) was collected and enriched tenfold.

### 2.2.11 *Isolation and culture of mouse BMMSCs*

Mouse BMMSCs were isolated based on CFU-F method [19]. BMCs were seeded at 10-20 x $10^6$ into 100 mm culture dishes. After 3 hours, they were washed with PBS twice to eliminate the non-adherent cells and the attached cells were cultured for 14-16 days. Attached colonies consisting of spindle-shaped cells were observed under a microscope. The colonies-forming attached cells were passed once. Cells were cultured with 20% FBS (Equitech-Bio), 2 mM L-glutamine (Nacalai), 55 μM 2-mercaptoethanol (Invitrogen), 100 U/ml penicillin and 100 μg/ml streptomycin; (Nacalai) in a-MEM (Invitrogen). Based on the MSC criteria [70], the colonies-forming cells were determined as previously [71]: 1) Flow cytometry demonstrated the immunophenotype of them positive to CD73, CD105, CD146, Sca-1 and SSEA-4 and negative to CD14, CD34 and CD45; 2) Mouse BMMSCs were evaluated to differentiate into osteoblasts, chondrocytes and adipocytes under corresponding specific culture conditions.

### 2.2.12 *CFU-F assay*

BMCs ($1.5x10^6$/flask) were seeded on T-25 flasks (Nunc). After 3 hours, the flasks were washed with PBS and cultured. After 16 days, they were treated with 2% PFA and 1% toluidine blue solution. Cell clusters containing $\geq$50 cells were recognized as a colony under a light microscopy. Total colony numbers were counted per flask.

### 2.2.13 *Population doubling assay*

Cells seeded on T-75 culture flasks (BD Biosciences) reached at sub-confluent condition, and passed. These steps were repeated until they lost the dividing capability. The PD score was calculated at every passage according to the equation: $\log_2$ (number of final harvested cells/number of initial seeded cells) and determined by the total score.

### 2.2.14 *Proliferation assay of mouse BMMSCs*

Mouse BMMSCs (10 x $10^3$/well) were seeded on 8-well chamber slides, incubated with BrdU solution (1:100) (Invitrogen) for 20 hours, and stained with a BrdU staining kit (Invitrogen). BrdU-positive cell number was calculated as a percentage to the total cell number on ten images per subject.

### 2.2.15 *In vitro osteogenic capacity of mouse BMMSCs*

Mouse BMMSCs were cultured under the osteogenic condition. The osteogenic medium consisted of 20% FBS (Equitech-Bio), 2 mM L-glutamine (Nacalai), 55 μM 2-mercaptoethanol (Invitrogen), 100 mM L-ascorbic acid 2-phosphate (WAKO), 2 mM b-glycerophosphate (Sigma), 10 nM dexamethasone (Sigma, St. Louis, MO) and 100 U/ml penicillin and 100 mg/ml streptomycin (Nacalai) in aMEM (Invitrogen) with or without CM of mouse BMCs, 10 nM recombinant mouse IL-17 (R&D Systems) and 1 mg/mL anti-mouse IL-17 antibody (R&D Systems). Four weeks after the induction, Alizarin Red-positive area was quantified by using NIH Image-J [25]. Furthermore, one-week after the inductions osteoblast-specific genes were analyzed.

### 2.2.16 *In vitro osteoclast assay*

Mouse BMCs (1x$10^6$/well) were co-cultured for 7 days with mouse calvarial cells or BMMSCs (each 0.1x$10^6$/well) pretreated with or without CM of mouse BMCs, 10 nM recombinant mouse IL-17 (R&D Systems) and 1 mg/mL anti-mouse interleukin IL-17 antibody (R&D Systems) for 3 days. The CM that enriched tenfold was mixed with the growth medium at the ratio of 1:9. Mouse calvarial cells were isolated from 2-3 day-old wild type C57BL/6 mice with a sequential enzyme treatment [19]. The osteoclastogeic medium contained 10% FBS (Equitech-Bio), 100 U/ml penicillin and 100 mg/ml

streptomycin (Nacalai), 10 nM vitamin $D_3$ (Wako) and 1 nM prostaglandin $E_2$ (Wako) in aMEM (Invitrogen). TRAP-positive multinucleated cells (>3 nuclei) were determined as osteoclast-like cells [19]. Osteoclast-specific genes were also assayed.

### 2.2.17 *Osteoblast- and osteoclast-specific gene analysis by RT-PCR*

Total RNA was isolated from the cultures using TRIzol (Invitrogen) and digested with DNase I. The cDNA was synthesized from 100 ng of total RNA using Superscript III (Invitrogen). PCR was performed using gene specific primers and Platinum PCR supermix (Invitrogen). Each amplified PCR product (5 μl) was analyzed by 2% agarose gel electrophoresis and visualized by ethidium bromide staining. The intensity of bands was measured by NIH Image-J software and normalized to *GAPDH*. The specific PCR primer pairs were summarized in **Table 3**.

### 2.2.18 *Induction assay of human IL-17-producing Th17 cells*

Human Th17 cells were induced as previously reported (Yamaza et al., 2010). Human CD4+CD25- naïve T lymphocytes ($1x10^6$ per well) were magnetically sorted from human PBMNCs (AllCells) using CD4+CD25+ regulatory T cell isolation kit (Miltenyi Biotec, Auburn, CA) and activated by plate-bounded anti-CD3 (5 mg/ml) (eBioscience) and soluble anti-CD28 (1 mg/ml) (eBioscience) antibodies for 3 days. The activated T cells were loaded on the MSC cultures ($20x10^3$ per well) with human transforming growth factor b1 (TGF-b1) (2 mg/ml) (R&D Systems) and interleukin 6 (IL-6) (50 mg/ml) (R&D Systems) for 3.5 days. Floating cells ($1x10^6$) were incubated with PerCP-conjugated anti-CD4, FITC-conjugated anti-CD8a, followed by the treatment with R-PE-conjugated anti-IL-17 and APC-conjugated anti-IFNg antibodies using a Foxp3 staining buffer kit (eBioscience) as previously (Yamaza et al., 2010), and then analyzed CD4+IL17+IFNg-

cells as TH17 cells on FACSVerse flow cytometer (BD Biosciences) by using FACSuit software (BD Biosciences). Collected supernatants were collected for further analysis.

**Table 3. List of primer pairs in Part II**

*ALP* (GenBank accession no. X14390)
sense: 5'-ACGTGGCTAAGAATGTCATC-3' (nucleotide 322-341)
antisense: 5'-CTGGTAGGCGATGTCCTTA-3' (779-797)

*calcitonin receptor* (NM_001042725)
sense: 5′-ACCGACGAGCAACGCCTACGC-3′ (1116-1136)
antisense: 5′-GCCTTCACAGCCTTCAGGTAC-3′ (1367-1387)

*cathepsin K* (NM_007802.3)
sense: 5′-GGAAGAAGACTCACCAGAAGC-3′ (138-158)
antisense: 5′-GTCATATAGCCGCCTCCACAG-3′ (580-600)

*GAPDH* (M33197)
sense: 5′-AGCCGCATCTTCTTTTGCGTC-3′ (12-32)
antisense: 5′-TCATATTTGGCAGGTTTTTCT-3′ (807-827)

*NFATC1* (NM_001164112)
sense: 5′-CTCGAAAGACAGCACTGGAGCAT-3′ (1023-1045)
antisense: 5′-CGGCTGCCTTCCGTCTCATAG-3′ (1339-1359)

*OCN* (X53698)
sense: 5′-CATGAGAGCCCTCACA-3′ (18-33)
antisense: 5′-AGAGCGACACCCTAGAC-3′ (316-332)

*RUNX2* (L40992)
sense: 5′-CAGTTCCCAAGCATTTCATCC-3 (880–900)
antisense: 5′-TCAATATGGTCGCCAAACAG-3′ (1304–1323).

### 2.2.19 Biochemical assay of biological (blood serum and urines) and culture (culture supernatant) samples

Albumin, anti- dsDNA IgG and IgM antibodies, ANA, and IL-17 in biological and culture samples were measured by using ELISA kits (Albumin, IL-17: R&D Systems; anti-dsDNA antibodies and ANA: Alpha Diagnostic, San Antonio, TX). Serum creatinine and urine

protein was assayed by using creatinine parameter assay kit (R&D Systems) and Bio-Rad protein assay (Bio-Rad, Hercules, CA), respectively.

### 2.2.20 Assay for mouse peripheral Th17 cells

Mouse peripheral blood cells ($0.1x10^6$ per 100 ml) were incubated with PerCP-conjugated anti-CD4 antibody (1 mg) (eBioscience) and treated with R-PE-conjugated anti-IL-17 (eBioscience) and APC-conjugated anti-IFNg (eBioscience) antibodies (each 1 mg) by using Fixation/permiabilization kit (eBioscience, San Diego, CA). As controls, the isotype-matched antibodies were used. Finally the number (percentage) of CD4+IL-17+IFNg- Th17 cells (per $10x10^3$) was measured on FACSVerse (BD Biosciences) by using FACSuit software (BD Biosciences).

### 2.2.21 *Statistical analysis*

Data were assayed by One-Way ANOVA F test. *P* values less than 0.05 were considered to be significant.

## 2.3 RESULTS

### 2.3.1 Systemic SHED- and hBMMSCs- transplantation ameliorates SLE disorders in MRL/*lpr* mice.

According to previous standard method [13], SHED and hBMMSCs ($0.1x10^6$ per 10 g body weight) were systemically transplanted through the right cervical vein into MRL/*lpr* mice at the age of 16 weeks old (**Figure 16A**), which expressed severe autoimmune disorders including abnormal autoantibody increment and severe renal nephritis [9]. The present systemic transplantation of SHED and hBMMSCs evaluated their immune therapeutic efficacy on the SLE-like disorders such as hyper-autoimmune antibody production and renal dysfunction in MRL/*lpr* mice 4 weeks (**Figures 16B, 16C)**, as previously [13,67].

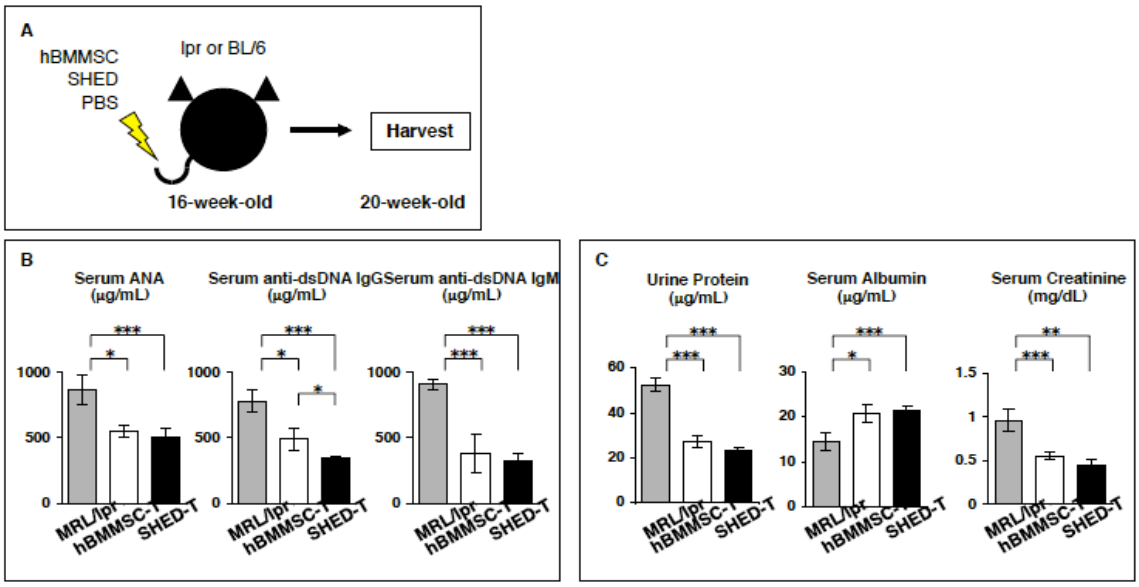


**Figure 16**. **Systemic transplantation of SHED and hBMMSCs improves serum hyper-autoantibody levels and renal dysfunction in MRL/*lpr* mice.** (**A**) A scheme of systemic transplantation of hBMMSCs and SHED into MRL/lpr mice. (**B**) ELISA of ANA (Serum ANA), anti-dsDNA IgG (Serum dsDNA IgG) and anti-dsDNA IgM (Serum dsDNA IgM) antibodies in the peripheral blood serum. (**C**) Levels of urine protein and serum albumin and creatinine. MRL/*lpr*: non-transplanted MRL/*lpr* group, hBMMSC-T: hBMMSC-transplanted MRL/*lpr* group, SHED-T: SHED-transplanted MRL/*lpr* group. **B, C:** n=5 for all group. **P*<0.05, ***P*<0.01, ****P*<0.005. The graph bar represents mean±SD.

(Ma et al. Stem Cells, in submission)

### 2.3.2 Systemic SHED- and hBMMSCs- transplantation improves the bone-loss secondary in MRL/*lpr* mice.

Severe osteoporosis with progressed trabecular bone breakdown is occurred secondary in SLE model MRL/*lpr* mice [9], as well as in SLE patients [57]. Enhanced osteoclastogenesis and suppressed osteoblastogenesis are responsible for the skeletal disruption in MRL/*lpr* mice [9]. Previous studies demonstrated that human MSC-transplantation improves the bone reduction of MRL/*lpr* mice [13,67]. However the cellular and molecular mechanisms have not been understood. To explore transplanted MSC-regulated skeletal condition, first of all, we examined the detailed *in vivo* skeletal metabolism in MRL/*lpr* mice 4 weeks after SHED transplantation. Micro-CT and histological analyses showed that the systemic transplantation of SHED recovered BMD and trabecular bone structures in MRL/*lpr* mice (**Figures 17A-17D**). By bone morphometric analysis, the number of osteoblasts on the bone surface increased in SHED-transplanted groups compared to non-transplanted group (**Figure 17E**). RT-PCR assay also demonstrated that the long bones of SHED-transplanted MRL/*lpr* mice expressed higher osteoblast-specific genes (*Runx2*, *Alp*, and *osteocalcin*) than that of non-transplanted MRL/*lpr* mice (**Figure 17F**). These bone reduction recovery functions were similar with hBMMSCs-transplantation group. Furthermore, SHED-transplantation as well as hBMMSC markedly reduced both the serum bone-resorption markers sRANKL and CTX by ELISA (**Figure 17G**) and the number of TRAP-positive cells in the epiphysis of long bones by histological analysis (**Figure 17H**) in comparison with non-transplanted mice. These findings suggest that SHED and hBMMSCs transplantation recovers the bone reduction via accelerated bone formation and suppressed bone resorption in MRL/*lpr* mice.

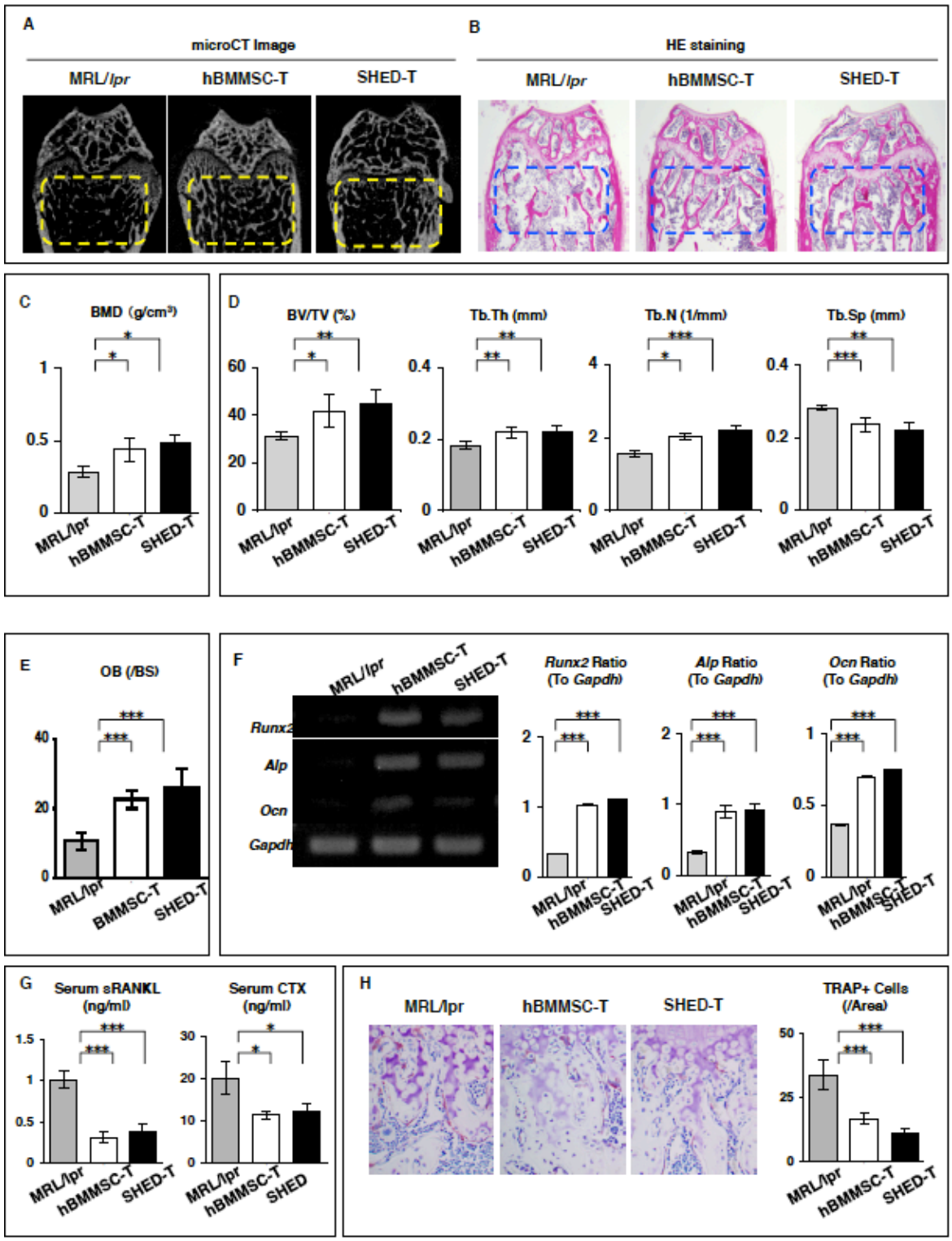


**Figure 17. Systemic transplantation of SHED and hBMMSCs ameliorates the bone-loss in MRL/*lpr* mice.**

←**Figure 17. Systemic transplantation of SHED and hBMMSCs ameliorates the bone-loss in MRL/*lpr* mice. (A-D)** Morphological analyses of mouse tibias. Representative microCT (**A**) and histological (**B**) images of trabecular bone structures (yellow and blue dot-circled areas). BMD (**C**). Trabecular bone parameter assay. BV/TV, Tb.Th, Tb.N, Tb.Sp (**D**). (**E, F**) *In vivo* osteogenic assay. Osteoblast number. OB/BS: osteoblast number per bone surface (**E**). Semi-quantitative RT-PCR analysis of osteoblast-specific genes. *Alp*, *Gapdh*, *Ocn*, *Runx2* (**F**). (**G**, **H**) *In vivo* osteoclast activity assay. ELISA of mouse serum. CTX, sRANKL (**G**). Histological analysis of recipient tibias with TRAP staining. TRAP+ Cells: TRAP-positive osteoclast-like cells (**H**). **A-H:** n=5 for all groups. MRL/*lpr*, hBMMSC-T, SHED-T: non-, hBMMSC-, and SHED-transplanted MRL/*lpr* mice. **C-H:** **P*<0.05, ***P*<0.01, ****P*<0.005. The graph bar represents mean±SD.

(Ma et al. Stem Cells, in submission)

### 2.3.3 Systemic SHED- and hBMMSCs- transplantation recovers dysregulation of osteoblast and osteoclast development via endogenous BMMSCs in MRL/*lpr* mice.

Dysregulation of osteoblast and osteoclast development in the marrow leads to a skeletal dysfunction. BMMSCs play a crucial role in the development of osteoblasts and osteoclasts in bone marrow [72-74]. Recent and present studies showed that endogenous BMMSCs impaired the osteogenic capacity [9,69] and demonstrated that SHED- and hBMMSC- transplanted mice expressed a skeletal phenotype with accelerated bone density (**Figure 17**) [13,67]. Therefore we hypothesized that endogenous BMMSCs participate in osteoporosis in SLE as a crisis and therapeutic target. Then, we isolated endogenous BMMSCs from non-, hBMMSC- and SHED-transplanted MRL/*lpr* mice, named MSC-MRL/*lpr*, MSC-hBMMSC and MSC-SHED, respectively. MSC-SHED exhibited similar effects in suppressing CFU-F numbers, high population doubling score and elevating cell proliferation rate with MSC-hBMMSC, when compared to MSC-MRL/*lpr* (**Figures 18A-18C**). Next, we examined the osteogenic capacity of endogenous BMMSCs. By Alizarin Red staining, MSC-MRL/*lpr* showed markedly lower mineral deposition than wild-type mice-derived MSCs (MSC-WT) 4 weeks after the osteogenic induction (**Figure 18D**). MSC-SHED and MSC-hBMMSC enhanced mineral

accumulation (**Figure 18D**) and osteoblast-specific gene expression (**Figure 18E**) in comparison with MSC-MRL/*lpr*.

Furthermore, we examined the effects of SHED-transplantation on endogenous BMMSC-depended osteoclast differentiation. Recipient BMMSCs were co-cultured with BMCs derived from wild-type mice (BMC-WT) under the stimulation with vitamin $D_3$ and prostaglandin $E_2$. MSC-MRL/*lpr* enhanced osteoclast induction compared to MSC-SHED (**Figure 18F**). This co-culture assay showed that MSC-SHED remarkably reduced the formation of TRAP-positive multinucleated cells (MNCs) (**Figure 18F**) and suppressed the expression of osteoclast-specific genes (*Nfatc, calcitonin receptor* and *cathepsin K*) (**Figure 18G**) when compared to MSC-MRL/*lpr*, which was also proved in MSC-hBMMSC group. Taken together, these data suggested that SHED-transplantation, likely hBMMSC-transplantation, improved dysfunction of endogenous BMMSCs on the induction of osteoblasts and osteoclasts to regenerate abnormal skeletal structures in MRL/*lpr* mice.

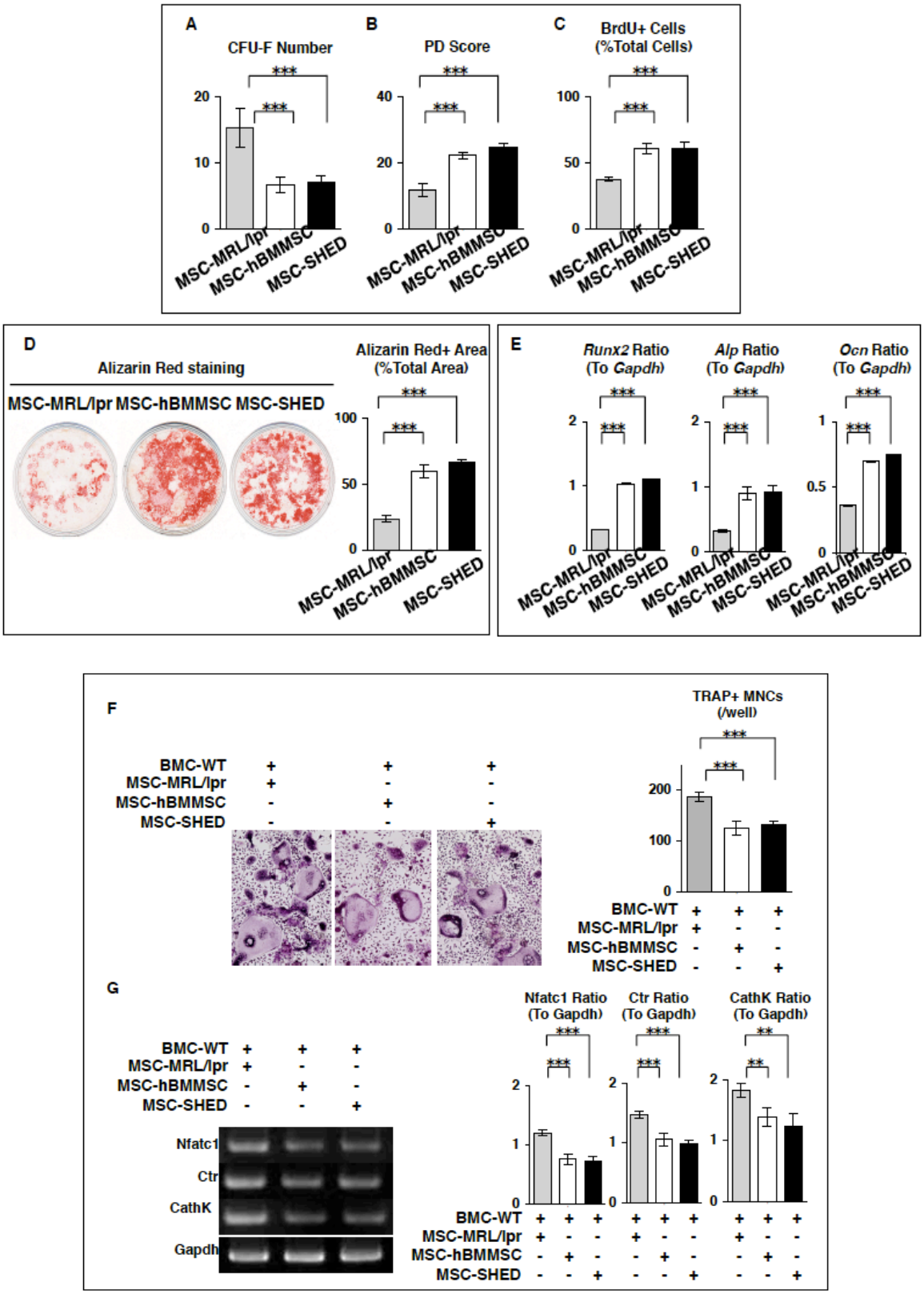


**Figure 18. Systemic transplantation of SHED and hBMMSCs recovers dysregulation of osteoblastogenesis and osteoclastogenesis development via endogenous BMMSCs in MRL/*lpr* mice.**

← **Figure 18. Systemic transplantation of SHED and hBMMSCs recovers dysregulation of osteoblastogenesis and osteoclastogenesis development via endogenous BMMSCs in MRL/*lpr* mice.** (**A-C**) Stemness of endogenous BMMSCs. CFU-F assay (**A**). Population doubling assay (**B**). Brd-U incorporate assay (**C**). (**D-E**) Osteogenic capacity of endogenous BMMSCs. Alizarin red staining 4 weeks after osteogenic induction (**D**). Semi-quantitative RT-PCR of osteoblast-specific genes 1 week after osteogenic induction. (**E**). (**F, G**) Osteoclastogenic capacity of endogenous BMMSCs under co-culture with wild type BL/6 mice-derived bone marrow cells (BMC-WT) through stimulation with 1a, 25-$(OH)_2$ vitamin $D_3$ and prostaglandin $E_2$. TRAP staining. TRAP+ MNCs: TRAP-positive multinucleated cells (**F**). Osteoclast-specific genes assay. *Nfatc1*: Nuclear factor of activated T-cells, cytoplasmic 1, *Ctr*: calcitonin receptor, *CathK*: cathepsin K, *Gapdh*: Glyceraldehyde 3-phosphate dehydrogenase (**G**). **A-G:** n=5 for all groups. . ** $P$<0.01, ***$P$<0.005. The graph bar represents mean±SD. MSC-MRL/*lpr*, MSC-hBMMSC, MSC-SHED: BMMSCs isolated from non-, hBMMSC-, and SHED-transplanted MRL/*lpr* mice, respectively.

(Ma et al. Stem Cells, in submission)

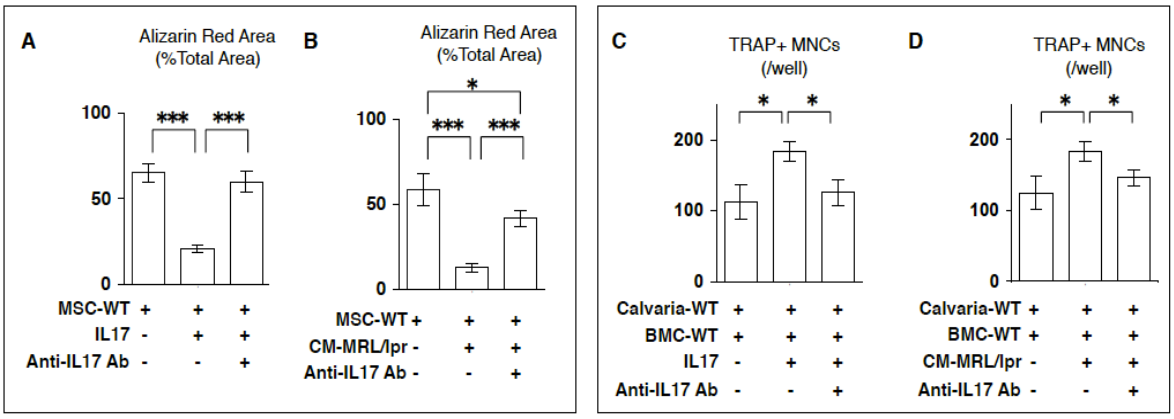


**Figure 19. Effects of IL-17 on osteogenic capacity and osteoclast differentiation.** (**A, B**) Alizarin Red staining 4 weeks after the osteogenic induction of MSC-WT under recombinant mouse IL-17 (IL17) (**A**) or conditioned medium of MRL/lpr mice-derived BMCs (CM-MRL/lpr) (**B**) in the presence and absence of anti-mouse IL-17 antibody (Anti-IL17 Ab). (**C, D**) TRAP staining after coculture of wild type mouse-derived BMCs (BMC-WT) and calvarial cells (Calvaria-WT) stimulated by 1α, 25$(OH)_2$ vitamin $D_3$ and prostaglandin $E_2$ under recombinant mouse IL-17 (IL17) (**C**) or CM-MRL/lpr (**D**) in the presence and absence of Anti-IL17 Ab. n=5 for all groups. *$P$<0.05, ***$P$<0.005. The graph bar represents mean±SD.

(Ma et al. Stem Cells, in submission)

### 2.3.4 Systemic SHED- and hBMMSCs- transplantation suppresses abnormal IL-17 production in the recipient bone marrow of MRL/*lpr* mice.

A pro-inflammatory cytokine IL-17, which is produced and secreted by a subset of helper T cells, called Th17 cells, contributes to the autoimmune progress in SLE [75,76]. We examined the immunoregulatory function of SHED on IL-17 production by using a co-culture system of SHED with human T cells in the presence of TGF-b1 and IL-6, and demonstrated that the SHED, similar with hBMMSC, were capable of suppressing both Th17 cell differentiation and IL-17 secretion by flow cytometric analysis and ELISA (**Figures 20A, 20B**). To confirm the *in vivo* immunological effects of SHED on IL-17 secretion, we analyzed peripheral levels of Th17 cells and IL-17 in MRL/*lpr* mice. Immunological analyses showed that SHED had lower capacity to suppressing systemic Th17 cell- IL-17-expression in MRL/*lpr* mice than hBMMSCs (**Figures 20C, 20D**).

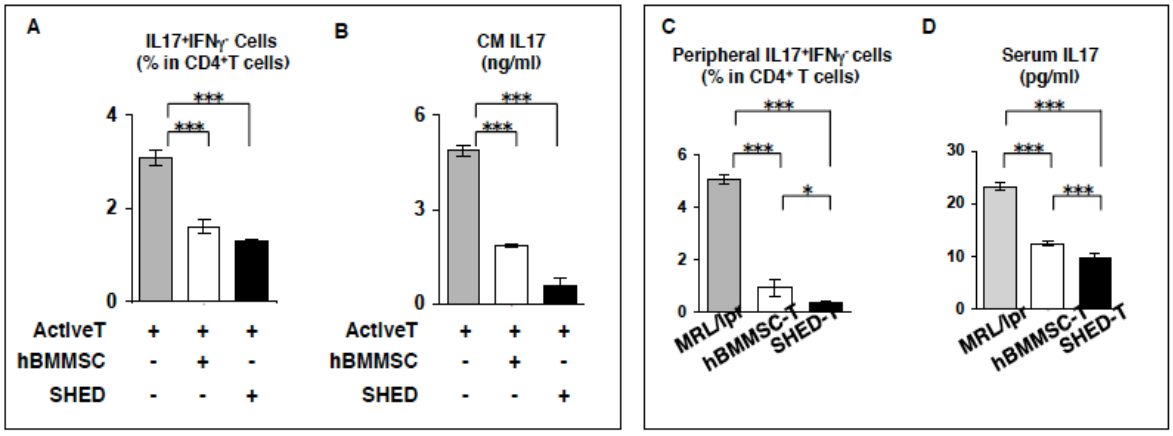


**Figure 20. Systemic transplantation of SHED and hBMMSCs suppresses peripheral Th17 cells in MRL/*lpr* mice.** (**A, B**) Suppression of Th17 cell differentiation and IL-17 secretion by hBMMSCs and SHED. Flow cytometry of peripheral $CD4^{+}IL\text{-}17^{+}IFNg^{-}$ (Th17) cells (**A**). ELISA of serum IL-17 (**B**). (**C, D**) Peripheral levels of Th17 cells and IL-17 in recipient MRL/*lpr* mice. Flow cytometry of peripheral $CD4^{+}IL\text{-}17^{+}IFNg^{-}$ (Th17) cells (**C**). ELISA of serum IL-17 (**D**). **A-D:** n=5 for all groups. **P*<0.05, ****P*<0.005. The graph bar represents mean±SD. MRL/*lpr*, hBMMSC-T, SHED-T: non-, hBMMSC-, and SHED-transplanted MRL/*lpr* mice.

(Ma et al. Stem Cells, in submission)

CFSE-labeled SHED were infused intravenously into MRL/*lpr* mice and found in the recipient bone marrow space on day 1 and 7 after the infusion, but the positive cell number was lower on day 7 than on day 1 (**Figure 21A**), suggesting the effect of homed SHED on immune condition in the recipient bone marrow, similar with homed hBMMSCs. IL-17 is significantly increased in bone marrow of MRL/*lpr* mice [9]. Then, we assessed bone marrow levels of IL-17 in SHED-transplanted MRL/*lpr* mice in comparison with non-transplanted mice. By immunofluorescent analysis, SHED-transplantation markedly decreased IL-17-positive cells in the recipient bone marrow (**Figure 21B**). Flow cytometric analysis and ELISA showed the reduction of $CD4^{+}IL17^{+}IFNg^{-}$ Th17 cells and IL-17 in recipient BMCs of SHED-transplanted group (**Figures 21C, 21D**). hBMMSC-transplanted group exhibited similar inhibitory to IL-17. To understand the productivity of IL-17 in the recipient bone marrow, we isolated BMC-MRL/*lpr*, BMC-hBMMSC and BMC-SHED from non-, hBMMSC- and SHED-transplanted MRL/*lpr* mice, respectively. Then we separately cultured the three different recipient BMCs under T-cell activation with anti-CD3 and anti-CD28 antibodies for 3 days and analyzed the IL-17-production in the CM by ELISA (**Figure 21E**). BMC-SHED and BMC-hBMMSC exhibited less production of IL-17 than BMC-MRL/*lpr* (**Figure 21F**). On the other hand, IL-17- and CM of BMC-MRL/*lpr*-treatments reduced the osteoblastogenic capacity of MSC-WT and enhanced osteoclast induction of MSC-WT from wild-type mice-derived calvarial cells (Calvarial-WT) (**Figure 19**). Taken together, these findings indicated that SHED-transplantation as well as hBMMSC- transplantation might suppress hyper immune condition, especially abnormal IL-17 production in the recipient bone marrow of MRL/*lpr* mice to modulate the condition of skeletal disorder via regulation of osteoblast and osteoclast differentiation in MRL/*lpr* mice.

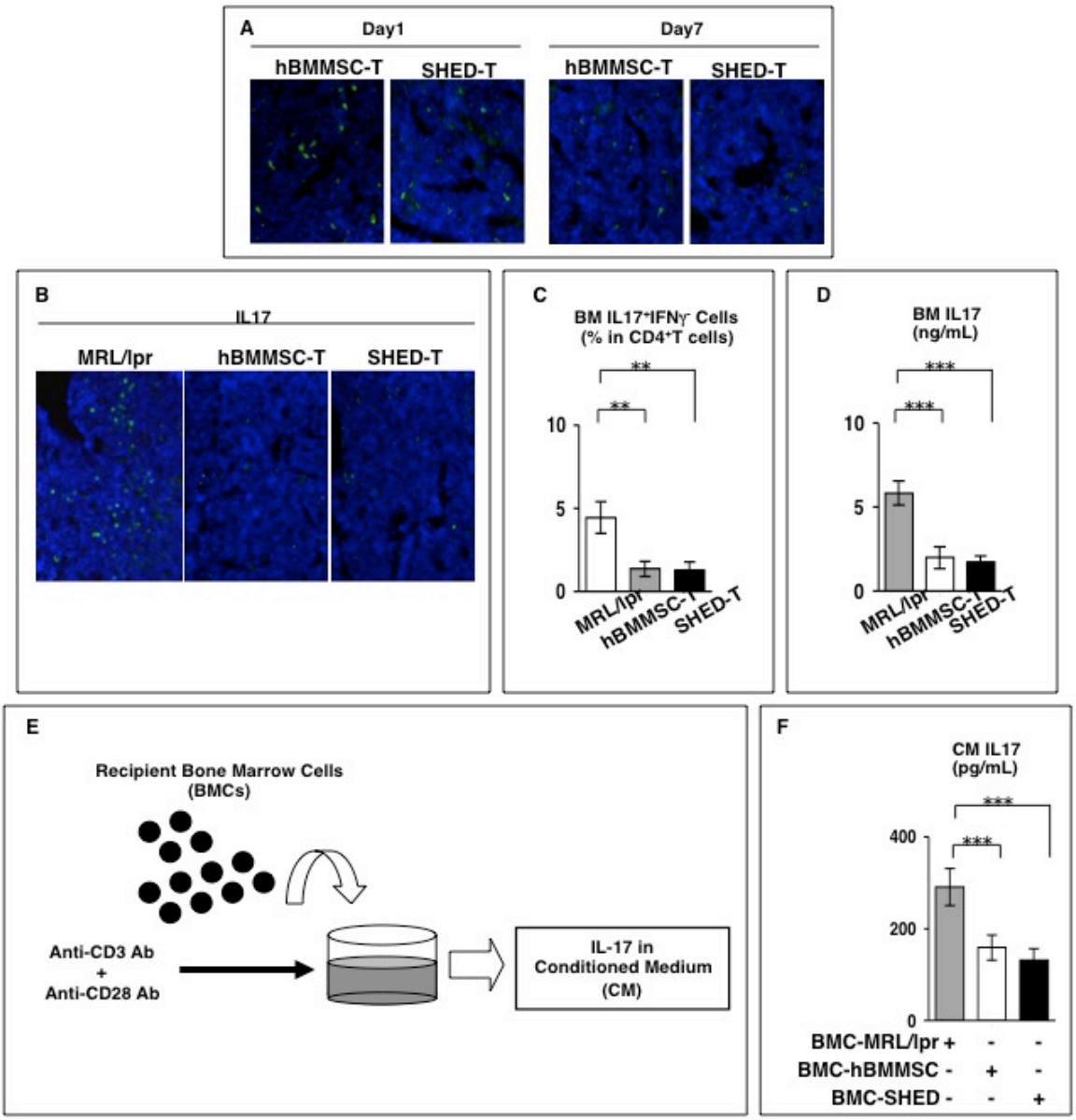


**Figure 21. Systemic transplantation of SHED and hBMMSCs into MRL/*lpr* mice suppressed IL-17-enhanced environment in the recipient bone marrow.** (**A**) *In vivo* homing assay of SHED and hBMMSCs in recipient bone marrow. Cell tracing assay with CSFE-labeling method. Nuclei are stained by DAPI. Day1: Cell infusion after 1 day, Day 7: Cell infusion after 7 days. (**B-D**) Levels of IL-17 and Th17 cells in recipient bone marrow. Immunofluorescence of IL-17. Nuclei are stained by DAPI (**B**). Flow cytometry of $CD4^{+}IL\text{-}17^{+}IFNg^{-}$ (Th17) cells in BM (**C**). ELISA of BM IL-17 (**D**). (**E, F**) Production assay of IL-17 in recipient BMCs. A scheme of the culture of recipient BMCs. BMCs were cultured under the stimulation of anti-CD3 and anti-CD28 antibodies and IL-17 was measured in the conditioned medium (CM) (**E**). ELISA of IL-17 in CM (CM IL-17) (**F**). **A-D, F:** n=5 for all groups. **A, C, D, F:** **P*<0.05, ***P*<0.01, ****P*<0.005. The graph bar represents mean±SD. **A-F:** MRL/*lpr*, hBMMSC-T, SHED-T: non-, hBMMSC-, and SHED-transplanted MRL/*lpr* mice. **F:** BMC-MRL/*lpr*, BMC-hBMMSC, BMC-SHED: BMCs isolated from non-, hBMMSC-, and SHED-transplanted MRL/*lpr* mice, respectively.

(Ma et al. Stem Cells, in submission)

### 2.3.5 Abnormal IL-17 expression in bone marrow impairs the osteogenic capacity of endogenous BMMSCs.

We examined whether IL-17-dependent immune condition in recipient bone marrow affects on endogenous BMMSC-mediated bone formation. Mouse BMMSCs were cultured under the osteogenic condition in the presence of ascorbic acid and inorganic phosphate with CM-MRL/*lpr*, CM-hBMMSC and CM-SHED, that were collected from BMC-MRL/*lpr*, BMC-hBMMSC and BMC-SHED cultures, respectively (**Figure 22A**). Alizarin Red Staining results showed that CM-MRL/*lpr* significantly suppressed osteogenic capacity of MSC-WT whereas CM-SHED and CM-hBMMSC expressed little suppressive effects on osteogenic capability of MSC-WT (**Figure 22B**). Meanwhile, Anti-IL-17 antibody-treatment successfully neutralized the CM-inhibited bone formation (**Figure 22B**), especially in CM-MRL/lpr group, suggesting the hyperactivity of IL-17 in CM-MRL/lpr may take responsibility for intense defective BMMSC-mediated bone formation.

Next, we checked the effect of SLE-like bone marrow immune condition on recipient BMMSCs-mediated bone formation. Recipient BMMSCs including MSC-SHED and MSC-hBMMSC were co-cultured with CM-MRL/*lpr* or IL17 under the osteogenic condition, separately. CM-MRL/*lpr*, as well as IL-17, significantly suppressed the mineralized formation of MSC-SHED and MSC-hBMMSC, similar to that of MSC-MRL/*lpr* (**Figure 22C, 22D**). However, anti-IL-17 antibody-treatment was able to neutralize the CM-MRL/*lpr* or IL-17 induced osteogenic capacity inhibition of MSC-SHED and MSC-hBMMSC (**Figure 22C, 22D**). These findings indicated that abnormal IL-17 in bone marrow impaired the osteogenic capacity of recipient BMMSCs.

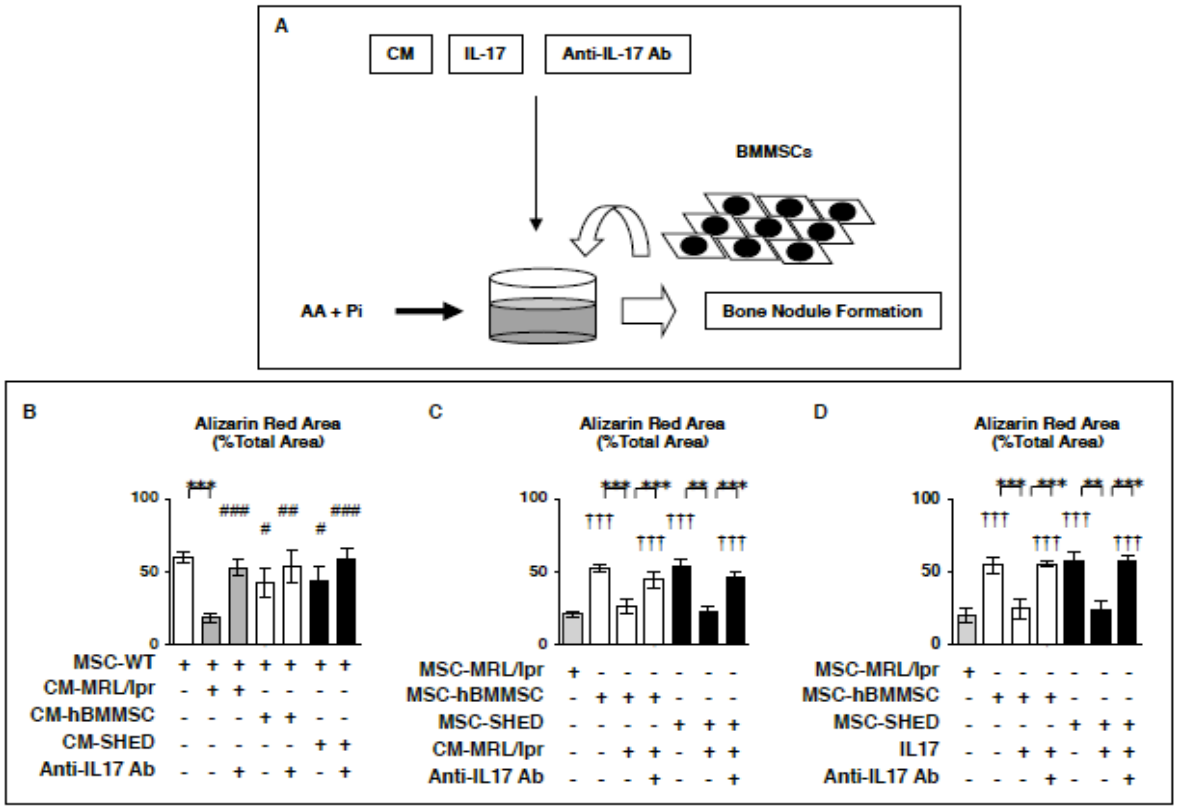


**Figure 22. Systemic transplantation of SHED and hBMMSCs recovers osteogenic capacity of recipient BMMSCs via suppressing bone marrow IL-17 in MRL/*lpr* mice.** (**A**) A scheme of osteogenic capacity of mouse BMMSCs. Mouse BMMSCs were induced by ascorbic acid (AA) and inorganic phosphate (Pi) treated with recipient BMC-derived CM in the presence or absence of anti-mouse IL-17 antibody (Anti-IL17 Ab) and recombinant mouse IL-17 (IL17). (**B-D**) Osteogenic assay by Alizarin Red staining 4 weeks after the osteogenic induction. **B-D:** MSC-WT: BMMSCs isolated from wild-type mice. MSC-MRL/*lpr*, MSC-hBMMSC, MSC-SHED: BMMSCs isolated from non-, hBMMSC-, and SHED-transplanted MRL/*lpr* mice, respectively. CM-MRL/*lpr*, CM-hBMMSC. CM-SHED; CM of BMC-MRL/*lpr*, BMC-hBMMSC, BMC-SHED cultures under the stimulation of anti-CD3 and CD28 antibodies, respectively. n=5 for all groups. The graph bar represents mean±SD. ***P*<0.01, ****P*<0.005. # *P*<0.05, ## *P*<0.01, ### *P*<0.005 (vs. MSC-WT). ††† *P*<0.005 (vs. MSC-MRL/*lpr*).

(Ma et al. Stem Cells, in submission)

### 2.3.6 Abnormal IL-17 expression in bone marrow enhances the osteoclastogenic capacity of recipient BMMSCs.

We examined whether IL-17-dependent immune condition in recipient bone marrow affects on endogenous BMMSC-mediated osteoclast formation. Calvarial-WT and recipient BMMSCs were pre-treated with recipient BMC-derived CM, recombinant mouse

IL-17 or anti-mouse IL-17 antibody for 3 days, then co-cultured with mouse BMCs in the presence of vitamin $D_3$ and prostaglandin $E_2$ (**Figure 23A**). In the co-culture of BMC-WT and Calvarial-WT, CM-MRL/*lpr*-pre-treatment significantly enhanced TRAP-positive MNC differentiation, but pre-treatment of CM-SHED and CM-hBMMSC showed less osteoclast induction compared to pre-treatment of CM-MRL/*lpr* (**Figure 23B, Figure 23D**). In the co-culture with Calvarial-WT, BMC-MRL/*lpr* also markedly induced TRAP-positive MNCs when compared to BMC-WT; however, BMC-SHED and BMC-hBMMSC exhibited less osteoclastogenesis than BMC-MRL/*lpr* (**Figures 23C, 23D**). In the case of CM-MRL/*lpr*- or IL-17-pre-treatment, BMC-SHED and BMC-hBMMSC exhibited enhanced TRAP-positive MNC-formation (**Figures 23C, 23D**). When anti-IL-17 antibody was also added in any pre-treatment of mouse BMMSCs, the accelerated osteoclastogenesis was completely neutralized (**Figures 23B-23D, Figures 19C, 19D**).

Next, in the co-culture of MSC-MRL/*lpr* with BMC-MRL/*lpr*, the pretreatment of CM-MRL/*lpr* remarkably induced TRAP-positive MNCs in comparison with non- treated MSC-MRL/*lpr*, but CM-SHED- or CM-hBMMSC-pretreatment showed less osteoclast induction compared to CM-MRL/*lpr*-pre-treatment (**Figures 23E, 23F**). Furthermore, in the co-culture with BMC-MRL/*lpr*, MSC-SHED and MSC-hBMMSC induced less TRAP-positive MNC-formation compared to MSC-MRL/*lpr* (**Figures 23F, 23G**). When pretreated with CM-MRL/*lpr*, TRAP-positive MNCs was enhanced in corresponding culture system, but the pretreatment effects in MSC-SHED and MSC-hBMMSC was less than that in MSC-MRL/*lpr* (**Figure 23F**). The pretreatment effects of IL-17 on recipient BMMSCs were resemble to the pretreatment effects of CM-MRL/*lpr* (**Figures 23G**). The neutralization with anti-IL-17 antibody suppressed the CM-MRL/*lpr*- and IL-17-induced osteoclastogenesis (**Figures 23F, 23G**). These findings indicated that IL-17-dependent hyper immune condition in recipient bone marrow of MRL/*lpr* mice affected abnormal

osteoclast formation through endogenous BMMSCs and suggested that SHED-transplantation as well as hBMMSCs-transplantation suppressed the bone marrow IL-17-accelerated osteoclast induction via endogenous BMMSCs.

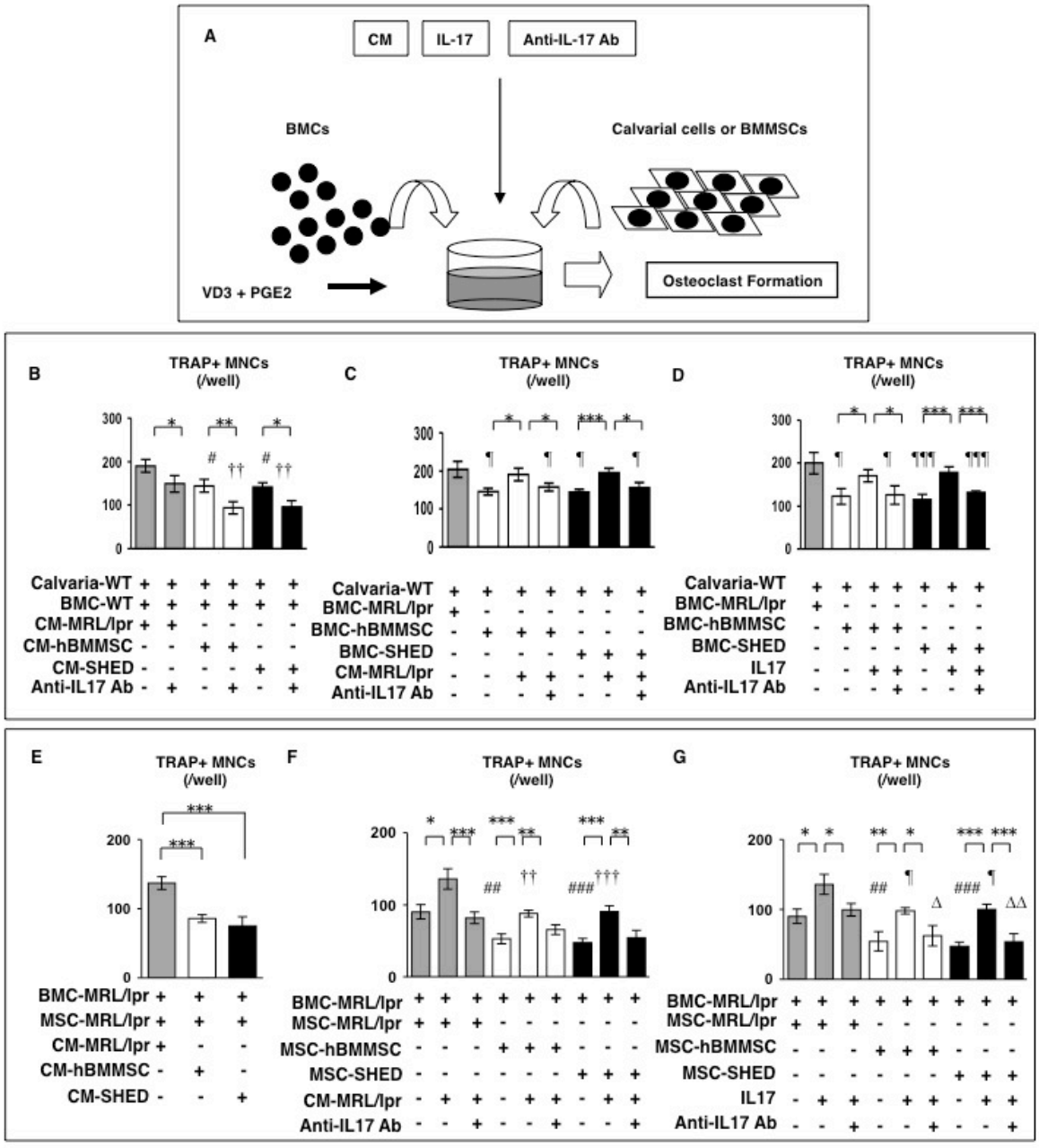


**Figure 23. Systemic transplantation of SHED and hBMMSCs into MRL/*lpr* mice inhibits endogenous BMMSC-mediated osteoclast differentiation via suppressing bone marrow IL-17.**

←**Figure 23. Systemic transplantation of SHED and hBMMSCs into MRL/*lpr* mice inhibits endogenous BMMSC-mediated osteoclast differentiation via suppressing bone marrow IL-17.** (**A**) A scheme of osteoclast induction. Mouse BMCs were co-cultured with wild-type mouse-derived calvarial cells or mouse BMMSCs under the stimulation with 1a, 25-$(OH)_2$ vitamin $D_3$ (VD3) and prostaglandin $E_2$ (PGE2). Calvarial cells or BMMSCs were pretreated with BMC-derived CM, recombinant mouse IL-17 (IL17) or anti-mouse IL-17 antibody (Anti-IL17 Ab). (**B-G**) Osteoclastogenic assay by TRAP staining. **B-G:** TRAP+ MNCs: TRAP-positive multinucleated cells. n=5 for all groups. **P*<0.05, ** *P*<0.01, ****P*<0.005. The graph bar represents mean±SD. Calvarial-WT: calvarial cells isolated form wild-type mice. BMC- WT: bone marrow cells isolated from wild-type mice. BMC-MRL/*lpr,* BMC-hBMMSC, BMC-SHED: bone marrow cells isolated from non-, hBMMSC-, and SHED-transplanted MRL/*lpr* mice, respectively. CM-MRL/*lpr*, CM-hBMMSC, CM-SHED: conditioned medium (CM) from BMC-MRL/*lpr*, BMC-hBMMSC, and BMC-SHED culture. MSC-MRL/*lpr*, MSC-hBMMSC, MSC-SHED: recipient BMMSCs isolated from control, hBMMSC-infused, SHED-transplanted MRL/*lpr* mice, respectively. **B:** # *P*<0.05 (vs. coculture with CM-MRL/*lpr*); †† *P*<0.01 (vs. coculture with CM-MRL/*lpr* and Anti-IL17 Ab). **C, D:** ¶ *P*<0.05, ¶¶ *P*<0.01, ¶¶¶ *P*<0.005 (vs. coculture of BMC-MRL/*lpr* with Calvarial-WT). **F, G:** ## *P*<0.01, ### *P*<0.005 (vs. coculture of BMC-MRL/*lpr* and MSC-MRL/*lpr*). **F:** †† *P*<0.01, ††† *P*<0.005 (vs. coculture of BMC-MRL/*lpr* and MSC-MRL/*lpr* with CM-MRL/*lpr*). **G:** ¶ *P*<0.05 (vs. coculture of BMC-MRL/*lpr* and MSC-MRL/*lpr* with IL17); Δ *P*<0.05, ΔΔ *P*<0.01 (vs. coculture of BMC-MRL/*lpr* and MSC-MRL/*lpr* with anti-IL17 Ab).

(Ma et al. Stem Cells, in submission)

## 2.4 DISCUSSION

The incidence of osteoporosis secondary in SLE patients ranges from 6.3% to 28% worldwide [77,78]. Osteoporosis is generally caused by the disruption to bone remodeling related to menopause and aging whereas osteoporosis secondary in SLE is multifactorial, mainly the underlying excessive systemic inflammation and the long-term anti-inflammatory/immunosuppressive medications such as glucocorticoids [72]. These risk factors lead to fragility fractures likely vertebral fractures, which can predict new fractures, increase mortality rate and reduce life quality [79,80]. Among many anti-osteoporosis drugs to prevent and treat the bone loss in SLE patients, bisphosphonates are selected as the first-line anti-resorptive agent, but show little effect on bone reconstruction and express side effects such as negative fetus development, osteonecrosis of the jaw and musculoskeletal pain. Other anti-osteoporotic choices likely estrogen, calcitonin or raloxifene exhibit different limits in potent, population and side effects [81]. Namely, from a view of a quality-of-life-based medicine, a novel therapeutics has been strongly desired to recover the bone loss in SLE patients. In this study, according to recent discovery of human MSC-based therapy [13,65-68], we systemically transplanted human SHED into the SLE model MRL/*lpr* mice with a severe osteoporotic phenotype and assessed the similar treatment effects towards the bone loss with hBMMSCs-transplantation, clarifying that SHED-based therapy presents a great value to ameliorate the bone reduction in MRL/*lpr* mice.

Once bone-remodeling balance by osteoblasts and osteoclasts becomes uncontrolled, skeletal system falls into a pathological situation. In bone marrow, BMMSCs serve not only as an original of osteoblasts, but also as a supporter of osteoclast differentiation [72-74]. Increasing evidences have showed the impaired function of BMMSCs derived from SLE patients [9,69,82,83] and SLE model mice [9], suggesting endogenous BMMSC

deficiency might participate in the pathology of osteoporosis secondary in SLE. However the recent [9,13,67] studies demonstrated that MSC transplantation into MRL/*lpr* mice improved the bone loss, no study focused on recipient BMMSCs in the bone regeneration process by systemic graft of MSCs. Therefore we hypothesized that the therapeutic efficacy of systemically transplanted MSCs on bone regeneration in SLE was mediated by reestablishment of the deficient host BMMSCs. Interestingly, in the present transplantation study, the grafted exogenous SHED recovered the impaired bone forming-capability of endogenous BMMSCs and reduce the abnormal osteoclast induction via endogenous BMMSCs in bone marrow environment of MRL/*lpr* mice, showing similar functions with hBMMSCs transplantation. These findings suggest that recovered endogenous BMMSCs play an important role in maintaining bone metabolism by regulating osteoblastogenesis and osteoclastogenesis after SHED- and hBMMSCs-transplantation. Furthermore studies will expect to explore the cellular and molecular mechanisms that exogenously grafted human MSCs improve deficiency of endogenous BMMSCs.

Inflammation shifts skeletal homeostasis to bone resorptive condition. Osteoporosis secondary in SLE is a complex interplay of hyperactivated immune reaction and abnormal bone metabolism. IL-17 is a pro-inflammatory cytokine produced by a special subset of helper T cells, called Th17 cells [84]. IL-17 concept has been investigated as a participant in a variety of autoimmune diseases [85,86]. In bone metabolism, IL-17 exerted to induce osteoclast differentiation through the osteoclastogenesis-supporting cells likely osteoblasts [87,88] while IL-17 directly inhibited osteoblast differentiation from MSCs [89], indicating that a novel potency of IL-17 was evaluated in bone diseases such as rheumatoid arthritis and osteoporosis [90,91]. In this study, systemic transplantation of hBMMSCs and SHED into MRL/*lpr* mice suppressed the increased expression of bone

marrow IL-17, as well as peripheral IL-17, and reconstructs the bone mineral loss via restoring the impaired functions of recipient BMMSCs on bone metabolism. The present neutralizing experiments also provided strong evidences that abnormal IL-17 expression in host bone marrow of MRL/*lpr* mice impaired endogenous BMMSC-mediated osteogenesis and endogenous BMMSC-dependent osteoclastogenesis. These findings suggest that hyper-activated IL-17 may be responsible for osteoporosis secondary via impairing endogenous BMMSCs in MRL/*lpr* mice. However NF-κB activation by proinflammatory cytokines including IL-17 affected the bone formation capacity of host BMMSCs [69,89], furthermore efforts will be required to figure out a crucial mechanism of IL-17 in the endogenous BMMSC-based pathology of osteoporosis secondary in SLE, leading to a novel endogenous BMMSC-targeting therapeutics for skeletal disorders.

In the present study, pathologic immune condition could affect endogenous MSCs and human MSC transplantation improved the bone reduction through restoring IL-17-impaired endogenous BMMSCs after migrating into the damaged bone marrow, suggesting the abnormal endogenous BMMSCs may require the correct recovery of the primary function supported by the post-transplantation actions of SHED and hBMMSCs. Although the therapeutic mechanism through migrated SHED and hBMMSCs in the target bone site has not been fully understood, several possibilities may be considered to involve in the post-transplantation behaviors of human MSCs in the impaired bone marrow. The migrated human MSCs had a potential to directly participate in bone regeneration by differentiating into osteoblasts and suppressing osteoclast differentiation [72-74], however the bone reconstruction was affected by proinflammatory cytokines at the bone defect sites [92]. In addition, MSCs acted as cellular modulators based on immunomodulatory and trophic effects [93]. The immunomodulatory function was inducted by cell-cell contact, including FasL-mediated T cell apoptosis [94], chemokine receptor 6-mediated

Th17 cell inhibition [95] and MSC-secreting molecules (eg. IL-10)-mediated Th17 cell suppression [96]. The trophic molecules released from MSCs could inhibit apoptosis and scar formation, such as macrophage inflammatory protein-1, Stromal cell-derived factor 1, TGF-b1 and vascular endothelial growth factor [97]. Therefore, exogenous SHED as well as hBMMSCs may exhibit a major contribution by the immunomodulatory and trophic activities via secreting bioactive molecules to re-establish impaired endogenous BMMSCs. Furthermore studies will be necessary to evaluate the molecular mechanism on grafted human MSCs mediated re-establishment of endogenous BMMSCs.

In conclusion, the present study demonstrated that systemic transplantation of SHED ameliorate severe bone reduction, as well as primary SLE disorders, in MRL/*lpr* mice. The therapeutic efficacy was similar with hBMMSCs-transplantation and mediated by recovering the impaired functions of recipient BMMSCs then regulating the osteogenesis and osteoclastogenesis via IL-17 suppression in bone marrow. These data indicate that IL-17, as an origin cause of osteoporosis secondary in SLE, might be a therapeutic target of transplanted SHED to the skeletal disorder. Furthermore researches will be necessary to explore new cellular and molecular strategy on endogenous BMMSC-based pathology of osteoporosis secondary in SLE, and to develop a novel endogenous/recipient BMMSC-targeting concept in MSC-based therapy for the skeletal disorder.

# SUMMARY

Stem cells have recently received much attention because of two-shared characteristic properties: a capacity to self-renewal and the potential to differentiate into various cell types. Medical advances bring the total population increase in the worldwide, especially the aging population. These changes create new challenges and arouse more demand for innovative therapeutic methods towards disease. Therefore, it is anticipated that stem cell-based therapy could provide new approaches for a variety of diseases, explore undiscovered etiology and develop new drugs with safety and effective. It is excited to see the progress in stem cell research and bright future in clinical application, which, we believe, can lead the current medical technology into a new era.

Embryonic stem (ES) cells have been mostly studied at the early stage of stem cell research, however, a series of ethical problems become their major obstacle in clinical application. Then, induced pluripotent stem (iPS) cells came into view [98], whose capacity can be competent with ES without worrying ethical issue. Unfortunately, ES and iPS both face the disadvantages to form teratomas [99, 100] and it seems that iPS induced teratomas are more malignant [101], which is considered a major concern by the U.S. Food and Drug Administration (FDA) [102].

MSCs can be isolated from various tissues and BMMSCs are the most intensively studied one. For years, MSCs have been widely used in animal models for preclinical study and patients for clinical treatment, including various degenerative diseases and immune disorders. These great therapeutic potentials are based on their multipotency and immunomodulatory capacity. Moreover, MSCs are free from ethical debate and show less tumorigenic risk compared with ES and iPS [103]. Currently, MSCs are the favorite stem cell types for translational medicine.

SHED are one of the most promising MSCs. Their largest advantages are derived from the natural discarded and least invasive tissue source — dental pulp from exfoliated deciduous teeth. Besides, SHED also presents the common MSCs properties, such as multipotency, immunomodulatory, in vitro and in vivo tissue regeneration. Compared with adult stem cells, SHED are less mature, suggesting the potent to differentiate into a wider range of tissue types. Moreover, SHED showed great therapeutic potential in preclinical settings as we discussed before. However, more and more problems should be considered for the actual clinical application of SHED.

In our study, we realized the importance of effective preservation method for stem cells and demonstrated that long-term cryopreservation of dental pulp tissue from exfoliated teeth would be a feasible approach for SHED banking, promising safe source and enough cell number for future SHED-based translational research. The success of cryopreservation of SHED built up our confidence for SHED-based therapy. We decided to move forward to apply SHED in real disease. Osteoporosis Secondary is often accompanied with SLE. SHED were transplanted into SLE model MRL/lpr mice and rescued the bone disorders, similar with hBMMSCs. Furthermore, in vitro and in vivo analysis to SHED- as well as hBMMSCs- transplantation pointed at one new pathogenesis which IL17 and endogenous BMMSC involve in, providing new therapeutic target for osteoporosis secondary.

However the current research of SHED is mainly limited to animal models, the human trial launch is urgent. The major question is how to translate the achievements in preclinical study into clinical applications, requiring a deep understanding of the complicated link between MSC and disease conditions. More efforts are needed for this career.

# ACKNOWLEDGMENTS

First and foremost I would like to express my deepest gratitude to my supervisor Prof. Kazuaki Nonaka (Department of Pediatric Dentistry) as well as Dr. Takayoshi Yamaza (Department of Molecular Cell Biology and Oral Anatomy) for providing me the opportunity to work on exciting projects under their guidance. Their endless enthusiasm on basic science, rigorous research attitude, and wide range of knowledge not only guided my research but also enlightened my pathway to scientific research. They truly take care of the students and are willing to listen the different voices. Their optimism, modesty and kindness have influenced me greatly over the years. Their understanding and tolerance on culture differences are highly appreciated.

My sincere thanks also extend to Prof. Toshio Kukita and Dr. Haruyoshi Yamaza for kind support and valuable advices to this work. And I also wanted to express my deep thanks to all members who worked in Department of Pediatric Dentistry. With their support I have got impressive experience on Pedodontic clinical treatment and education.

In my personal life, I would like to thank all of my friends for accompanying me in Japan so memorable and full of laughter. They continuously gave me encouragements and advices when I was upset and disappointed. Moreover, I am forever indebted to my beloved family members, without whom my achievements would not have been possible.

And at last I must express my deep appreciation to China Scholarship Council of Education Ministry, which covered my four-year living cost, and to Ministry of Education, Culture, Sports, Science and Technology of Japan, which supported my research and conference study.

# REFERENCES


1. Porada CD, Almeida-Porada G. (2010) Mesenchymal stem cells as therapeutics and vehicles for gene and drug delivery. *Advanced Drug Delivery Reviews* 62: 1156-1166.
2. Kwan MD, Slater BJ, Wan DC, Longaker MT. (2008) Cell-based therapies for skeletal regenerative medicine. *Human Molecular Genetics* 17: R93-98.
3. Panetta NJ, Gupta DM, Quarto N, Longaker MT. (2009) Mesenchymal cells for skeletal tissue engineering. *Panminerva Medica* 51: 25-41.
4. Aggarwal S, Pittenger MF. (2005) Human mesenchymal stem cells modulate allogeneic immune cell responses. *Blood* 105: 1815-1822.
5. Nauta AJ, Fibbe WE. (2007) Immunomodulatory properties of mesenchymal stromal cells. *Blood* 110: 3499-3506.
6. Le Blanc K, Rasmusson I, Sundberg B, Götherström C, Hassan M, Uzunel M, Ringd én O. (2004) Treatment of severe acute graft-versus-host disease with third party haploidentical mesenchymal stem cells. *The Lancet* 363: 1439-1441.
7. Koç ON, Gerson SL, Cooper BW, Dyhouse SM, Hayneswothr SE, Caplan AI, Lazarus HM. (2000) Rapid hematopoietic recovery after coinfusion of autologous-blood stem cells and culture-expanded marrow mesenchymal stem cells in advanced breast cancer patients receiving high-dose chemotherapy. *Journal of Clinical Oncology* 18: 307-316.
8. Noort WA, Kruisselbrink AB, in't Anker PS, Kruger M, van Bezooijen RL, de Paus RA, Heemskerk MH, Löwik CW, Falkenburg JH, Willemze R, Fibbe WE. (2002) Mesenchymal stem cells promote engraftment of human umbilical cord blood-derived CD34 cells in NOD/SCID mice. *Experimental Hematology* 30: 870–878.

9. Sun L, Akiyama K, Zhang H, Yamaza T, Hou Y, Zhao S, Xu T, Le A, Shi S. (2009) Mesenchymal Stem Cell Transplantation Reverses Multi-Organ Dysfunction in Systemic Lupus Erythematosus Mice and Humans. *Stem Cells* 27: 1421-1432.
10. Miura M, Gronthos S, Zhao M, Lu B, Fisher LW, Robey PG, Shi S. (2003) SHED: Stem cells from human exfoliated deciduous teeth. *Proc Natl Acad Sci USA* 100: 5807-5812.
11. Seo BM, Sonoyama W, Yamaza T, Coppe C, Kikuiri T, Akiyama K, Lee JS, Shi S. (2008) SHED repair critical-size calvarial defects in immunocompromised mice. *Oral Diseases* 14: 428-434.
12. Zheng Y, Liu Y, Zhang CM, Zhang HY, Li WH, Shi S, Le AD, Wang SL. (2009) Stem cells from deciduous tooth repair mandibular defect in swine. *Journal of Dental Research* 88: 249-254.
13. Yamaza T, Akiyama K, Chen C, Liu Y, Shi Y, Gronthos S, Wang S, Shi S. (2010) Immunomodulatory properties of stem cells from human exfoliated deciduous teeth. *Stem Cell Research & Therapy* 1:5.
14. Wood EJ, Benson JD, Agca Y, Crister JK. (2004) Fundamental cryobiology of reproductive cells and tissues. *Cryobiology* 48: 146-156.
15. Friedenstein AJ. (1980) Stromal mechanisms of bone marrow: cloning in vitro and retransplantation in vivo. *Haematology and Blood Transfusion* 25: 19-29.
16. Shi S, Gronthos S, Chen S, Reddi A, Counter CM, Robey PG, Wang CY. (2002) Bone formation by human postnatal bone marrow stromal stem cells is enhanced by telomerase expression. *Nature Biotechnology* 20: 587-591.
17. Bi Y, Ehirchiou D, Kilts TM, Inkson CA, Embree MC, Sonoyama W, Li L, Leet AI, Seo BM, Zhang L, Shi S, Young MF. (2007) Identification of tendon stem/progenitor

cells and the role of the extracellular matrix in their niche. *Nature Medicine* 13: 1219-1227.

18. Gronthos S. Zannettino AC, Hay SJ, Shi S, Graves SE, Kortesidis A, Simmons PJ. (2003) Molecular and cellular characterisation of highly purified stromal stem cells derived from human bone marrow. *Journal of Cell Science* 116: 1827-1835.
19. Yamaza T, Miura Y, Bi Y, Liu Y, Akiyama K, Sonoyama W, Patel V, Gutkind S, Young M, Gronthos S, Le A, Wang CY, Chen W, Shi S. (2008) Pharmacologic stem cell based intervention as a new approach to osteoporosis treatment in rodents. *PLoS ONE* 3: e2615.
20. Danjo A, Yamaza T, Kido MA, Shimohira D, Tsukuba T, Kagiya T, Yamashita Y, Nishijima K, Masuko S, Goto M, Tanaka T. (2007) Cystatin C stimulated the differentiation of mouse osteoblastic cells and bone formation. *Biochemical and Biophysical Research Communications* 360: 199-204.
21. Shi S, Gronthos S. (2003) Perivascular Niche of Postnatal Mesenchymal Stem Cells Identified in Human Bone Marrow and Dental Pulp. *Journal of Bone and Mineral Research* 18: 696-704.
22. Kerkis I, Kerkis A, Dozortsev D, Stukart-Parsons GC, Gomes Massironi SM, Pereira LV, Caplan AI, Cerruti HF. (2006) Isolation and characterization of a population of immature dental pulp stem cells expressing OCT-4 and other embryonic stem cell markers. *Cells Tissues Organs*. 184: 105-116.
23. Lizier NF, Kerkis A, Gomes CM, Hebling J, Oliveira CF, Caplan AI, Kerkis I. (2012) Scaling-up of dental pulp stem cells isolated from multiple niches. *PLoS One* 7: e39885.

24. Miura Y, Gao Z, Miura M, Seo BM, Sonoyama W, Chen W, Gronthos S, Zhang L, Shi S. (2006) Mesenchymal stem cell-organized bone marrow elements: an alternative hematopoietic progenitor resource. *Stem Cells* 24: 2428-2436.
25. Yamaza T, Miura Y, Akiyama K, Bi Y, Sonoyama W, Gronthos S, Chen W, Le A, Shi S. (2009) Mesenchymal stem cell-mediated ectopic hematopoiesis alleviates aging-related phenotype in immunocompromised mice. *Blood* 113: 2595-2604.
26. Morrison SJ, Prowse KR, Ho P, Weissman IL. (1996) Telomerase activity in hematopoietic cells is associated with self-renewal potential. *Immunity* 5: 207-216.
27. Yang J, Yang X, Zou H, Chu Y, Li M. (2011) Recovery of the immune balance between Th17 and regulatory T cells as a treatment for systemic lupus erythematosus. *Rheumatology* 50: 1366-1372.
28. Liu Y, Wang L, Kikuiri T, Akiyama K, Chen C, Xu X, Yang R, Chen W, Wang S, Shi S. (2011) Mesenchymal stem cell-based tissue regeneration is governed by recipient T lymphocytes via IFN-gamma and TNF-α. *Nature Medicine* 17: 1594-1601.
29. de Mendonça Costa A, Bueno DF, Martins MT, Kerkis I, Kerkis A, Fanganiello RD, Cerruti H, Alonso N, Passos-Bueno MR. (2008) Reconstruction of large cranial defects in nonimmunosuppressed experimental design with human dental pulp stem cells. *The Journal of Craniofacial Surgery* 19: 204-210.
30. Sakai VT, Zhang Z, Dong Z, Neiva KG, Machado MA, Shi S, Santos CF, Nör JE. (2010) SHED differentiate into functional odontoblasts and endothelium. *Journal of Dental Research* 89:791-796.
31. Nourbakhsh N, Soleimani M, Taghipour Z, Karbalaie K, Mousavi SB, Talebi A, Nadali F, Tanhaei S, Kiyani GA, Nematollahi M, Rabiei F, Mardani M, Bahramiyan H, Torabinejad M, Nasr-Esfahani MH, Baharvand H. (2011) Induced in vitro

differentiation of neural-like cells from human exfoliated deciduous teeth-derived stem cells. *The International Journal of Developmental Biology* 55: 189-195.

32. Kerkis I, Ambrosio CE, Kerkis A, Martins DS, Zucconi E, Fonseca SA, Cabral RM, Maranduba CM, Gaiad TP, Morini AC, Vieira NM, Brolio MP, Sant'Anna OA, Miglino MA, Zatz M. (2008) Early transplantation of human immature dental pulp stem cells from baby teeth to golden retriever muscular dystrophy (GRMD) dogs: Local or systemic? *Journal of Translational Medicine* 6: 35.
33. Zheng Y, Wang XY, Wang YM, Liu XY, Zhang CM, Hou BX, Wang SL. (2012) Dentin regeneration using deciduous pulp stem/progenitor cells. *Journal of Dental Research* 91: 676-682.
34. Sakai K, Yamamoto A, Matsubara K, Nakamura S, Naruse M, Yamagata M, Sakamoto K, Tauchi R, Wakao N, Imagama S, Hibi H, Kadomatsu K, Ishiguro N, Ueda M. (2012) Human dental pulp-derived stem cells promote locomotor recovery after complete transection of the rat spinal cord by multiple neuro-regenerative mechanisms. *The Journal of Clinical Investigation* 122: 80-90.
35. Korbling M, Estrov Z. (2003) Adult stem cells for tissue repair—a new therapeutic concept? *The New England Journal of Medicine* 349: 570-582.
36. Woods EJ, Pollok KE, Byers MA, Perry BC, Purtteman J, Heimfeld S, Gao D. (2007) Cord blood stem cell cryopreservation. *Transfusion Medicine and Hemotherapy* 34: 276-285.
37. D'Ippolito G, Schiller PC, Ricordi C, Roos BA, Howard GA. (1999) Age-related osteogenic potential of mesenchymal stromal stem cells from human vertebral bone marrow. *Journal of Bone and Mineral Research* 14: 1115-1122.

38. Stenderup K, Justesen J, Clausen C, Kassem M. (2003) Aging is associated with decreased maximal life span and accelerated senescence of bone marrow stromal cells. *Bone* 33: 919-926.

39. Stolzing A, Jones E, McGonagle D, Scutt A. (2008) Age-related changes in human bone marrow-derived mesenchymal stem cells: consequences for cell therapies. *Mechanism of Ageing and Development* 129: 163-173.

40. Garvin G, Connie F, Sharp JG, Berger A. (2007) Does the number or quality of pluripotent bone marrow stem cells decrease with age? *Clinical Orthopaedics and Related Research* 465: 202-207.

41. Muschler GF, Boehm C, Easley K. (1997) Aspiration to obtain osteoblast progenitor cells from human bone marrow: The influence of aspiration volume. *The Journal of Bone and Joint Surgery. American Volume* 79: 1699-1709.

42. Zuk PA, Zhu M, Mizuno H, Huang J, Futrell JW, Katz AJ, Benhaim P, Lorenz HP, Hedrick MH. (2001) Multilineage cells from human adipose tissue: implications for cell-based therapies. *Tissue Engineering* 7: 211-228.

43. Erices A, Conget P, Minguell JJ. (2000) Mesenchymal progenitor cells in human umbilical cord blood. *British Journal of Haematology* 109: 235-242.

44. Gronthos S, Mankani M, Brahim J, Robey PG, Shi S. (2000) Postnatal human dental pulp stem cells (DPSCs) in vitro and in vivo. *Proc Natl Acad Sci USA* 97: 13625-13630.

45. Hubel A. (1997) Parameters of cell freezing: implications for the cryopreservation of stem cells. *Transfusion Medicine Reviews* 11: 224-233.

46. Areman E, Sacher R, Deeg H. (1990) Processing and storage of human bone marrow: A survey of current practices in North America. *Bone Marrow Transplantation* 6: 203-209.

47. Watt SM, Austin E, Armitage S. (2007) Cryopreservation of hematopoietic stem/progenitor cells for therapeutic use. *Methods in Molecular Biology* 368: 237-259.

48. Perry BC, Zhou D, Wu X, Yang FC, Byers MA, Chu TM, Hockema JJ, Woods EJ, Goebel WS. (2008) Collection, cryopreservation, and characterization of human dental pulp-derived mesenchymal stem cells for banking and clinical use. *Tissue Engineering. Part C, Methods* 14: 149-156.

49. Seo BM, MiuraM, SonoyamaW, Coppe C, Stanyon R, Shi S. (2005) Recovery of stem cells from cryopreserved periodontal ligament. *Journal of Dental Research* 84: 907-912.

50. Ding G, Wang W, Liu Y, An Y, Zhang C, Shi S, Wang S. (2010) Effect of cryopreservation on biological and immunological properties of stem cells from apical papilla. *Journal of Cellular Physiology* 223: 415-422.

51. Zhao ZG, Li WM, Chen ZC, You Y, Zou P. (2008) Hematopoiesis capacity, immunomodulatory effect and ex vivo expansion potential of mesenchymal stem cells are not impaired by cryopreservation. *Cancer Investigation* 26: 391-400.

52. Sonoyama W, Liu Y, Fang D, Yamaza T, Seo BM, Zhang C, Liu H, Gronthos S, Wang CY, Wang S, Shi S. (2006) Mesenchymal stem cell-mediated functional tooth regeneration in swine. *PLoS One* 1: e79.

53. Sonoyama W, Liu Y, Yamaza T, Tuan RS, Wang S, Shi S, Huang GT. (2008) Characterization of the Apical Papilla and Its Residing Stem Cells from Human Immature Permanent Teeth: A Pilot Study. *Journal of Endodontics* 34: 166-171.

54. Cooper C. (2003). Epidemiology of osteonecrosis. In: *primer on the Metabolic Bone Disease and Disorders of Mineral Metabolism*. Favus M, ed. American Society for Bone and Mineral Research, Washington DC, pp 307-313.

55. Walker-Bone K. (2012). Recognizing and treating secondary osteoporosis. *Nature Reviews. Rheumatology* 8:480-492.

56. Lane NE. (2006). Therapy Insight: osteoporosis and osteonecrosis in systemic lupus erythematosus. *Nature Clinical Practice. Rheumatology* 2:562-569.

57. Bultink IE. (2012). Osteoporosis and fractures in systemic lupus erythematosus. *Arthritis Care & Research* 64:2-8.

58. Pittenger MF, Mackay AM, Beck SC, Jaiswal RK, Douglas R, Mosca JD, Moorman MA, Simonetti DW, Craig S, Marshak DR. (1999). Multilineage potential of adult human mesenchymal stem cells. *Science* 284:143-147.

59. Keating A. (2008). How do mesenchymal stromal cells suppress T cells? *Cell Stem Cell* 2:106-108.

60. Nauta AJ, Fibbe WE. (2007). Immunomoduratory properties of mesenchymal stem cells. *Blood* 110:3499-3506.

61. González MA, Gonzalez-Rey E, Rico L, Büscher D, Delgado M. (2009). Adipose-derived mesenchymal stem cells alleviate experimental colitis by inhibiting inflammatory and autoimmune responses. *Gastroenterology* 136:978-989.

62. Sun L, Wang D, Liang J, Zhang H, Feng X, Wang H, Hua B, Liu B, Ye S, Hu X, Xu W, Zeng X, Hou Y, Gilkeson GS, Silver RM, Lu L, Shi S. (2010). Umbilical Cord Mesenchymal Stem Cell Transplantation in Severe and Refractory Systemic Lupus Erythematosus. *Arthritis and Rheumatism* 62:2467–2475.

63. Wang D, Zhang H, Liang J, Li X, Feng X, Wang H, Hua B, Liu B, Lu L, Gilkeson GS, Silver RM, Chen W, Shi S, Sun L. (2012). Allogeneic mesenchymal stem cell transplantation in severe and refractory systemic lupus erythematosus: 4 years experience. *Cell Transplantation*: In press.

64. Theofilopoulos AN, Dixon FJ. (1985). Murine models of systemic lupus erythematosus. *Advances in Immunology* 37:269-390.

65. Zhou K, Zhang H, Jin O, Feng X, Yao G, Hou Y, Sun L. (2008). Transplantation of human bone marrow mesenchymal stem cell amelionates the autoimmune pathogenesis in MRL/lpr mice. *Cellular & Molecular Immunology* 5:417-424.

66. Gu Z, Akiyama K, Ma X, Zhang H, Feng X, Yao G, Hou Y, Lu L, Gilkeson GS, Silver RM, Zeng X, Shi S, Sun L. (2010). Transplantation of umbilical cord mesenchymal stem cells alleviates lupus nephritis in MRL/lpr mice. *Lupus* 19:1502-1514.

67. Ma L, Makino Y, Yamaza H, Akiyama K, Hoshino Y, Song G, Kukita T, Nonaka K, Shi S, Yamaza T. (2012). Cryopreserved dental pulp tissues of exfoliated deciduous teeth is a feasible stem cell resource for regenerative medicine. *PLoS One* 7:e51777.

68. Makino Y, Yamaza H, Akiyama K, Ma L, Hoshino Y, Nonaka K, Terada Y, Kukita T, Shi S, Yamaza T. (2013). Immune therapeutic potential of stem cells from human supernumerary teeth. *Journal of Dental Research* 92:609-615.

69. Tang Y, Xie H, Chen J, Geng L, Chen H, Li X, Hou Y, Lu L, Shi S, Zeng X, Sun L. (2013). Activated NF-κB in bone marrow mesenchymal stem cells from systemic lupus erythematosus patients inhibits osteogenic differentiation through downregulating Smad signaling. *Stem Cells and Development* 22:668-678.

70. Dominici M, Le BK, Mueller I, Slaper-Cortenbach I, Marini F, Krause D, Deans R, Keating M, Prockop D, Horwitz E. (2006). Minimal criteria for defining multipotent mesenchymal stromal cells. The International Society for Cellular Therapy position statement. *Cytotherapy* 8:315-317.

71. Yamaza T, Ren G, Akiyama K, Chen C, Shi Y, Shi S. (2011). Mouse mandible contains distinctive mesenchymal stem cells. *Journal of Dental Research* 90:317-324.

72. Manolagas SC, Jilka RL. (1995). Bone marrow, cytokines, and bone remodeling. Emerging insights into the pathophysiology of osteoporosis. *The New England Journal of Medicine* 332:305-311.

73. Oshita K, Yamaoka K, Udagawa N, Fukuyo S, Sonomoto K, Maeshima K, Kurihara R, Nakano K, Saito K, Okada Y, Chiba K, Tanaka Y. (2011). Human mesenchymal stem cells inhibit osteoclastogenesis through osteoprotegerin production. *Arthritis and Rheumatism* 63: 1658-1667.

74. Varin A, Pontikoglou C, Labat E, Deschaseaux F, Sensebé L. (2013). CD200R/CD200 inhibits osteoclastogenesis: new mechanism of osteoclast control by mesenchymal stem cells in human. *PLoS One* 8: e72831.

75. Kurasawa K, Hirose K, Sano H, Endo H, Shinkai H, Nawata Y, Takabayashi K, Iwamoto I. (2000). Increased interleukin-17 production in patients with systemic sclerosis. *Arthritis and Rheumatism* 43:2455-2463.

76. Wong CK, Ho CY, Li EK, Lam CW. (2000). Elevation of proinflammatory cytokine (IL-18, IL-17, IL-12) and Th2 cytokine (IL-4) concentrations in patients with systemic lupus erythematosus. *Lupus* 9:589-593.

77. Souto MI, Coelho A, Guo C, Mendonça LM, Pinheiro MF, Papi JA, Farias ML. (2012). The prevalence of low bone mineral density in Brazilian patients with systemic lupus erythematosus and its relationship with the disease damage index and other associated factors. *Journal of Clinical Densitometry* 15:320-327.

78. Jacobs J, Korswagen LA, Schilder AM, van Tuyl LH, Dijkmans BA, Lems WF, Voskuyl AE, Bultink IE. (2013). Six-year follow-up study of bone mineral density in patients with systemic lupus erythematosus. *Osteoporosis International* 24:1827-1833.

79. Oleksik A, Lips P, Dawson A, Minshall ME, Shen W, Cooper C, Kanis J. Health-related quality of life in postmenopausal women with low BMD with or without prevalent vertebral fractures. (2000). *Journal of Bone and Mineral Research* 15:1384-1392.

80. Hasserius R, Karlsson B, Jonsson B, Redlund-Johnell I, Johnell O. (2005). Long-term morbidity and mortality after a clinically diagnosed vertebral fracture in the elderly – a 12 and 22 year follow-up of 257 patients. *Calcified Tissue International* 76:235-242.

81. Miller PD, Derman RJ. (2010). What is the best balance of benefits and risks among anti-resorptive therapies for postmenopausal osteoporosis? *Osteoporosis International* 21:1793-1802.

82. Sun LY, Zhang HY, Feng XB, Hou YY, Lu LW, Fan LM. (2007). Abnormality of bone marrow-derived mesenchymal stem cells in patients with systemic lupus erythematosus. *Lupus* 16:121-128.

83. Tang Y, Ma X, Zhang H, Gu Z, Hou Y, Gilkeson GS, Lu L, Zeng X, Sun L. (2012). Gene expression profile reveals abnormalities of multiple signaling pathways in mesenchymal stem cell derived from patients with systemic lupus erythematosus. *Clinical & Developmental Immunology* 2012: 826182.

84. Yao Z, Fanslow WC, Seldin MF, Rousseau AM, Painter SL, Comeau MR, Cohen JI, Spriggs MK. (1995). Herpesvirus Saimiri encodes a new cytokine, IL-17, which binds to a novel cytokine receptor. *Immunity* 3:811-821.

85. Harrington LE, Hatton RD, Mangan PR, Turner H, Murphy TL, Murphy KM, Weaver CT. (2005). Interleukin 17-producing CD4+ effector T cells develop via a lineage distinct from the T helper type 1 and 2 lineages. *Nature Immunology* 6:1123-1132.

86. Park H, Li Z, Yang XO, Chang SH, Nurieva R, Wang YH, Wang Y, Hood L, Zhu Z, Tian Q, Dong C. (2005). A distinct lineage of CD4 T cells regulates tissue inflammation by producing interleukin 17. *Nature Immunology* 6:1133-1141.

87. Kotake S, Udagawa N, Takahashi N, Matsuzaki K, Itoh K, Ishiyama S, Saito S, Inoue K, Kamatani N, Gillespie MT, Martin TJ, Suda T. (1999). IL-17 in synovial fluids from patients with rheumatoid arthritis is a potent stimulator of osteoclastogenesis. *Journal of Clinical Investigation* 103:1345-1352.

88. Sato K, Suematsu A, Okamoto K, Yamaguchi A, Morishita Y, Kadono Y, Tanaka S, Kodama T, Akira S, Iwakura Y, Cua DJ, Takayanagi H. (2006). Th17 functions as an osteoclastogenic helper T cell subset that links T cell activation and bone destruction. *The Journal of Experimental Medicine* 203:2673-2682.

89. Chang J, Liu F, Lee M, Wu B, Ting K, Zara JN, Soo C, Al Hezaimi K, Zou W, Chen X, Mooney DJ, Wang CY. (2013). NF-κB inhibits osteogenic differentiation of mesenchymal stem cells by promoting β-catenin degradation. *Proc Natl Acad Sci (USA)* 110: 9469-9474.

90. Okamoto K, Takayanagi H. (2011). Osteoclasts in arthritis and Th17 cell development. *International Immunopharmacology* 11: 543-548.

91. Zhao R. (2013). Immune regulation of bone loss by Th17 cells in oestrogen-deficient osteoporosis. *European Journal of Clinical Investigation* 43:1195-1202.

92. Liu Y, Wang L, Kikuiri T, Akiyama K, Chen C, Xu X, Yang R, Chen W, Wang S, Shi S. (2011). Mesenchymal stem cell–based tissue regeneration is governed by recipient T lymphocytes via IFN-Gamma and TNF-Alpha. *Nature Medicine* 17: 1594-1601.

93. Caplan AI, Correa D. (2013). The MSC: An injury drugstore. *Cell Stem Cell* 9: 11-15.

94. Akiyama K, Chen C, Wang D, Xu X, Qu C, Yamaza T, Cai T, Chen W, Sun L, Shi S. (2012). Mesenchymal-stem-cell-induced immunoregulation involves FAS-ligand-FAS-mediated T cell apoptosis. *Cell Stem Cell* 10: 544-555.

95. Ghannam S, Pène J, Moquet-Torcy G, Jorgensen C, Yssel H. (2010). Mesenchymal stem cells inhibit human Th17 cell differentiation and function and induce a T regulatory cell phenotype. *Journal of Immunology* 185: 302-312.

96. Qu X, Liu X, Cheng K, Yang R, Zhao RC. (2012). Mesenchymal stem cells inhibit Th17 cell differentiation by IL-10 secretion. *Experimental Hematology* 40: 761-770.

97. Murphy MB, Moncivais K, Caplan AI. (2013). Mesenchymal stem cells: environmentally responsive therapeutics for regenerative medicine. *Experimental & Molecular Medicine* 45:e54.

98. Takahashi K, Yamanaka S. (2006). Induction of pluripotent stem cells from mouse embryonic and adult fibroblast cultures by defined factors. *Cell* 126:663-676.

99. Wong DJ, Liu H, Ridky TW, Cassarino D, Segal E, Chang HY. (2008). Module map of stem cell genes guides creation of epithelial cancer stem cells. *Cell Stem Cell* 2:333–344.

100. Miura K, Okada Y, Aoi T, Okada A, Takahashi K, Okita K, Nakagawa M, Koyanagi M, Tanabe K, Ohnuki M, Ogawa D, Ikeda E, Okano H, Yamanaka S. (2009). Variation in the safety of induced pluripotent stem cell lines. *Nature Biotechnology* 27:743–745.

101. Gutierrez-Aranda I, Ramos-Mejia V,Bueno C, Munoz-Lopez M, Real PJ, Mácia A, Sanchez L, Ligero G, Garcia-Parez JL, Menendez P. (2010). Human induced pluripotent stem cells develop teratoma more efficiently and faster than human embryonic stem cells regardless the site of injection. *Stem Cells* 28:1568–1570.

102. Fink DW Jr. (2009). FDA regulation of stem cellbased products. *Science* 324:1662–1663.

103. Ren G, Chen X, Dong F, Li W, Ren X, Zhang Y, Shi Y. (2012). Concise review: mesenchymal stem cells and translational medicine: emerging issues. *Stem Cells Translational Medicine* 1:51-58.